UNIVERSIDADE DO ALGARVE

DEPARTAMENTO DE CIÊNCIAS

BIOMÉDICAS E MEDICINA

Investigating the role and function of Tribbles 2 (TRIB2) in drug resistance within cancer

Laura Guerreiro Colaço

Dissertação para a obtenção do Grau de Mestre em Ciências Biomédicas

Trabalho efetuado sob a orientação de:

Professor Doutor Wolfgang Link
Professor Doutor Richard Hill

2014

UNIVERSIDADE DO ALGARVE

DEPARTAMENTO DE CIÊNCIAS

BIOMÉDICAS E MEDICINA

Investigating the role and function of *Tribbles 2* (TRIB2) in drug resistance within cancer

Dissertação apresentada à Universidade do Algarve para cumprimento dos requisitos necessários à obtenção do grau de Mestre em Ciências Biomédicas, realizada sob a orientação do Professor Doutor Wolfgang Link e do Professor Doutor Richard Hill (Departamento de Ciências Biomédicas e Medicina e Centro de Biomedicina Molecular e Estrutural - CBME).

Laura Guerreiro Colaço

2014

Investigating the role and function of *Tribbles 2* (TRIB2) in drug resistance within cancer

Declaração de autoria de trabalho

Declaro ser a autora deste trabalho, que é original e inédito. Autores e trabalhos consultados estão devidamente citados no texto e constam da listagem de referências incluída.

ASSINATURA: **_____**

ACKNOWLEDGEMENTS

Foremost, I would like to express my sincere gratitude to my supervisors Dr. Wolfgang Link and Dr. Richard Hill for their patience, motivation, enthusiasm, and immense knowledge. Their guidance helped me in all the time of research and writing of this thesis. I could not have imagined having a better supervisors and mentors.

I would like to thank all of my closest friends and my boyfriend for all the support that they gave me over the last year.

Last but not the least, I would like to thank my parents, Jacinto Colaço e Maria Helena Guerreiro, for all the love and support that they give me every single day.

"When you've fighting for it all your life
You've been working every day and night
That's a how a superhero learns to fly
(Every day, every hour, turn that pain into power)"

Danny O'Donoghue and Mark Sheehan

CHAPTER 1

ABSTRACT

1. ABSTRACT

Cancer is one of the major causes of death worldwide, with Melanoma being the one of the ten most frequent malignancy in a number of countries. Melanoma is an extremely aggressive cancer and concomitant to this aggressiveness, patient prognosis is poor. As a result, novel therapies and cellular targets are desperately needed. Nowadays, the chemical compound BEZ235 has demonstrated significant potential as an anti-cancer agent. The PTEN/PI3K/AKT pathway constitutes an important signaling regulator of multiple biological processes such as apoptosis, metabolism, cell proliferation and cell growth. The PTEN is a dual protein/lipid phosphatase which most important substrate is the phosphatidyl-inositol-3,4,5-triphosphate (PIP3), the product of PI3K. An increase in PIP3 recruits AKT to the membrane where it is activated by other kinases also dependent on PIP3. TRIB2, a gene that has been reported to be up-regulated in some cancers, has also been implicated in the negative regulation of the FOXO signaling cascade, specifically the negative regulation of FOXO3a. Consequently TRIB2 has been implicated in Melanoma resistance to various classical chemotherapeutics, like DTIC, and to some PI3K inhibitors, like BEZ235. As the abrogation of FOXO function is a key feature of many tumor cells, regulation of FOXO factors is receiving increasing attention in cancer research.

BEZ235 is a potent inhibitor of PI3Ks that are constitutively active in many cancers, including Melanoma. This deregulation results in the inactivation of the FOXO family of transcription factors, critical regulators of the cell cycle and apoptosis. Here we investigate how TRIB2 mediates PI3K inhibitor resistance and the role(s) of FOXO3a in this response. Our finding implicate TRIB2 influencing apoptosis (although not the cell cycle) and that this occurs at the level of transcription. Our findings also indicate that the over expression of TRIB2 significantly attenuates BEZ235 induced apoptosis and confer resistance to p53-dependent chemotherapeutics that induce apoptosis. However, in contrast to BEZ235 exposure, we note that DTIC treatment stabilizes p53 in cells with an over expression of TRIB2. Our findings indicate that cellular balance between p53 and MDM2 is disrupted. Here we note also that TRIB2 transcription and protein expression is significantly higher in Melanoma patient samples compared to normal skin tissue.

Keywords: Cancer, Melanoma, TRIB2, FOXO3a, p53, BEZ235, Signaling

1.1. Resumo

O cancro é uma das maiores causas de morte em tudo o mundo e é causado por um série de alterações somáticas no DNA que, consequentemente, causam uma proliferação celular descontrolada. A grande maioria destas alterações são causadas por erros aquando da replicação, por defeitos no processo de reparação do DNA ou pela exposição a cancerígenas. Casualmente, as patologias cancerígenas podem ser causadas por uma alteração num gene dominante (oncogene), que estimula a que ocorra uma proliferação celular desregulada. Na sua grande maioria e, porventura, em todos os tipos de cancro que ocorrem nos humanos existem, como principais características dos mesmos, seis alterações essenciais à fisiologia das células: a autossuficiência no que diz respeito a sinais de crescimento, uma evidente insensibilidade a sinais inibitórios externos de crescimento, uma evasão à morte celular programada, um ilimitado potencial replicativo, uma angiogénese sustentada pela própria célula e uma capacidade metastática para outros tecidos do organismo.

O Melanoma é a forma mais agressiva de cancro que se desenvolve a partir dos melanócitos e, ainda, uma das mais frequentes patologias oncológicas em diversos países. É mais comum em pessoas com idades compreendidas entre os 30 e os 60 anos e, o aumento anual no seu número de casos nos últimos cinco anos, tem causado um consequente significativo aumento na taxa de mortalidade associada a este tipo de cancro. Os Melanomas podem desenvolver-se em pessoas com todo o tipo de cor de pele, contudo existe uma maior incidência deste tipo de tumor em pessoas que possuam uma pele mais clara. Sendo esta uma patologia heterogénea, a mesma apresenta diferentes e diversas alterações genéticas e, ainda, uma extensa variedade de subtipos histológicos. Este tipo de doença oncológica é extremamente agressivo, conferindo, aos pacientes, um prognóstico pessimista. Tendo em conta o referido anteriormente, é de extrema importância que sejam descobertos novos alvos celulares e novas terapias contra esta doença cancerígena. Desta forma, a investigação científica nesta área tem sido vasta, obtendo-se, através de estudos recentes, resultados que demonstram que sinalização da PI3K está desregulada na grande maioria dos Melanomas. Atualmente, o composto químico BEZ235 tem demonstrado ser detentor de um significante potencial como agente anticancerígeno.

A via de sinalização PTEN/PI3K/AKT é um importante regulador de diversos processos biológicos, como, por exemplo, o metabolismo, o crescimento celular, a proliferação celular e a apoptose. O PTEN é uma fosfatase com características de proteína e de lípido, e que tem, como principal substrato, o fosfatidil inositol 3,4,5-trifosfato (PIP3), que é o produto da PI3K. O aumento do níveis de PIP3 faz com que ocorra o recrutamento de AKT para a membrana, permitindo que o mesmo seja ativado por outras quinases que também são dependentes de PIP3.

O TRIB2 é um gene que tem sido descrito como sendo um dos que demonstram possuir uma regulação superior em diversos tipos de cancro, inclusive em Melanomas, onde a sua sobre expressão proteica é um obstáculo à eficiência dos tratamentos aplicados a este tipo de patologia oncológica. Este mesmo gene, também tem sido implicado na regulação negativa da via de sinalização do FOXO, especialmente na regulação negativa do FOXO3a. Como consequência das características atrás mencionadas, o TRIB2 tem sido considerado como uma das causas para a resistência aos quimioterapêuticos clássicos (como o DTIC) e aos inibidores da PI3K (como o BEZ235), por parte de pacientes com Melanoma. Tendo em conta que a supressão da função do fator de transcrição FOXO é uma característica fundamental para inúmeras células tumorais, a regulação desses mesmos fatores tem sido, cada vez mais, uma das linhas de investigação mais seguidas contra o cancro.

O BEZ235 é um potente inibidor das PI3Ks, as quais se encontram desregulamente ativas nos mais variados tipos de cancro, incluindo no Melanoma. Esta desregulação, tem como consequência a inativação da família dos fatores de transcrição FOXO, os quais exercem funções como reguladores cruciais do ciclo celular e da apoptose. Neste trabalho, foi investigado o processo sobre como o TRIB2 medeia a resistência aos inibidores da PI3K e, também, qual a função do FOXO3a em resposta a esse mesma resistência. No decorrer da investigação inerente a este trabalho, foi constatado que o TRIB2 exerce uma determinada influência sobre a apoptose, a nível da transcrição, contudo o mesmo não acontece sobre o ciclo celular. Posteriormente, também foi verificado que a sobre expressão de TRIB2 atenua, significativamente, a apoptose induzida pelo inibidor da PI3K BEZ235, tendo sido observado que, após o tratamento com esse mesmo inibidor, as células onde a expressão de TRIB2 estava presente, demonstraram possuir níveis proteicos de Caspase-3 clivada inferiores e que essas mesmas células são, fenotipicamente, caracterizadas por uma redução significativa na população celular na fase Sub-G1, comparativamente às células que não sobre expressam TRIB2.

Neste trabalho, foi também verificado que a sobre expressão de TRIB2 confere resistência aos quimioterapêuticos, que induzem a apoptose, dependentes do supressor tumoral p53. Contudo, e em contraste com a exposição ao BEZ235, foi verificado que o tratamento com o quimioterapêutico convencional DTIC estabiliza o p53 nas células que sobre expressam TRIB2. Estes resultados indicam que o balanço celular proteico entre o p53 e o MDM2 está corrompido.

Todos as evidências atrás verificadas foram realizadas em amostras *in-vitro*. Contudo, aquando da realização deste projeto, foi possível ter acesso a amostras de Melanoma e a amostras normais *ex-vivo*. Nas amostras de pacientes com Melanoma, foi verificado um aumento significativo nos níveis de AKT fosforilada, comparativamente às amostras normais. De acordo com a ativação da via do AKT referida

acima, foi também verificado a existência de níveis altos de FOXO3a fosforilado nas células dos pacientes com Melanoma. Em concordância com as observações atrás mencionadas, foi verificado que as células normais expressam uma maior quantidade das proteínas reguladas pelo FOXO3a, FasL e BIM, comparativamente às células de pacientes com Melanoma. Estas observações podem ser devidas ao facto das células cancerígenas precisarem de evitar a apoptose, de forma a continuarem a divisão celular, particularmente no último estádio da doença. Por último, foi também constatado que, tanto a transcrição como a expressão proteica de TRIB2, estão ambas significativamente elevadas nas amostras de pacientes com Melanoma, comparativamente às amostras de células normais.

Palavras-chave: Cancro, Melanoma, TRIB2, FOXO3a, p53, BEZ235, Sinalização

TABLE OF CONTENTS

FIGURES LIST

TABLES LIST

APPENDIX LIST

ABBREVIATIONS LIST

AJCC	American Joint Committee on Cancer
AKT	Protein kinase B
ATF4	Activating transcription factor 4
BRAF	B-type Raf kinase
ChIP	Chromatin Imunnoprecipitation
Co-IP	Co-Imunnoprecipitation
DNA	Deoxyribonucleic acid
DTIC	Dacarbazine
FACS	Fluorescent Activated Cell Scanning
FasL	Fas ligand
FDA	Food and Drug Administration
FOXO	Forkhead transcription factor
IGF-1	Insulin-like growth factor 1
IgG	Immunoglobulin G
Il-2	Interleukin-2
IP	Immunoprecipitation
KD	Kinase Domain
MAPK	Mitogen-activated protein kinases
MAPKK	Mitogen-activated protein kinase kinase
MDM2	Mouse double minute 2 homolog
mTOR	Mechanistic target of rapamycin
p70S6K	Phosphorylation of 40S ribosomal protein S6
PBS	Phosphate buffered saline
PDK1	Pyruvate dehydrogenase lipoamide kinase isozyme 1
PI3K	Phosphatidylinositol 3 kinase
PIP3	Phosphatidylinositol (3,4,5)-trisphosphate
PRAS40	proline-rich AKT substrate of 40 kDa
PTEN	Phosphatase with tensin homology
RTK	Receptor tyrosine kinases
USA	United States of America
UV	Ultraviolet

CHAPTER 2

INTRODUCTION

2. <u>INTRODUCTION</u>

2.1. Cancer.

Cancer is caused by a series of somatic alterations in DNA and the consequence of these events is an uncontrolled cellular proliferation. The majority of these alterations are caused by replication errors, defective DNA repair processes or exposure to carcinogens[1,2]. However, occasionally cancers can be caused by an alteration in a dominant gene that drives uncontrolled cell proliferation. The genes that can promote cell growth when altered are often called *oncogenes*[3].

Most and perhaps all types of human cancers are characterized by six essential alterations in cell physiology: self-sufficiency in growth signals, insensitivity to growth-inhibitory signals, evasion of programmed cell death, limitless replicative potential, sustained angiogenesis, and tissue invasion and metastasis. These properties are exclusive from the cancer cell and are not found in the normal adult cell from which the tumor is derived[4].

2.2. Melanoma.

2.2.1. *General Issues.*

Pigmented lesions are among the most common findings on skin examination. The challenge is to distinguish Melanomas, which account for the overwhelming majority of deaths resulting from skin cancer, from the remainder, which with rare exceptions are benign[5]. Cutaneous Melanoma, is a form of aggressive cancer that develops from melanocytes (Figure 1.2.1.1). It is most common in people between 30 and 60 years of age. This type of cancer is a heterogeneous disease that presents different genetic alterations and diversity of histological subtypes[6,7]. Having regarded what was referred before, the scientific investigation in this area has been vast. Recent studies have revealed that PI3K signaling is deregulated in a high proportion of Melanomas[8,9]. Despite all the research that has been done, Melanoma patients have only experienced a minor increase in life expectancy in stark contrast to other types of cancer. The rising number of cases per year has resulted in Melanoma mortality rising sharply over the along the last five decades[10].
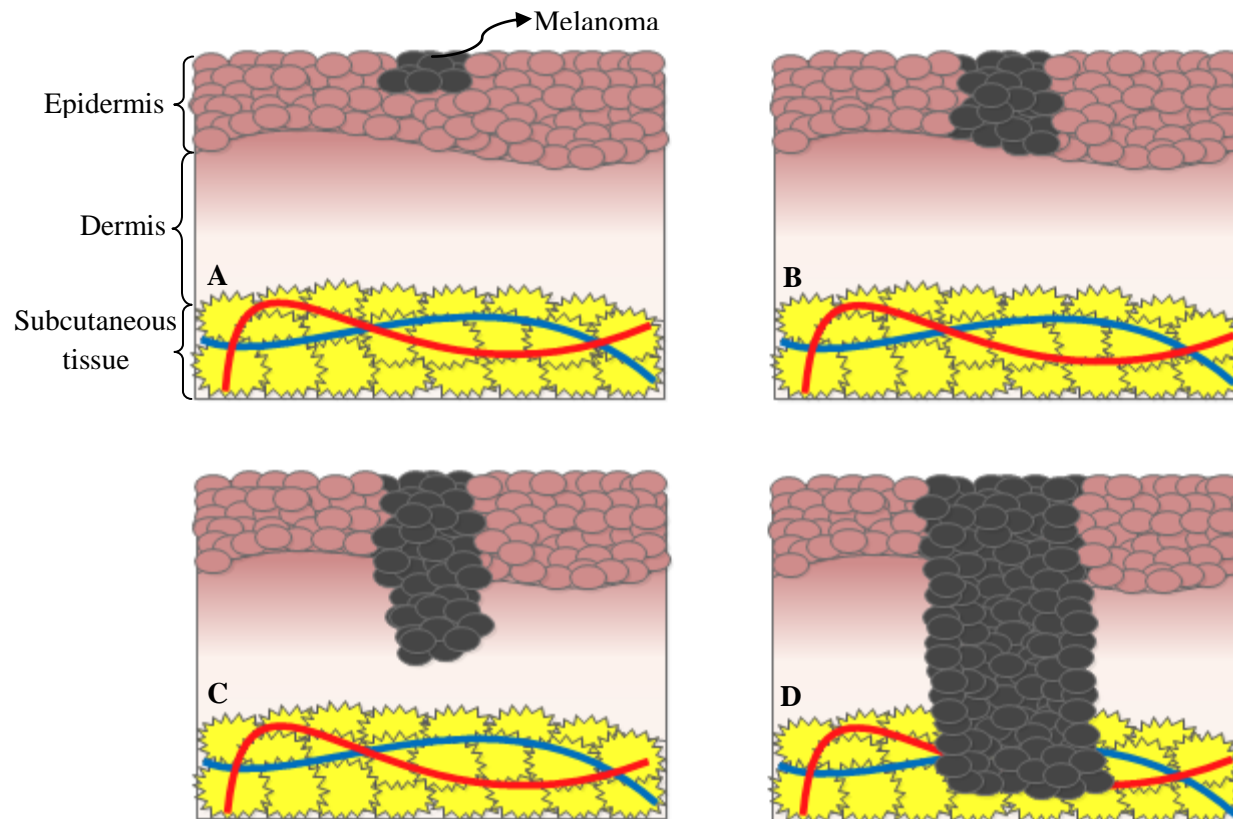
Figure 2.2.1.1: Schematic illustration of the process and development of Melanoma and its metastases (from A to D).

2.2.2. Epidemiology.

Melanomas can occur in adults of all ages (the median age at diagnosis is the late fifties), in people of all colors and men are affected slightly more than women (1.3/1). It is located on the skin and originates following the transformation of melanocytes, the pigment-producing cells in the neural crest that migrate mainly to skin, mucous membranes, upper esophagus and eyes[6,7]. The highest incidence rates occurs in white-skinned peoples living at low latitudes. Accordingly, the association between sun exposure and Melanoma have been explored. An important risk factor for Melanoma is UV irradiation upon sun exposure[10].

Melanoma primarily grows horizontally within the epidermis (Melanoma *in situ*) but in an advance stage it can grow in depth and penetrates into the dermis (invasive Melanoma)[8]. At this point, the patient prognosis is good, with surgical resection of the tumor conferring a 53-97% survival. However, if a distant metastasis is present, the patients exhibit a less than 5% survival independently of the therapeutic intervention. It is estimated that there were more than 1 million Melanoma survivors living in the USA as of January 1, 2014, and an additional 76 100 people will be diagnosed in 2014. Melanoma incidence rates have

been increasing for at least 30 years. About 84% of Melanomas are diagnosed at a localized stage, when they are highly curable[7,11].

2.2.3. Treatment of Melanoma by Stage.

The stage of a Melanoma is a description of how widespread it is. This includes its thickness in the skin, whether it has spread to nearby lymph nodes or any other organs, and certain other factors. A staging system is a standard way to sum up how far a cancer has spread. The system most often used to stage Melanoma is the American Joint Commission on Cancer (AJCC) system[12,13] (Table 1.2.2.1).

Stage	Description of Melanoma's Characteristics
0	It is in the epidermis but has not spread to the dermis
I	It is smaller than 1.0 mm in thickness and has not been found in lymph nodes or distant organs
II	It is thicker than 4.0 mm and is ulcerated. It has not been found in lymph nodes or distant organs
III	It can be of any thickness, but it is not ulcerated. It has spread to 1 - 3 lymph nodes near the affected skin area (no distant spread)
IV	It has spread beyond the original area of skin and nearby lymph nodes to other organs such as the lung, liver, or brain, or to distant areas of the skin, subcutaneous tissue, or distant lymph nodes

Table 2.2.3.1: American Joint Commission on Cancer (AJCC) system, which is used to stage Melanoma.

Surgery to remove the tumor and surrounding tissue is the primary treatment for most Melanomas. Less than 3% of all patients with Melanoma undergo radiation therapy. However, almost one-half (45%) of patients with metastatic disease who receive either chemotherapy or immunotherapy also receive radiation therapy[14,15]. Patients with stage III Melanoma are often offered adjuvant immunotherapy with interferon for about a year. However, this treatment has side effects that make it very difficult to tolerate. Treatment for patients with stage IV Melanoma has changed in recent years and typically includes immunotherapy or targeted therapy drugs. Patients with localized or regional metastatic disease are identified for surgical resection and could benefit from interferon-α adjuvant therapy, despite the significant toxicity associated with this treatment. In patients with distant metastasis, surgery is unlikely to be offered and the only therapeutic option available is systemic drug administration[12,15,16].

2.2.4. Conventional Chemotherapy .

Conventional chemotherapy is based on the use of alkylating agents such as Fotemustine (Muphoran), Dacarbazine (DTIC), and Temozolomide (Temodal) which trigger cytotoxic effects by blocking cell replication. However, these chemotherapy drugs promote only 10% of objective response with

no improvement of overall survival[15,17]. Since the major advance realized in 2011 with the FDA approval of Vemurafenib, for mutated *BRAF* Melanomas, these drugs are limited to patients harboring non-*BRAF* mutated Melanomas or for patients who developed resistance to previous treatments[18,19].

It has been well documented that Melanoma is an immunogenic tumor but metastatic Melanoma cells have developed mechanisms to escape from immune surveillance in order to survive. The immune system involvement in protection against Melanoma is supported by the increased of Melanoma incidence under immunosuppression conditions[20]. In 1998, the first immunotherapy to be approved by the Food and Drug Administration (FDA) for treatment of advanced Melanoma was Interleukin-2 (IL-2) but, like Dacarbazine, response rates were low even at high-doses of treatment. Its use in clinical practice is limited by the severe toxic side-effects[21,22]. However, substantial advances in systemic cancer therapies have been reported since 2009 and a new immunotherapeutic drug (anti-CTL4-4 antibody) Ipilimumab[23].

2.2.5. *Novel Therapy.*

The recent characterization of the molecular alterations in Melanoma leads to the development of targeted therapies in order to finish with the resistance to therapeutic agents, both chemical or biological, which remains the main problem in the management of the therapy in Melanoma. These treatments are designed to target tumors according to their molecular diversity and activated intracellular signaling pathways[24–27]. Advanced studies led to the development of inhibitors of PI3K which selectively target only the catalytic sites. The PI3K inhibitors, GSK2126458 and BEZ235, were evaluated in vitro showing an enhanced cell growth inhibition[28–30].

The use of novel therapeutics should ideally be made following an immunological and genetic mutation screen of the patients tumor, in order to the treatment be specifically adapted based on mutations of a patient who have cancer. However, there are no currently available immunological biomarkers and those targeted agents for which mutations can be tested, frequently develop secondary resistance. New biomarkers could be useful for many different things like screening, early diagnosis, disease staging as well as for the identification of those patients who are in high risk of disease recurrence[31,32].

2.3. The AKT Pathway.

2.3.1. *General Issues*

The AKT is a serine/threonine kinase downstream of PTEN/ PI3K, that exists as three isoforms in mammals (AKT1, AKT2 and AKT3) , which are encoded by three different genes. They are ubiquitously

expressed, but their levels are variable, depending upon the tissue type[33,34]. In Melanoma cells, AKT3 is the form preferentially expressed. The AKT3 activation is found in about 60% of sporadic Melanomas[35]. The AKT kinase regulates multiple biological processes including cell survival, proliferation, growth, and glycogen metabolism through phosphorylation of many physiological substrates[33]. A variety of growth factors (e.g. IGF-1), hormones (e.g. Thyroid Hormone T_3), cytokines (e.g. IL-2) and certain oncogenes (e.g. Ras) activate AKT, by binding their cognate receptor tyrosine kinase (RTK) and triggering activation of the lipid kinase PI3K[36–39]. For instance, Ras activation of the AKT pathway confers protection from apoptosis in fibroblasts in response to DNA damage or oncogenic Myc. Although several AKT targets have been reported, it is not fully understood how AKT promotes survival[9,40,41].
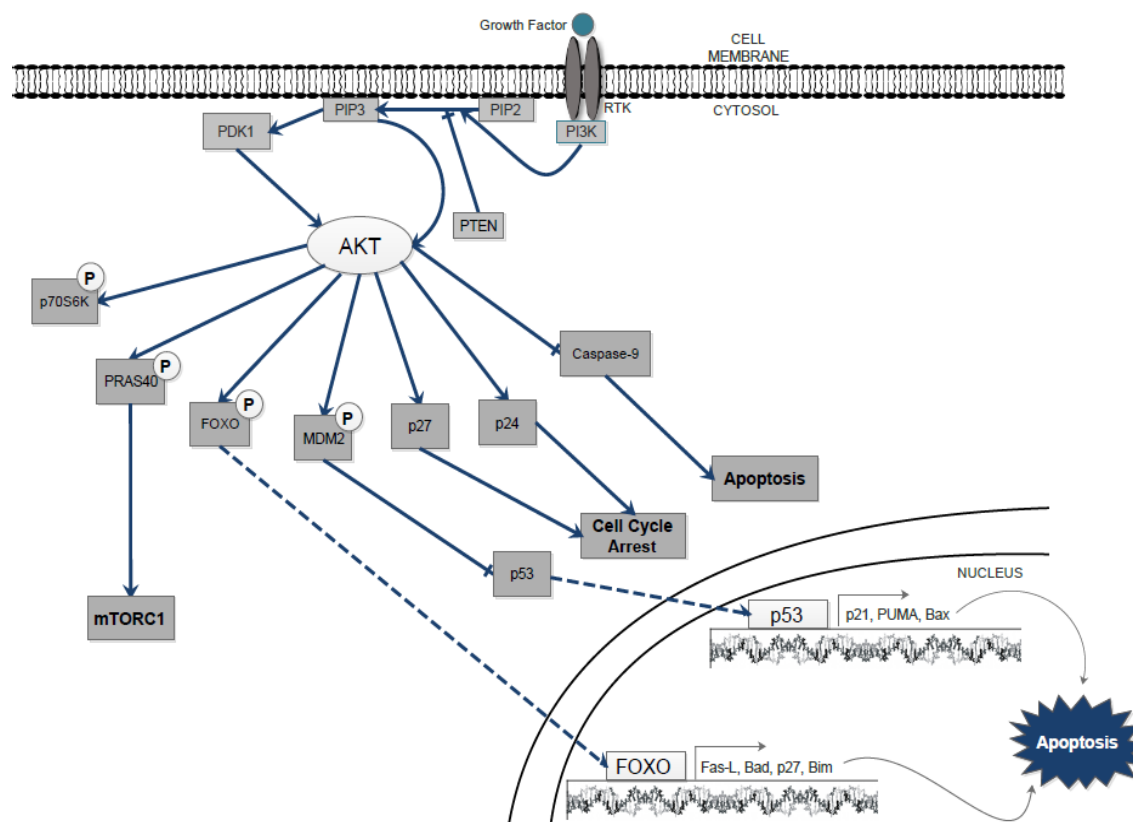
Figure 2.3.1.1: General scheme of the PTEN/PI3K/AKT pathway.

2.3.2. The Activation of AKT.

The PTEN is a dual lipid and a protein phosphatase. Its primary target is the lipid phosphatidylinositol-3,4,5-triphosphate (PIP3), the product of the phosphatidylinositol-3-kinase (PI3K)[42,43]. The loss of function of the PTEN (which has been implicated in many human cancers), as well as the activation of the PI3K, results in accumulation of PIP3 triggering for the activation of its downstream effectors, PDK1, AKT and Rac1[44,45]. The activation of PI3K is induced by growth factors and insulin targeting by the catalytic subunit to the membrane where it is in close proximity with its substrate, mainly

PIP2. PDK1 contains a C-terminal pleckstrin homology (PH) domain, which binds the membrane bound PIP3 triggering PDK1 activation. Activated PDK1 phosphorylates AKT at Thr308 activating its ser/thr kinase activity and further activation occurs by PDK2 by phosphorylation at Ser473[46,47]. Activation of AKT results in the suppression of apoptosis induced by a number of stimuli including growth factor withdrawal, detachment of extracellular matrix, UV irradiation and cell cycle discordance[9]. Furthermore, the abnormal expression and activity of the PI3K/AKT pathway proteins has been shown to promote Melanomagenesis by inducing cell survival signaling in Melanoma cells. Therefore, members of this signaling cascade are attractive targets for inhibiting Melanoma[9].

2.3.3. The Importance of p53.

The PI3K-AKT pathway has recently been reported to inhibit the transcriptional activity of p53 and reduce the proapoptotic functions of it. The p53 is a tumor suppressor which plays a key role in the induction of apoptosis and cell cycle arrest in response to a variety of genotoxic stresses and to the activation of some oncogenes such as Myc, thereby preventing the propagation of damaged cells[48,49]. Its function is controlled by several mechanisms, including the regulation of p53 protein stability. Central to this process is MDM2, a ubiquitin ligase that targets p53 for ubiquitination and allows export of p53 from the nucleus to the cytoplasm, where p53 degradation by proteasomes takes place[50].

Under normal circumstances, p53 is maintained at very low levels by continuous ubiquitination and degradation. Activation of p53 in response to cellular stresses is mediated partly by inhibition of MDM2 and rapid stabilization of p53 protein. The deregulated activation of mitogenic signals, caused by the oncogenic activation of Ras or Myc for example, leads to the activation of p53, which provides a mechanism to prevent the abnormal proliferation associated with tumor development[51,52]. However, this activation of p53 by mitogenic signals must be suppressed during normal cell proliferation to prevent p53 from inducing cell cycle arrest or apoptosis. Therefore, it appears reasonable to assume that mitogenic signals elicit both p53-activating and -inactivating signals[53,54]. Recent studies have indeed shown that Ras can inhibit or activate p53, depending on the cellular contexts and the duration of Ras activation. The Raf/MEK/MAPK pathway has been shown to mediate Ras activation of p53. Therefore, it is possible that the PI3K/AKT pathway opposes the MAPK pathway in activation of p53. However, it has yet to be determined how AKT suppresses p53[55–57].

2.3.4. *The role of FOXO proteins.*

As mentioned above, the AKT promotes cell survival directly by its ability to phosphorylate and inactivate several pro-apoptotic targets, like Bim, and the forkhead transcription factors (FOXO)[58]. The FOXO proteins (including FOXO3a) play an important role in longevity and tumor suppression by regulating a wide range of genes involved in stress resistance, metabolism, cell cycle arrest and apoptosis. Previous studies have shown that BEZ235 treatment of malignant Melanoma cells induces FOXO3a-dependent gene expression following the inhibition of PI3K1. Activation of this pathway can directly result in phosphorylation of FOXOs and their subsequent cytoplasmic sequestration and/or degradation via the ubiquitin-proteasome pathway. When FOXO is activated by the inhibition of the PI3K/AKT pathway, FOXO's promotes a wide range of effects including cell cycle arrest, cell differentiation, autophagy and apoptosis via various mechanisms[59,60].
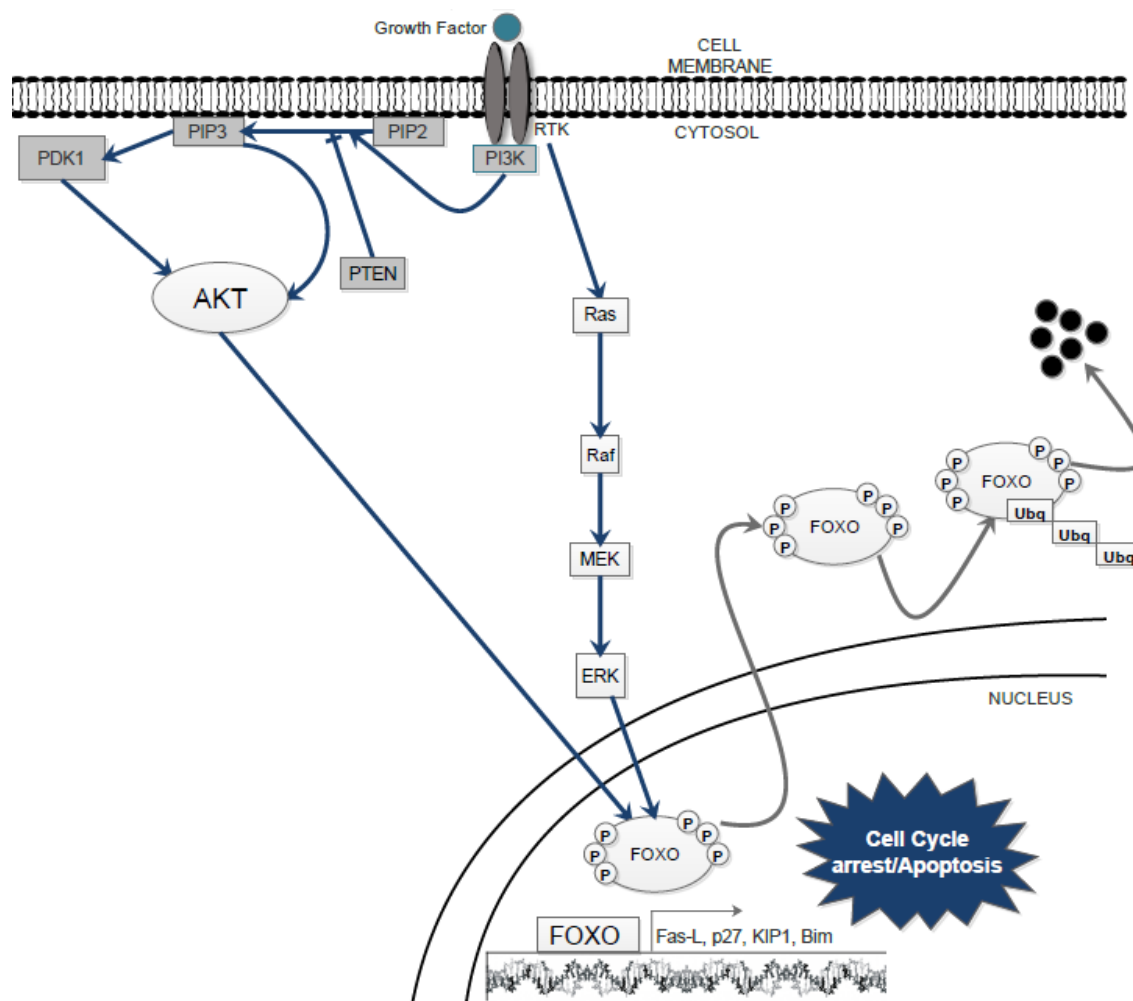
Figure 2.3.4.1: General scheme of PTEN/PI3K/AKT pathway inhibition and FOXOs posphorilation, with FOXOs subsquent cytoplasmatic sequestration.

2.4. The Tribbles Pseudokinases Family.

The Tribbles (TRIB) pseudokinases family members are the human homolog of Drosophila tribbles protein, which regulates the cell cycle during oogenesis and morphogenesis, and influences proliferation, motility, metabolism, and oncogenic transformation. All three TRIB (TRIB1, TRIB2, and TRIB3) pseudokinases are associated with a variety of human malignancies, acting as adaptors in important cellular signaling pathways extending from mitosis and cell activation to apoptosis and modulation of gene expression[59]. The members of Tribbles family have been reported to interact and modulate the activity of signal transduction pathways, including the PI3K/AKT and the MAPK systems, and with various signaling molecules and transcription factors, including ATF4, p65, CtIP, MAPKK, AKT and COP1[60,61].

The TRIB2 (and the others Tribbles proteins) are characterized by a central serine/threonine kinase-like domain (KD) and a C-terminal binding site for E3 ubiquitin ligases. However, these proteins are considered to be catalytically inactive because they lack conserved residues from the characteristic adenosine triphosphate binding site and catalytic core motif within the KD[61]. Therefore, Tribbles probably function as adapter or scaffold proteins. Although the three members of Tribbles family proteins are highly homologous in the KD and in the C-terminal E3 ubiquitin ligase binding site, they show restricted similarity in the N- and C-terminal domains[62]. The TRIB2 domains responsible for protein binding or functional/oncogenic activity are unknown. On the other hand, the integrity of the KD domains is required for both of these activities, and a mutation of critical residues within the KD interferes with these activities. Additionally, the binding of COP1 to the TRIB2 C-terminus is essential for TRIB2-induced AML. In the nonexistence of COP1 binding, Leukemia does not occur[59,63,64].

Furthermore, TRIB2 has been implicated in the negative regulation of FOXO3a. The restoration of FOXO proteins have been suggested as a promising strategy to treat various types of cancer and accordingly the forced expression of nuclear FOXO has been shown to induce apoptosis in a wide range of in vitro cancer cell line models[59,63]. Additionally, the TRIB2, which is highly expressed in metastatic Melanoma cells, has been implicated in the resistance of various cancers to a range of chemotherapeutics, including PI3K inhibitors that are under clinical trial. It is hypothesized that this resistance is due to the repression of FOXO family members[59,61,65].

2.5. Hypothesis.

Our group discovered that the kinase-like protein TRIB2 was highly expressed in metastatic Melanoma samples (and recently colon and pancreatic malignancies). Recent data within our laboratory revealed that the over expression of TRIB2 conferred drug resistance to a range of chemotherapeutic agents

and importantly conferred resistance to a number of phosphatidylinositol 3-kinases (PI3Ks) inhibitors that are being tested in Melanoma clinical trials.

These results indicate that TRIB2 confers chemotherapeutic resistance. Based on our laboratory research, the present work intends to elucidate some of the mechanism(s) of action about how TRIB2 mediates PI3K inhibitor resistance and the role(s) of FOXO3a in this response.

In order to test our hypothesis, we need to confirm the inhibition effectiveness of our PI3K inhibitor and the cellular phenotype following TRIB2 over expression and to examine the recruitment of FOXO3a and the promoters of cell cycle arrest.

CHAPTER 3

MATERIALS AND METHODS

3. <u>MATERIALS AND METHODS</u>

3.1. Cell Culture and Tissue Samples.

The cell lines used for this work and their respective information are represented in Table 3.1.1. The cells were cultivated in DMEM (Sigma) with 10% heat inactivated FCS (Sigma) supplemented with Pen/Strep (Gibco) and within 35 mm plates. The U2OS and the 293T cell lines was previously transfected with a plasmid containing the TRIB2. The G361 and the SK-Mel28 cell lines was stably transfected with a TRIB2 shRNA expressing plasmid. We treated the cells with several chemotherapeutic drugs. The chemotherapeutic drugs and their respective concentrations are represented in Table 3.1.2. We did several drug time courses with the different chemotherapeutic drugs.

<u>Cell Line</u>	<u>Origin</u>
U2OS	Human Osteosarcoma
293T	Human Renal Cancer
MCF-7	Human Breast Cancer
MDA-489	Human Breast Cancer
A375	Human Melanoma
G361	Human Melanoma
M14	Human Melanoma
SK-Mel28	Human Melanoma
UACC62	Human Melanoma

Table 3.1.1: Cell lines used in this work and their origin.

<u>Chemotherapeutic Drugs</u>	<u>Concentration</u>
DTIC (Dizcarbacine)	100nm
BEZ235	100nm
BAYER COMPOUNDS (236; 439; 766; 931)	10nm
Cyclohexamide	10ug
Actinimycin D	10ug
MG132	10ug/ml

Table 3.1.2: Chemotherapeutics drugs used in this work and their respective concentrations.

All used Melanoma and Normal tissue samples are represented in Table 3.1.3, and were provided by Dr Selma Ugurel (Julius-Maximilians-Universität Würzburg, Germany). They were sectioned for Immunohistochemistry (Faro Hospital) and the remaining tissue used for protein analysis.

Melanoma Samples			Normal Samples
Stable Disease	Complete response	Progressive Disease	////////
CSM002	CSM066	CSM105	1274
CSM178	CSM209	CSM108	1440
CSM200	CSM203	CSM143	1454
CSM214	CSM068	CSM060	1425
CSM099	CSM006	CSM057	1408
		CSM027	1474
		CSM094	1412
		CSM038	1489
		CSM111	1428
		CSM213	1508

Table 3.1.3: Melanoma and Normal tissue samples used in this work.

3.2. Protein Extraction and Quantification.

The protein extraction is the total protein that was extracted from each cell line or our tissue samples.

For cellular extraction, the cells were collected from the culture plates by first removing the growth medium and to then scrape the cells in 1 ml of PBS. This suspension was then transferred into a clean Eppendorf and spinned at 1100 rpm for 5 min at 4ºC. The PBS was removed from the pellet and RIPA buffer (Tris-HCL ph 7.4, NaCl, 10% Nonidet P-40, 10% sodium deoxycholate, 100 mM EDTA, PIC, 200 mM NA-F, 100mM Na3VO4 and protease inhibitors cocktail) was added to the pellet. The pellet was resuspended in this total lysis buffer and incubated on ice for 30 minutes. After 30 minutes the lysed cells were spun 15 minutes at 13000 rpm (maximum speed). The supernatant (containing our proteins) was collected and transferred to a fresh eppendorf prior to quantification.

For protein extraction from our tissue samples, tissue sections were placed inside a manual homogenizer (Sigma) with 500 μL of the RIPA buffer (described above) and vigorously homogeneized. After homogenization samples were incubated on ice for 30 minutes. Lysed samples were spun at 13000 rpm and the supernatant transferred to a fresh eppendorf prior to protein quantification. For both extraction protocols all extracted proteins were stored at -80ºC until required.

To determine the protein concentrations (protein quantification) in each sample we used the Quick Strat™ Bradford Protein Assay (BioRad) and the NanoDrop 2000 UV-Vis Spectrophotometer (ThermoScientific) following the manufacturers guidelines.

3.3. Western Blotting.

Our extracted protein samples were diluted in to 2x lammeli loading buffer (containing β-mercaptoethanol) and heatedat 95ºC for 5 minutes. Samples were loaded into our 10% SDS-PAGE gels. Separated proteins within each gel were transferred on to nitrocellulose membranes (Amersham) and were blocked with 5% BSA (in Tris-buffered-saline [TBS]) for 1 hour (preventing non-specific antibody binding). After blocking, membranes were immunoblotted with several primary antibodies (dilution of 1/1000 into BSA) overnight at 4ºC. The primary antibodies used in this work and their respective information are represented in Table 3.3.1.

After incubation, membranes were washed (x3) with TBS 0.1% tween20. After washing, corresponding secondary antibodies were added (dilution of 1/5000 into BSA) at room temperature for 1 hour. The secondary antibodies used in this work and their respective information are represented in Table 3.3.2. The membranes were washed (x3) times with TBS 0.1% tween20 and visualized using ECL$^+$. Images were obtained using a Molecular Imager® ChemiDoc™ XRS System (BioRad).

Primary Antibodies	Supplier and Information
Total AKT	C-20; sc-1618; Goat; Santa Cruz Biotechnology
p-AKT	Ser 473; sc-7985; Rabbit; Santa Cruz Biotechnology
Total FOXO (FKHRL1)	N-16; sc-9813; Goat; Santa Cruz Biotechnology
p-FOXO (p-FKHRL1)	Ser253; sc-101683; Rabbit; Santa Cruz Biotechnology
TRIB2	Custom, Rabbit, Madrid
Fas-L	C-178; sc-6237; Rabbit; Santa Cruz Biotechnology
MDM2	C-18; sc-812; Rabbit;Santa Cruz Biotechnology
PTEN	A2B1; sc-7974; Mouse; Santa Cruz Biotechnology
P53	DO-1; sc-126; Mouse; Santa Cruz Biotechnology
BIM	H-191; sc-11425; Rabbit; Santa Cruz Biotechnology
Total PRAS40	H-216; sc-67042; Rabbit; Santa Cruz Biotechnology
p-PRAS40	Thr246; sc-32629; Rabbit; Santa Cruz Biotechnology
Total p70S6K	C-18; sc-230; Rabbit; Santa Cruz Biotechnology
Actin	I-19; sc-1616; Goat; Santa Cruz Biotechnology
Caspase-3	E-8; sc-7272; Mouse; Santa Cruz Biotechnology
Cleaved Caspase-3	h176; sc-22171; Rabbit; Santa Cruz Biotechnology
Total PDK1	C-20; sc-7140; Goat; Santa Cruz Biotechnology
p-PDK1	Ser241; #3061; Rabbit; Cell Signaling Technology
14-3-3σ	N-14; sc-7681; Goat; Santa Cruz Biotechnology

Table 3.3.1: Primary antibodies used in this work and their respective information.

Secondary Antibodies	Supplier and Information
Anti-rabbit	IgG-HRP; sc-2004; Goat; Santa Cruz Biotechnology
Anti-goat	IgG-HRP; sc-2020; Donkey; Santa Cruz Biotechnology
Anti-mouse	IgG-HRP; sc-2314; Donkey; Santa Cruz Biotechnology

Table 3.3.2: Secondary antibodies used in this work and their respective information.

3.4. Co-Imunnoprecipitation (Co-IP).

The cells were washed with medium. Trypsin was added to the plate with the cultivated cells and then the cells were scraped. The solution was collected to new Eppendorf tubes and centrifuged, and the supernatant was collected to new tubes. The protein A/G-agarose beads (Sigma) were washed for 2 times with PBS and a 50% protein A/G agarose working solution (in PBS) was made. Each indicated antibody was added to the beads for 1 hour. After 1 hour the beads were washed (x2) with PBS. 500 μg of total protein lysate was added to each set of beads and incubated overnight at 4ºC. Samples were centrifuged (max speed), the pellet was kept, and washed with pre-chilled PBS (x3). SDS-loading buffer was added to beads and the samples heated to 95ºC for 5 minutes. Samples were extracted and run on an appropriate percentage SDS-gel.

3.5. JetPrime Transfection Protocol.

In order to transfect some of ours cell lines (see Table 3.1.1 from 3.1), we followed the JetPrime transfection Protocol. We started the protocol diluting 2 μg of our DNA into 200 μl jetPRIME® buffer and, after that, we mixed both by vortexing. Then, it was added 4 μl of jetPRIME® to the mix and then, the new mix, was vortexed for 10 seconds and, after that, spun down briefly. At that time, the mix was incubated for 10 minutes at room temperature. Following the incubation, it was added 200 μl transfection mix (drop wise), per plate and evenly, onto the cells in serum containing medium. Finally, the plates was gently rocked and, then, placed into the incubator for 24 hours.

3.6. Chromatin Imunnoprecipitation (ChIP).

The plates were washed with medium, and a 1% formaldehyde/PBS solution was added to cross-link proteins to DNA. The solution was removed, and the plates were washed with ice cold PBS (x3). Cells were scraped from the plates with 1M Tris-HCl with 10mM DTT, and transferred to Eppendorf tubes. After centrifugation, the pellets were washed with Buffer I and II. After centrifugation, the pellet was resuspended in lysis buffer (made fresh with PIC). The cells were sonicated (6 times for 10 sec each sample) on ice, to shear DNA to an average fragment size of 200-500 base pairs. After centrifugation (at max speed for 15 minutes) to pellet cell debris, the supernatant was transferred into a new Eppendorf. 300 µl of Buffer D and PIC were added to each sample. 100 µl input samples were removed at this stage. The input samples were heated overnight at 65°C.

To the remaining sample (after the inputs were removed), we added sheared salmon sperm DNA, the antibody of interest and protein G-fast flow beads (Sigma) and Buffer D. After incubation overnight at 4ºC, the beads were pulled down and washed with TSE I, II and III. Afterwards the beads were washed with ice cold TE. The DNA was extracted with three washes with a solution of NaCHO3 and SDS. Once extracted the samples were transferred to a fresh Eppendorf and heated overnight at 65ºC. Our input and the ChIP samples were loaded into Sigma-PCR clean-up columns and after washing our immunoprecipitated DNA eluted with 30 µl dH2O. Samples were stored at -20ºC

3.7. Fluorescent Activated Cell Scanning (FACS).

For cellular extraction (after treatment), we first collected the growth medium and then transferred this into a clean 15 ml Falcon Tube. After that, we added 1mL of Trypsin to the cells and then we placed them in an incubator for 15 minutes. After 15 minutes we detached the cells by mixing up and down. The trypsinized cells were then added to the corresponding Falcon Tube and spinned at 1100 rpm for 5 minutes. The medium/trypsin was removed from the pellet and 1 ml of cold PBS was added to the pellet. The pellet was resuspended in the PBS and spinned at 1100 rpm for 5 minutes. The PBS was removed from the pellet and 1 ml of 70% Ethanol was added to the pellet. The pellet was resuspended in the 70% Ethanol and then was stored at 4ºC until required for FACS.   Samples were run on FACS after propidium iodide (2.5 mg mL-1) was added to the fixed, stained cells prior to analysis. 50,000 gated, total events were scored per study from triplicate studies. Data was analyzed using FACS-express 3 (De Novo software).

CHAPTER 4

RESULTS

4. <u>RESULTS</u>

4.1. TRIB2 protein expression conferred resistance to classical chemotherapeutic modalities.

Previous data from our laboratory demonstrated that the TRIB2 protein negatively regulated FOXO3a. However, the exact mechanism of this resistance remained elusive. Considering that forkhead transcription factors are important effector proteins following chemotherapeutic treatment, we hypothesized that elevated TRIB2 protein expression could confer resistance to a range of chemotherapeutic drugs. To test this hypothesis, we took matched cell lines (with either stable over expressed TRIB2-GFP or shRNA knocked down TRIB2). These cell lines are summarized in my materials and methods (Table 3.1.1, section 3.1, page 22). Prior to examining cell line sensitivity, we confirmed each cell line TRIB2 protein expression level (Figure 4.1.1)
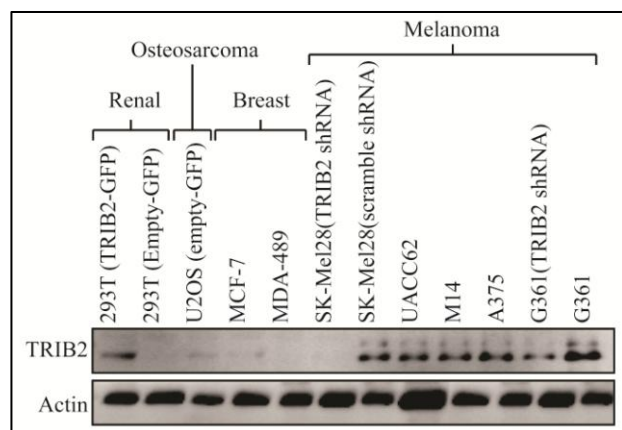
Figure 4.1.1: A representative western blot showing the expression level of TRIB2 and actin in our isogenic cell lines. 50 μg of total protein lysate was loaded per lane and separated on a 10% SDS-PAGE gel.

Having confirmed that our cell lines had matched TRIB2 protein expression levels, we questioned if these isogenic lines show any significant viability difference when exposed to 20 μM dazcarbizine (DTIC), 10 μM gemcitabine (Gem) or 50 μg/ml 5-fluorouracil (5-FU). We note that 72 hours post treatment, cells with increased TRIB2 protein expression were significantly more resistant to each chemotherapy modality that they were exposed to (Figure 4.1.2).
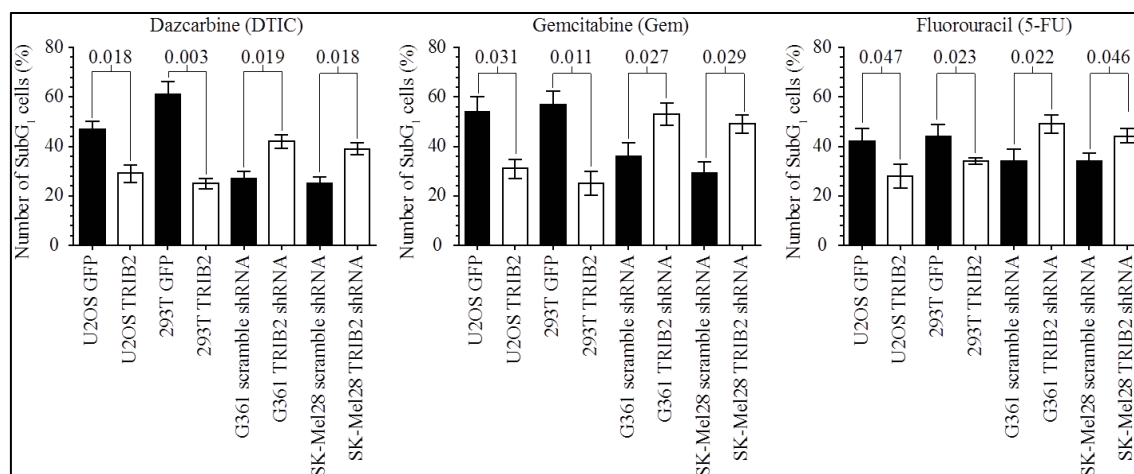
Figure 4.1.2: Cell viability was measured 72 hours post exposure to each indicated chemotherapeutic agent. The percentage of subG$_1$ cells were measured by FACS analysis after 50,000 total events (N=3). *P* values are indicated for each isogenic cell line comparison and error bars are indicative of standard deviation.

Recently, a wide range of PI3K inhibitors have been developed to treat Melanoma and in particular metastatic Melanoma that typically presents an extremely poor clinical prognosis. Considering the highly significant resistance to conventional chemotherapeutic modalities (including the standard Melanoma treatment agent DTIC), we next questioned if TRIB2 status conferred resistance to PI3K inhibitors. One of the most extensively tested agents is the PI3K inhibitor BEZ235 (Novartis) that, in combination with DTIC is the standard treatment regime.

4.2. TRIB2 expression conferred resistance to the PI3K inhibitor BEZ235.

We exposed our isogenic cell lines to 100 nM BEZ235 for 24, 48 and 72 hours. Prior to BEZ235 exposure, there was no significant difference in terms of cell cycle distribution or proliferation rate between each isogenic cell line (data not shown). However, 48 hours post 100 nM BEZ235 treatment we note a number of highly significant differences. In cells that do <u>not</u> over express the TRIB2 protein there is an almost complete loss of the G$_2$ (*4N*) population (white bars in Figure 4.2.1, 4.2.2 and 4.2.3) and a significantly increased sub-G$_1$ population (the black bars shown in Figure 4.2.1, 4.2.2 and 4.2.3).

In contrast, cell lines with increased TRIB2 protein expression display a more distinct G$_1$ population (dark grey bars in Figure 4.2.1, 4.2.2 and 4.2.3). Furthermore the sub-G$_1$ population is significantly lower, indicative of viable cells. Overall these results indicate that the over expression of TRIB2 conferred significant resistance to the PI3K inhibitor BEZ235
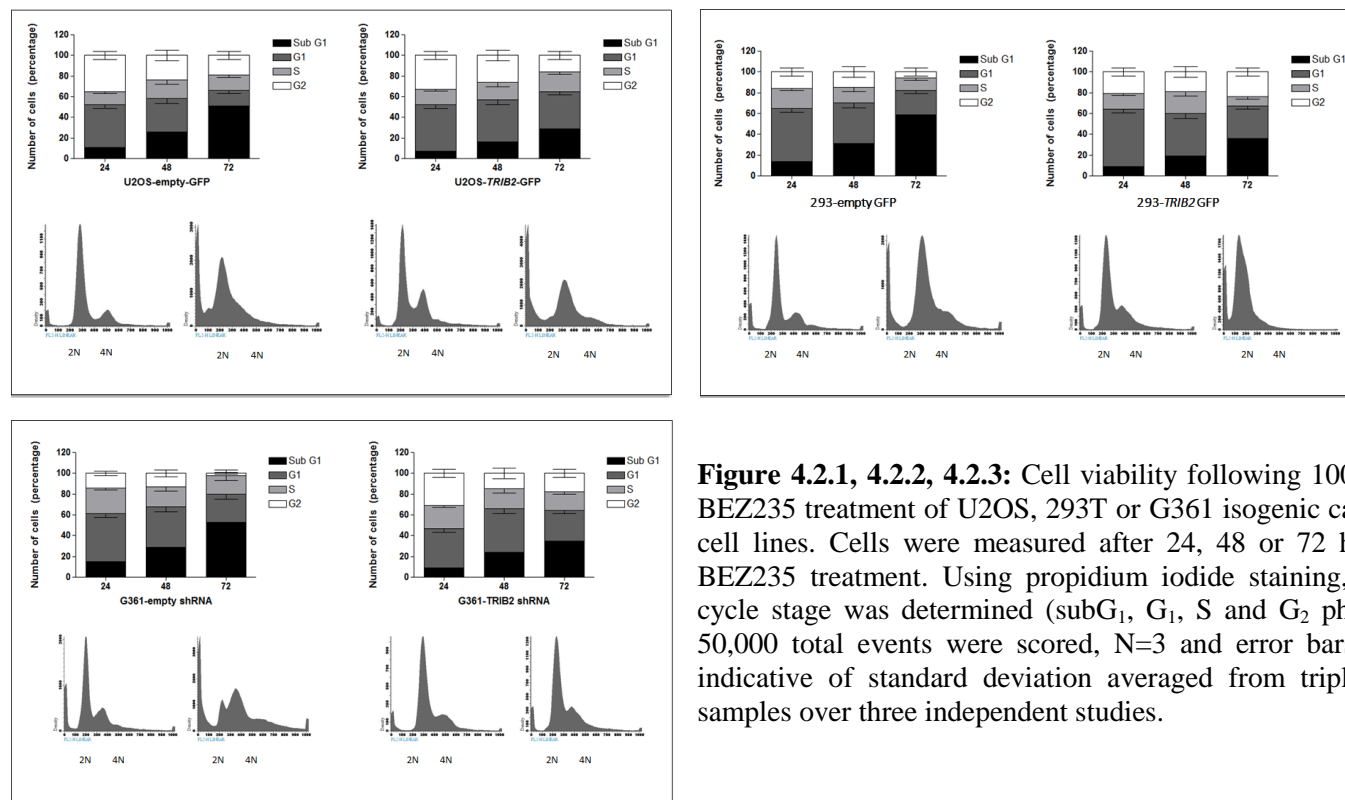
Figure 4.2.1, 4.2.2, 4.2.3: Cell viability following 100 nM BEZ235 treatment of U2OS, 293T or G361 isogenic cancer cell lines. Cells were measured after 24, 48 or 72 hours BEZ235 treatment. Using propidium iodide staining, cell cycle stage was determined (subG$_1$, G$_1$, S and G$_2$ phase). 50,000 total events were scored, N=3 and error bars are indicative of standard deviation averaged from triplicate samples over three independent studies.

4.3. Increased TRIB2 expression significantly attenuates BEZ235 induced apoptosis.

Our data indicated that high TRIB2 protein significantly increased cell line viability (hence a lower subG1 cell population) to both conventional as well as novel chemotherapeutics. However, we do not know if this resistance was due to a reduction in apoptosis (programmed cell death) or more generalized (such as necrosis). To address this question, we treated our U2OS-empty-GFP and U2OS-TRIB2-GFP isogenic cells with 100 nM BEZ or 20 μM DTIC, and evaluated the expression of caspase-3 and cleaved (active) Caspase-3 up to 48 hours post-treatment (Figure 4.3.1).
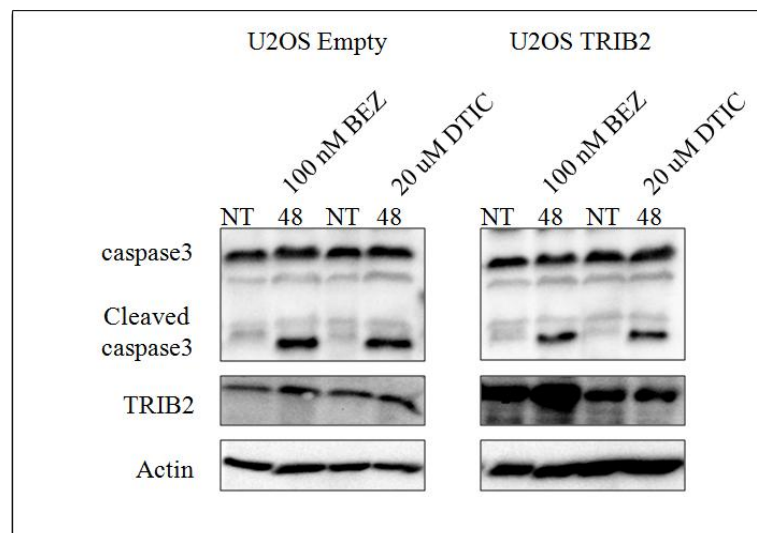
Figure 4.3.1: Representative immunoblots for caspase-3/cleaved Caspase-3, TRIB2 and actin following 100nM BEZ235 or 20 μM DTIC. For each SDS-PAGE gel, 100 μg of total protein was loaded. Antibodies were used as described in the materials and methods section.

In each cell line prior to treatment we observe little to no Caspase-3 cleavage consistent with healthy, non-apoptotic cells. In addition up to 48 hours post treatment (BEZ235 or DTIC) that there was no significant change in the total protein level of Caspase-3 (top band in Figure 4.3.1). However, strikingly 48 hours post BEZ235 or DTIC treatment there was a significant accumulation of cleaved Caspase-3 (indicative of apoptosis induction). Strikingly, in cell lines with increased TRIB2 protein expression, there was reduced Caspase-3 cleavage and therefore less apoptosis (lane 2 and 4 compared to lane 6 and lane 8 in Figure 4.3.1). Taking into account that Caspase-3 cleavage is a critical process in both the classical and non-classical apoptotic cascade, we can conclude, consistent with cell morphology and detachment (observed under the microscope) that TRIB2 over expressing cells are significantly less apoptotic than isogenic cells with low/endogenous TRIB2 protein expression. Strikingly cells that over express TRIB2 show significantly reduced caspase-3 cleavage and that are consistent with the resistance to BEZ treatment (as well as other PI3K inhibitors).

When we examined TRIB2 protein expression, we note a very interesting result. While the total level of TRIB2 protein did not change following DTIC treatment (Figure 4.3.1 middle panel, lane 3-4 and lane 7-8), when cell lines were treated with the PI3K inhibitor BEZ235, the level of total TRIB2 protein significantly increased (Figure 4.3.1, lane 1-2 and lane 5-6). It is tempting to suggest that this increase in independent of *TRIB2* transcription for a number of reasons. In the U2OS-TRIB2-GFP cells, *TRIB2* expression in under the control of a cytomegalovirus (CMV) promoter. Consequently, the transcription rate from this promoter is unlikely to change as it is already a high-expression promoter. We cannot rule out an increase in endogenous *TRIB2* transcription in each cell line although considering that expression is already extremely high in U2OS-TRIB2-GFP cells, it is tempting to hypothesize that this increase in TRIB2 protein expression is independent of transcription and could be the result of post-translational modification(s). This is unexpected result is under intense investigation in our group.

Our results so far have only examined one time point (48 hours) post chemotherapeutic treatment and while we note a striking difference in the amount of Caspase-3 cleavage between U2OS-empty versus U2OS-TRIB2 cells, we wanted to examine Caspase-3 cleavage over more time points (Figure 4.3.2).
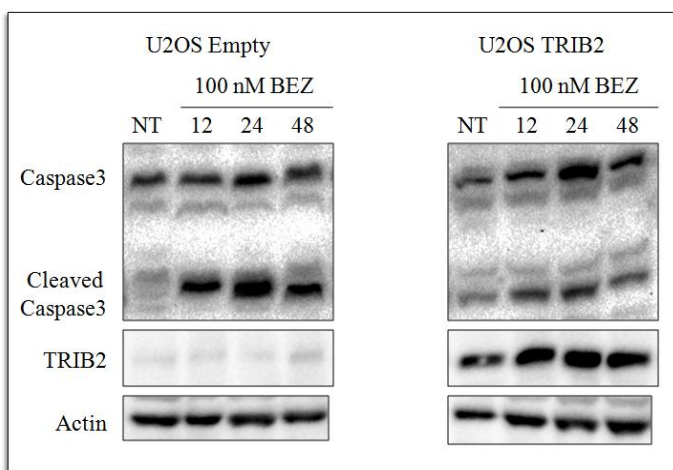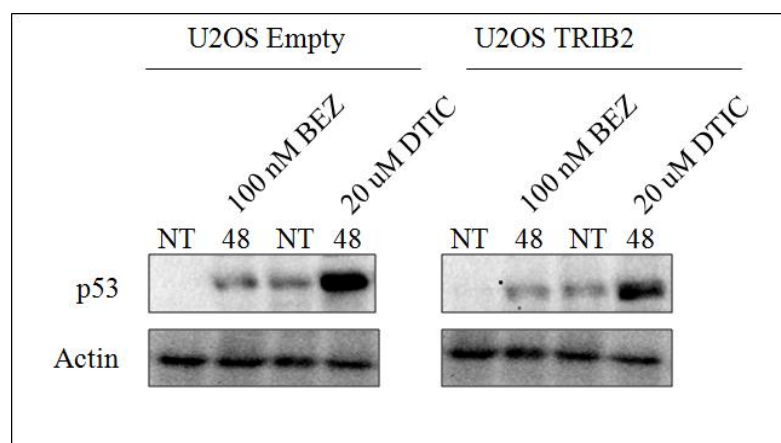
Figure 4.3.2: Representative immunoblots for caspase-3/cleaved Caspase-3, TRIB2 and actin following 100nM BEZ235. For each SDS-PAGE gel, 50 μg of total protein was loaded. Antibodies were used as described in the materials and methods section.

Consistent with our previous Caspase-3 immunoblots, we note no significant difference between the levels of non-cleavage Caspase-3 over time in each cell line. In contrast however (and again consistent with Figure 4.3.1), we note that compared to matched isogenic cells, U2OS-TRIB2 cells show significantly lower Caspase-3 cleavage after BEZ235 exposure. Strikingly, by halving the amount of total protein per lane (50 μg compared to 100 μg) that this difference is even more striking. Furthermore, it is now extremely difficult to detect endogenous TRIB2 protein expression in our U2OS-empty cell line (Figure 4.3.2 lane 2, 3 and 4). We note that in our U2OS-TRIB2 cells, that following BEZ235 exposure that as early as 12 hours post treatment that there was a noticeable increase in the total level of TRIB2 protein (compare Figure 4.3.2 lane 5 versus lane 6). Considering that this increase can be seen as early as 12 hours post-BEZ235 treatment, it supports the hypothesis that the increase is independent of transcription as this is a short time point to consider a transcriptional response. In contrast, a post-translational response increasing the stability of TRIB2 is highly plausible. However, this aspect is still only a hypothesis and significantly more investigation is required at this point. Interestingly, cells treated with the chemotherapeutic DTIC show little to no TRIB2 stabilization after DTIC treatment (Figure 4.3.1). This suggests that the stabilization of TRIB2 (whether a transcritional or post-translational) is PI3K-dependent. These results clearly shows that cell lines with significantly elevated TRIB2 have considerably lower Caspase-3 cleavage and that following PI3K inhibition that TRIB2 protein levels accumulate. Our actin immunoblot confirms an equivalent protein load per lane in our immunoblots.

4.4. In contrast to BEZ235 exposure, DTIC treatment stabilizes p53.

We note that following DTIC or BEZ235 exposure cells that do not over express TRIB2 show significant apoptotic cell death compared to isogenic cells that have high levels of the TRIB2 protein. This is a striking observation as these chemotherapeutic agents have highly divergent mechanisms of action (as described in my introduction). As an alkylating agent, we questioned if the tumour suppressor p53 (a protein that is extremely similar to FOXO3a) was affected following the exposure to DTIC. We also included BEZ235 treatment hypothesizing that p53 would not be affected by PI3K inhibition (Figure 4.4.1).

Figure 4.4.1: Representative immunoblots for total p53 (DO1) and actin following 100nM BEZ235 or 20 μM DTIC exposure. For each SDS-PAGE gel, 50 μg of total protein was loaded. Antibodies were used as described in the materials and methods section.

We note that U2OS-empty cells show a small increase in total p53 up to 48 hours post BEZ235 (100nM) treatment that was not unexpected. U2OS-empty cells show robust induction of apoptosis at this time point (see Figure 4.1.2). Consequently, within this cellular environment, with approximately 30-40% of the cells inducing apoptosis, we would expect a slight accumulation of p53. However strikingly, we note that following DTIC treatment that there was a significant accumulation of p53 (Figure 4.4.1 lane 3-4 and lane 7-8). Furthermore, in cell lines with high TRIB2 protein expression that p53 accumulation was lower compared to matched isogenic cell lines (see Figure 4.4.1 lane 4 versus lane 8). From this result we can conclude that DTIC exposure leads to the robust accumulation of p53, that BEZ235 treatment does not trigger p53 accumulation and that importantly, cell lines with high TRIB2 expression show attenuated p53 accumulation compared to control cells.

4.5. A role for p53?

Based on our results described in 4.4, we hypothesized that DTIC would trigger the subG1 accumulation and apoptosis in a p53-dependent manner. To address this question, we used the Vogelstein isogenic HCT-116 colon cancer cell line with matched p53 status. These cell lines were grown to 70% confluence and treated with 20 µM DTIC or 100 nM BEZ235. At 48 hours post exposure to either agent, cells were analyzed via FACS (Figure 4.5.1).
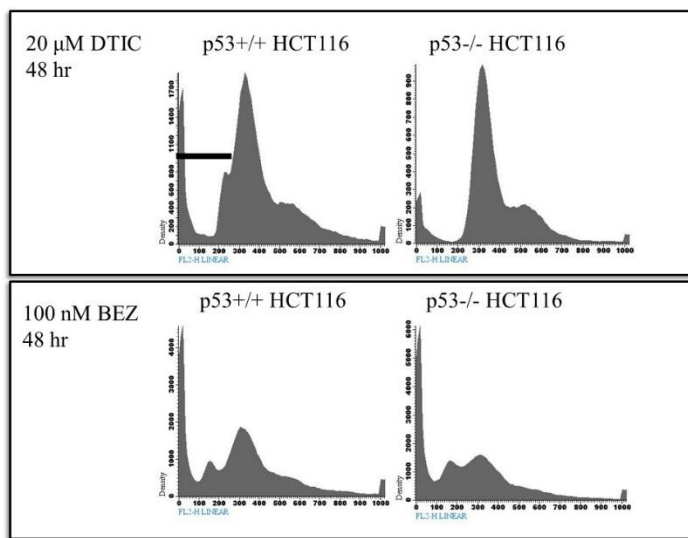
Figure 4.5.1: Representative FACS profiles for $p53^{+/+}$ and $p53^{-/-}$ HCT116 cell viability 48 hours following 20 µM or 100 nM BEZ235 treatment. Using propidium iodide staining, cell cycle stage was determined (subG$_1$, G$_1$ phase, S and G$_2$ phase). 50,000 total events were scored, N=3

As we would have predicted based on our previous immunoblot analysis, we note that $p53^{+/+}$ cells are highly sensitive to DTIC treatment (Figure 4.5.1 top left FACS plot). In contrast, $p53^{-/-}$ HCT-116 cells are extremely resistant to DTIC (Figure 4.5.1 top right FACS plot). In contrast, BEZ235 treatment induced significant cell death/subG$_1$ accumulation in a p53-independent manner (Figure 4.5.1 bottom left and bottom right FACS plots). The most striking aspect of the data we have accumulated suggests that increased TRIB2 protein expression confers resistance to both DTIC (a p53-dependent chemotherapeutic) and BEZ235 (a PI3K inhibitor and likely FOXO3a-dependent chemotherapeutic).

As a negative regulator of FOXO3a, our data unexpectedly raised the hypothesis that TRIB2 could confer resistance to p53-dependent chemotherapeutics. To investigate this further we carried out immunoblotting for total p53 and the E3-ubiquitin ligase (and negative regulator of p53) mouse double minute 2 homolog (MDM2) in our isogenic U2OS cell lines (Figure 4.5.2).
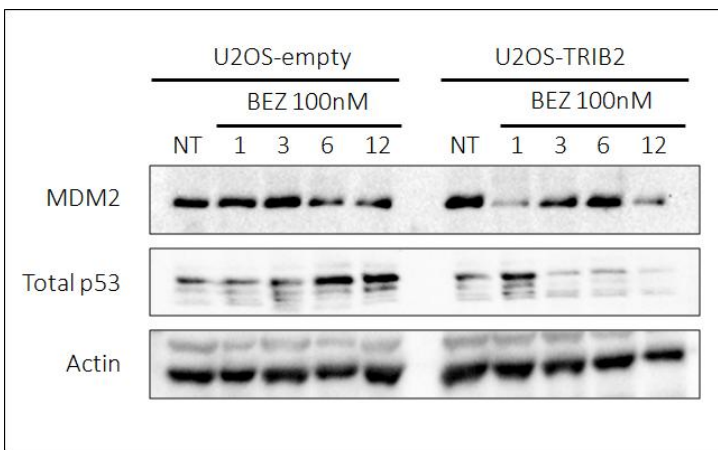
**Figure 4.5.2:** Representative immunoblots for MDM2, total p53 (DO1) and actin following 100nM BEZ235 exposure. For each SDS-PAGE gel, 100 μg of total protein was loaded. Antibodies were used as described in the materials and methods section.

First we note that incontrast to U2OS-empty cells that U2OS-TRIB2 cells have a slightly higher level of MDM2 under non-treatment conditions (Figure 4.5.2. lane 1 compared to lane 6). Second, following BEZ exposure, U2OS-empty cells show a steady reduction in MDM2 protein levels (Figure 4.5.2 lane 2-5). Unexpectedly, U2OS-TRIB2 cells show a rapid decrease in MDM2 protein expression and then a rapid rise in MDM2 protein level, oscillating up and down. As we would predict, U2OS-empty cells show a steady increase in total p53 level consistent with MDM2 levels decreasing (Figure 4.5.2, middle panel, lanes 2-5). Strikingly, while U2OS-TRIB2 cells have p53, the accumulation of total p53 is significantly attenuated (Figure 4.5.2 lane 5 versus lane 10). We note that U2OS-empty cells show a gradual increase in total p53 up to 12 hours post BEZ treatment. In contrast, U2OS-TRIB2 cells show a significantly lower level of p53 protein under non-treated conditions, an initial increase 60 minutes post BEZ exposure and then a noticeable decrease up to 12 hours post BEZ incubation. Strikingly, the exact opposite trend was observed for MDM2 raising the hypothesis that in cells which over express TRIB2, the p53/MDM2 regulatory balance is disrupted.

4.6. TRIB2 and MDM2 interaction.

The next question we asked after observing the deregulated p53/mDM2 axis in TRIB2 over expressing cells was if TRIB2 and MDM2 could interact. This question is particularly important as very little is known regarding TRIB2 protein regulation although it has been reported that TRIB2 can be regulated by ubiquitination[66,67]. We carried out co-immunoprecipitation (co-IP) assays 12 hours post 100 nM BEZ235 treatment or after mock-drug treatment in our isogenic U2OS cell line model, asking if TRIB2 would interact with MDM2, AKT or FOXO3a (Figure 4.6.1).
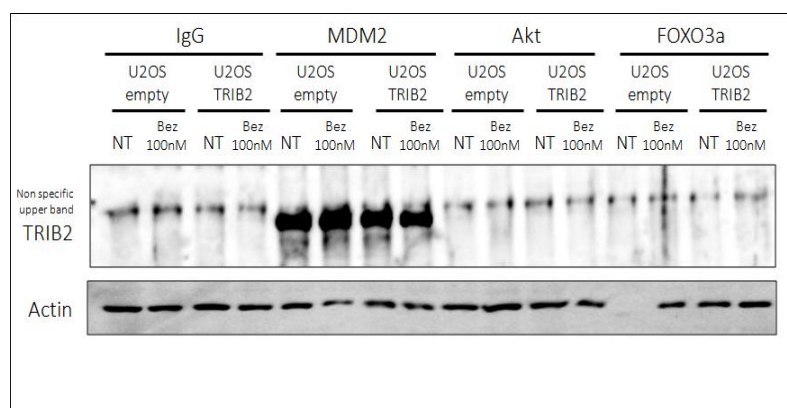
Figure 4.6.1: SDS-PAGE gel following IgG, MDM2, AKT or FOXO3a co-IP. Captured lysates were probed for TRIB2. 500 μg of total protein was captured per sample and run in each lane. 25 μg of total protein lysate was run on a separate SDS-PAGE gel and probed for actin to ensure equivalent protein loading N=3.

Our co-IP studies indicate that TRIB2 and MDM2 interact, raising the hypothesis that MDM2 could, in principle regulate TRIB2. Overall, this result indicates that the TRIB2 and MDM2 interact and that the overexpression of TRIB2 perturbs the p53/MDM2 regulatory balance. This supports our previous data where unexpectedly, TRIB2 over expression confers cell line resistance to chemotherapeutics that induce p53-dependent apoptosis (including gemcitabine and 5-FU).

4.7. TRIB2 Expression and Stress Signaling.

So far, our data indicates that DTIC induces a potent p53-dependent apoptotic response in contrast to BEZ235 that causes cell death independently of p53. This raised two questions, specifically "*how does BEZ235 induce cell death?*" and "*would these drugs in combination significantly increase cell death?*" To address these questions we used our isogenic U2OS and 293T cell lines. Each cell line was treated with either 100 nM BEZ235, 20 μM DTIC or both chemotherapeutics (representative of the combinational therapy used to treat malignant Melanoma) for 48 hours. Following this drug treatment, total cell lysates were collected and immunoblot analysis conducted for a number of key signaling proteins and downstream effector proteins from these signaling networks (Figure 4.7.1).
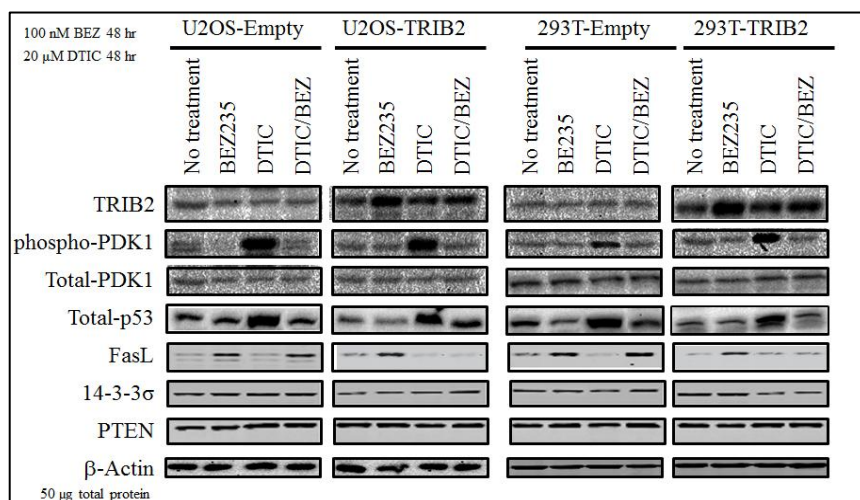
Figure 4.7.1: Representative immunoblots for each indicated protein after 100nM BEZ235 or 20 μM DTIC exposure. 50 μg of total protein was loaded per lane. Antibodies were used as described in the materials and methods section.

We initially investigated the protein expression levels for TRIB2, total-PDK1, phospho-PDK1, PDK1, total p53, FasL, 14-3-3σ, PTEN and β-Actin in our matched U2OS and 293T cell lines. These proteins are key components of the PI3K and PI3KK signaling networks. In particular PDK1 and PTEN being key members of the AKT signaling cascade, p53 (as the "*guardian of the genome*"), FasL (as a critical effector protein of the pro-apoptotic FOXO cascade) and 14-3-3σ (a protein regulated by p53, directing cell cycle arrest and regulating FOXO localization).

We note that in cell lines with low TRIB2 protein expression that BEZ235 exposure triggered the robust accumulation of FasL, a FOXO3a regulated gene. In contrast, DTIC did not induce any significant amount of FasL. Furthermore, BEZ235 exposure induced the de-phosphorylaion of PDK1, indicative of inhibiting PI3K signaling. As we would predict, DTIC treatment had no effect on PDK-1 phosphorylation indicating that the PI3K signaling pathway remains active in the presence of DTIC. PTEN protein expression remained constant regardless of chemotherapeutic exposure while 14-3-3σ protein expression also did not significantly change. When we look at these pathways in cells with increased TRIB2 expression, we see a striking observation; BEZ235 and dual DTIC/BEZ treated cells do not induce significant amounts of FasL, consistent with a lower overall sensitivity to these chemotherapies. This observation is very apparent in dual treated cells and while the lower protein accumulation is not as clear-cut in BEZ235 only TRIB2 over expressing cells, the accumulation of FasL is lower in both U2OS-TRIB2 and 293T-TRIB2 cells compared to their matched controls. This result implied that the high level of TRIB2 was affecting at least FasL protein expression, consistent with our previously published work showing TRIB2-dependent inhibition of FOXO3a[59]. Interestingly, our immunoblots for p53 also indicate that in high TRIB2 expressing cells that there is a slightly lower accumulation of p53 following DTIC treatment.

4.8. Implicating AKT and FOXO.

Based on our initial screen in Figure 4.7.1, we noticed that following BEZ235 and dual BEZ235/DTIC treatment that there was reduced (or ablated) FasL expression. As *FasL* is regulated by FOXO3a and is a critical effector protein of apoptosis, we questioned if other components of the PI3K network were affected by TRIB2 status and was contributing to resistance to BEZ235. To address these questions, we treated our matched U2OS cells with 100 nM BEZ235 and via immunoblotting, examined key components of the AKT signaling cascade (Figure 4.8.1).
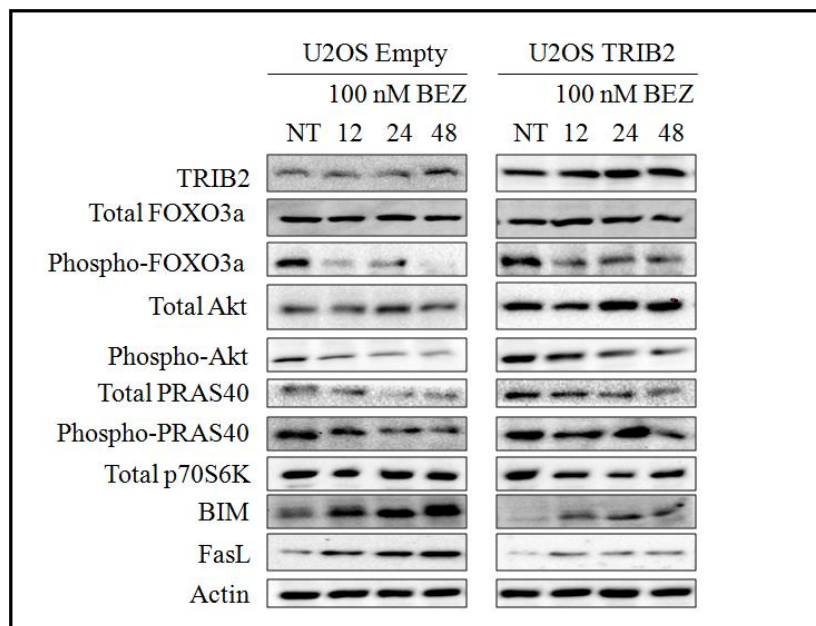
Figure 4.8.1: Representative immunoblots for each indicated protein after 100nM BEZ235 exposure. 50 μg of total protein was loaded per lane. Antibodies were used and bands visualized as described in the materials and methods section.

After conducting this protein expression and modification screen we note a number of important observations. First, consistent with the data we have shown previously, following BEZ235 exposure, the TRIB2 protein level accumulates (Figure 4.8.1 top panel). This is noticeable in both U2OS-empty cells (that have low TRIB2 protein expression) and in U2OS-TRIB2 cells (that have extremely high TRIB2 protein levels). Second, we note that regardless of TRIB2 status and irrespective of BEZ235 presence/absence that the total level of FOXO3a does not change (Figure 4.8.1 panel two). In contrast however we note that there are significant differences regarding phosphorylated FOXO3a (Figure 4.8.1 panel 3). In our U2OS-empty cells, treatment wth BEZ235 induced the rapid de-phosphorylation of FOXO3a (ser253) consistent with the inhibition of AKT. Strikingly, in the U2OS-TRIB2 cell line, there was a significantly higher level of ser253-FOXO3a in non-treated cells (Figure 4.8.1 panel 3, compare lane 1 and lane 5). Furthermore, despite the robust inhibition of AKT, in U2OS-TRIB2 cells, at 12, 24 and 48 hours post BEZ235 treatment, there is still high levels of ser253 phosphorylated FOXO3a. In U2OS-empty cells FOXO3a phosphorylation is completely ablated at 48 hours. Concomitant to this observation, we note the same pattern regarding AKT with an even more prominent profile; the level of both total AKT and ser473 phosphorylated AKT is significantly higher in U2OS-TRIB2 cells compared to their matched empty control cells (Figure 4.8.1 panel 4 and 5). The same profile was noted for total and phosphorylated PRAS40 (Figure 4.8.1 panel 6 and panel 7). In contrast, there was no significant protein expression change regarding total p70S6K. Unfortunately at the time of writing, our lab has not received the phosphorylated p70S6K antibody. Finally we examined the expression of the key FOXO3a regulated proteins BIM and FasL (Figure 4.8.1 panel 9 and panel 10). We would hypothesize a similar expression profile to FOXO3a and PRAS40 as p70S6K is downstream target of

AKT. Based on these results, we can conclude that increased TRIB2 protein expression directly or indirectly increases and activates the AKT cascade. As a result, FOXO3a mediated cell cycle arrest and apoptosis following chemotherapeutic treatment (BEZ235) is significantly attenuated.

In order to address this aspect further, we questioned what the cellular phenotype would be if we stably knocked FOXO3a expression down in both our U2OS-empty and U2OS-TRIB2 cell lines. We developed four different FOXO3a knockdown constructs and transfected these into our cell lines. Following transfection, they were selected and analyzed for FOXO3a knock down efficiency (Figure 4.8.2).
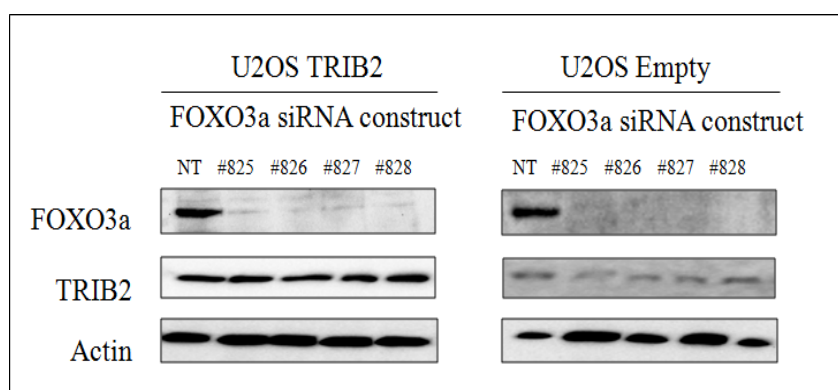
Figure 4.8.2: Immunoblots for FOXO3a and TRIB2 after transfection of FOXO3a shRNA constructs. 100 μg of total protein was loaded per lane. Antibodies used are described in the materials and methods section.

We note that each of our four FOXO3ashRNA expression constructs ablated FOXO3a protein expression. The stable knockdown of FOXO3a had no effect regarding the total level of TRIB2 in either our U2OS-TRIB2 or U2OS-empty cell lines.

After generating a range of isogenic cell lines with FOXO3a knocked down with either high or low (endogenous) TRIB2 protein expression, we exposed these cell lines to 100 nM BEZ235 for up to 72 hours (similarly to the data shown in Figure 4.2.1, 4.2.2 and 4.2.3).
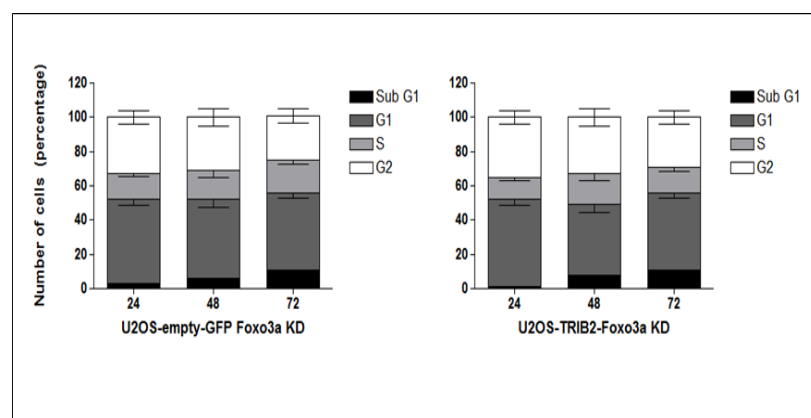
Figure 4.8.3: Cell viability following 100 nM BEZ235 treatment of U2OS-empty-FOXO3aKD or U2OS-TRIB2-FOXO3aKD cancer cells. Viability and cell cycle distribution was measured 24, 48 or 72 hours post BEZ235 treatment. Using propidium iodide staining, cell cycle stage was determined (subG$_1$, G$_1$, S and G$_2$ phase). 50,000 total events were scored, N=3 and error bars are indicative of standard deviation averaged from triplicate samples over three independent studies. Construct #826 was used for these studies but the same data was noted for each of the other constructs.

Our previous data (shown in section 4.2) demonstrated that TRIB2 significantly increased cell line resistance to BEZ235. We note that when FOXO3a is stably knocked down that there is significantly increased cell line resistance to BEZ235 independent of TRIB2 status. Second, the knockdown of FOXO3a had no effect at all regarding cell cycle distribution in either U2OS-empty or U2OS-TRIB2 cells. Third both cell lines with FOXO3a knocked down are significantly more resistant to BEZ235 treatment than either the U2OS-empty or U2OS-TRIB2 cell lines. This indicates that BEZ235-mediated cell death is principally via FOXO3a. The data that we have presented at this stage suggest that TRIB2-dependent negative regulation of FOXO3a previously reported, rather than being direct, could be via the cellular master switch AKT.

4.9. TRIB2 protein expression in primary clinical samples.

All the results described previously were obtained from in *in-vitro* samples. We wanted to consider our findings in a clinical context. We initially obtained primary, colon and pancreatic patient samples. We extracted the total RNA and protein from these *ex vivo* samples. First of all we determined TRIB2 protein expression in our colon and pancreatic samples (Figure 4.9.1). Note that for each patient, the normal sample, is matched patient control tissue.
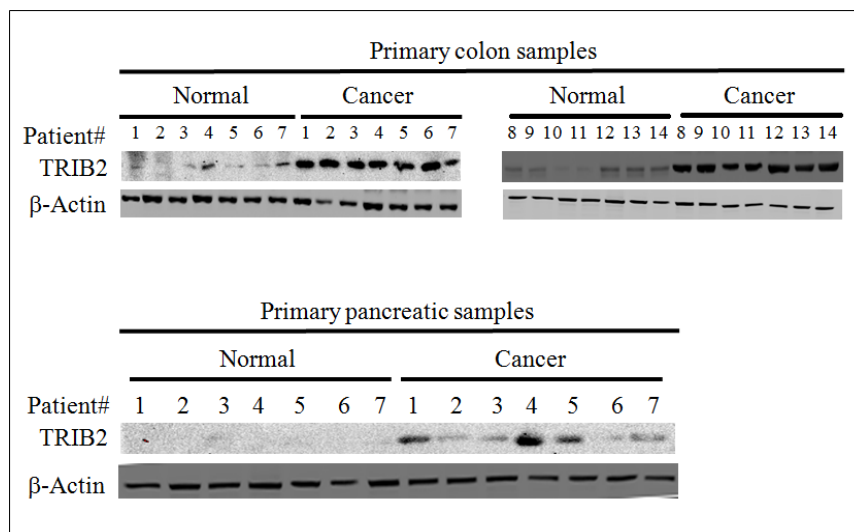
Figure 4.9.1: Immunoblots for TRIB2 and actin in our primary *ex vivo* clinical samples. 100 μg of total protein was loaded per lane. Antibodies used are described in the materials and methods section.

Strikingly we note that in both colon and pancreatic patient samples that there was noticeably higher TRIB2 protein expression, suggesting that the protein over expression of TRIB2 is a feature of these cancers.

Having noted the significant over expression of TRIB2 in these colon and pancreatic cancer samples, we wanted to broaden this investigation to include primary Melanoma samples and examine if we see the TRIB2-dependent deregulation of the FOXO3a/p53 network. We obtained a range of primary metastatic Melanoma samples that have been extensive clinical history, including patient outcome (complete response,

stable disease or progressive disease). We processed these samples for total RNA and protein. Having obtained the total protein, we questioned if there was significantly higher TRIB2 expression (Figure 4.9.2).
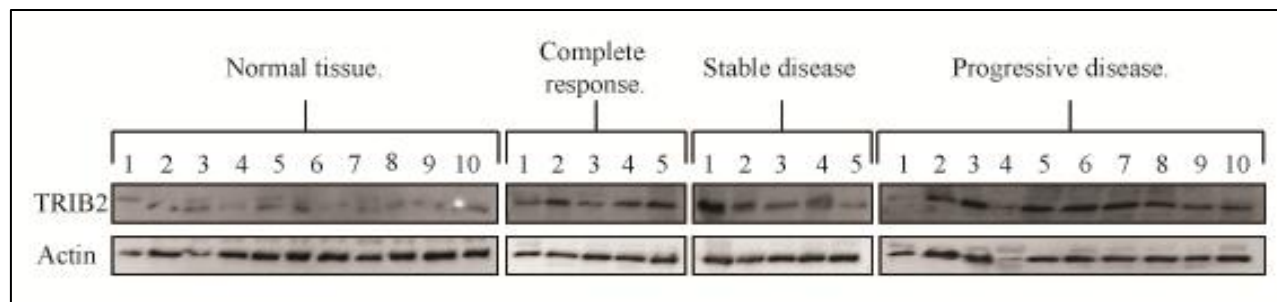

Figure 4.9.2: Immunoblots for TRIB2 and actin in our primary *ex vivo* Melanoma clinical samples. 100 μg of total protein was loaded per lane. Antibodies used are described in the materials and methods section.

Similar to primary colon and pancreatic cancer samples, we note that in the Melanoma samples (complete response, stable disease and progressive disease samples) that TRIB2 protein expression was significantly higher than normal tissue samples. In contrast to our primary colon and pancreatic cancer samples, the normal tissue samples are not matched (i.e. normal tissue sample #1 and complete response sample #1 are not from the same patient). Overall, metastatic Melanoma patients have significantly higher TRIB2 protein compared to non-cancerous skin tissue from healthy donors.

As a logical follow up to our studies shown in Figure 4.9.2, we questioned if in these primary samples, there was deregulated AKT/FOXO3a/p53 networks. We analyzed the protein expression for key components of these pathways in a similar manner to our *in vitro* studies shown in 4.7 and 4.8). The protein expression analysis is shown on the next page in Figure 4.9.3.
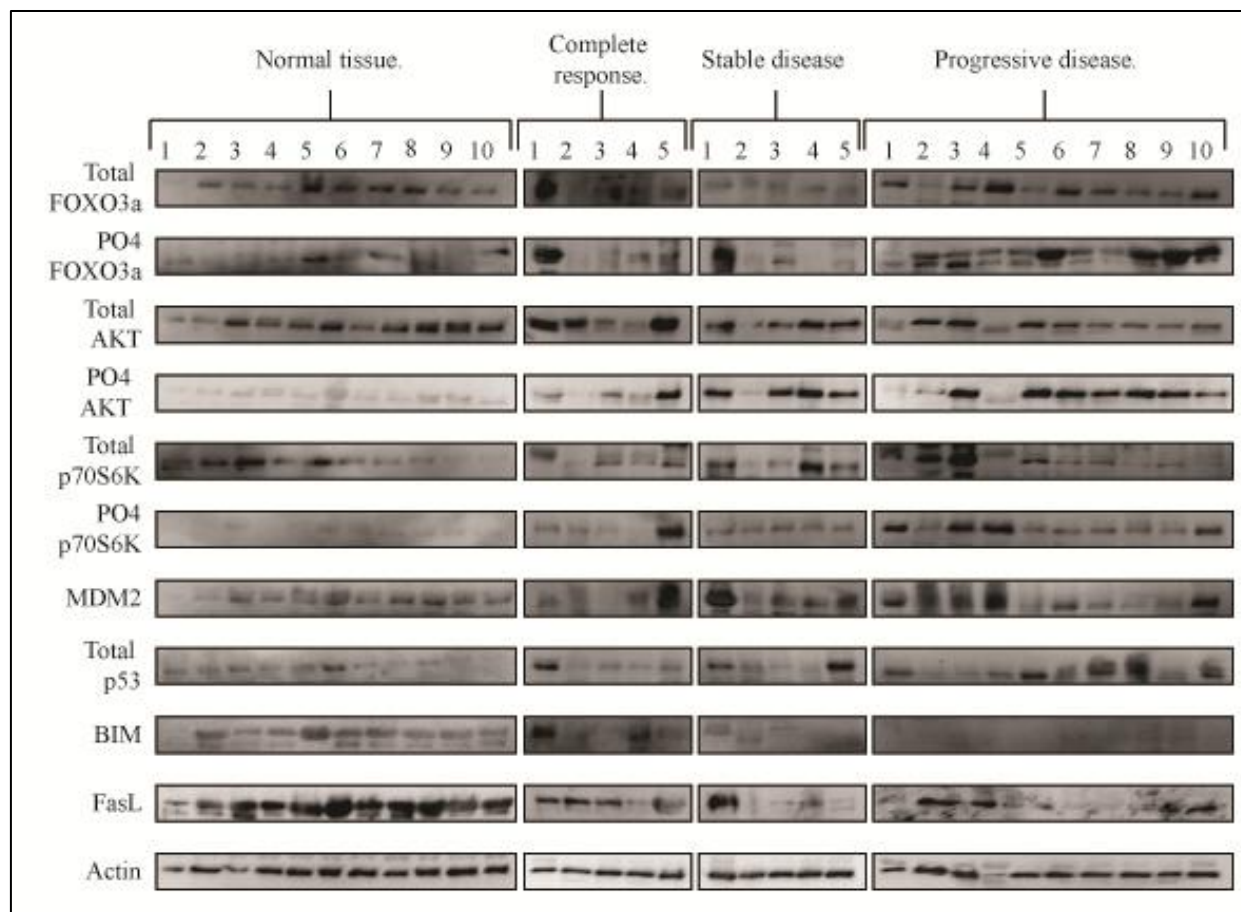
Figure 4.9.3: Immunoblots for each indicated protein and actin (from figure 4.9.2) in our primary *ex vivo* Melanoma clinical samples. 100 μg of total protein was loaded per lane. Antibodies used are described in the materials and methods section.

Strikingly, in support of our *in vitro* observations, we see that Melanoma clinical samples have significantly higher levels of ser473 phosphorylated AKT in each Melanoma sample and that there is a concomitant increase in the level of phosphorylated FOXO3a, phosphorylated p70S6K. Furthermore, there is the suppression of both Bim and FasL protein expression in metastatic Melanoma samples whereas these proteins can be robustly detected in the normal tissue samples. Strkingly MDM2 protein expression is significantly higher in metastatic Melanoma samples (Figure 4.9.3 panel 7). AKT is known to activate MDM2 and thus can suppress the p53-response to chemotherapeutics. Interestingly, we note that the level of total p53 in the clinical samples (particularly the progressive disease samples) was higher than normal, complete response or stable disease lanes (Figure 4.9.3, panel 8). There are a number of reasons for this that are considered in more detail in the discussion, including tumour heterogeneity, hypoxic regions, normal cell infiltration as well as potential p53 function(s). Overall there is very good correlation between our *in vitro* results shown and to our clinical studies.

CHAPTER 5

DISCUSSION AND CONCLUSION

5.   DISCUSSION AND CONCLUSION

Melanoma is one of the deadliest types of cancer that is due to late disease diagnosis and the lack of effective treatments once diagnosed at this stage. In addition to the lack of effective diagnostic tools, another major issue within the Melanoma field is the high molecular heterogeneity within Melanoma patients (and all cancers in general) compared to Melanoma cell lines. This results in a significant barrier for the effective development and testing of novel therapies and drug prior to their testing within the clinic, or indeed their successful testing within the laboratory (*in vitro* and *in vivo*) before failing in clinical trial.

Previous work within our group indicated that there was increased expression of TRIB2 in malignant Melanoma (and suggested a pathogenic role in this type of cancer) and recent findings by our group and others has highlighted that a significant obstacle in the effective treatment of cancer is the over expression of the protein TRIB2 within tumors. How TRIB2 can direct this chemo-resistance is unknown although some of the work presented here has begun to address this important issue.

In this project investigation we show that TRIB2 over expressing cells show clearly less caspase-3 cleavage and are phenotypically characterized by a significantly reduced Sub-G1 population of cells following BEZ treatment compared to matched non-TRIB2 over expressing cells. Remarkably, our FACS analysis demonstrated that prior to BEZ exposure, there was no significant difference between all of TRIB2 over expressing cells and our empty vector control cells. This results suggesting that the TRIB2 phenotype we have observed is independent of the cell cycle. In addition, we demonstrate that the BEZ treatment of TRIB2 over expressing cells resulted in an increase in the total level of TRIB2 protein.

Another stimulating result was the fact that cells treated with the chemotherapeutic DTIC exhibited that TRIB2 is not stabilized after chemotherapeutic treatment. Oppositely, in cells treated with BEZ235 we note that TRIB2 levels were stabilized after treated with this PI3K inhibitor. These results let us conclude that TRIB2 conferred resistance to chemotherapeutics like DTIC, one of the most chemotherapeutics used nowadays in the treatment against Melanoma. This deductions show that the over expression of TRIB2 has no effect on the cell cycle, and promotes resistance to chemotherapy by the inhibition of PI3K, a key regulator of the transcription factor FOXO3a. Our evidence indicates that cells that over express TRIB2, following BEZ235 treatment has a significantly lower accumulation of both Bim and Fas-L (two key pro-apoptotic proteins regulated by FOXO3a) compared to our matched control cell line.

We confirmed in our cell line models that BEZ235 was functioning precisely, examining the expression and post-translational modifications of key proteins regulated by PI3K. BEZ235 treatment directed the loss of phosphorylated AKT, causing its inactivation, and since FOXO3a is a downstream target

of AKT, we note FOXO3a activation. This suggests that TRIB2 confers resistance to BEZ through the inhibition of FOXO3a mediated pro-apoptotic gene expression.

Since p53 and FOXO3a are similar transcription factors controlling the same processes and the importance of p53 in many types of human cancer, we interrogated if TRIB2 and BEZ235 impacted the p53 pathway. Therefore, p53 and MDM2 (the negative regulator of p53) were tested. We prove that in our non-over expressing TRIB2 cell line, that there is an increase in the accumulation of p53, while TRIB2 cells display a deregulated p53 response, characterized by significantly elevated MDM2 and reduced overall p53. These results permit us to say that the PI3K inhibitor BEZ235 only has a insignificant effect on p53 and, in contrast, the chemotherapeutic DTIC induces p53. Once more, this highlights that the over expression of TRIB2 could promote chemo-resistance.

All the results above were performed in *in-vitro* samples. Considering that our laboratory had access to Melanoma *ex-vivo* samples, we carried an immunoblotting with those samples for TRIB2 and β-Actin. We note that primary colon samples and primary pancreatic samples cells shows higher levels of TRIB2 then the Normal ones, respectively. All of the Normal and the Cancer cells of both kinds of samples express β-Actin. The over expression of TRIB2 in Melanoma cell lines was evident by our immunoblotting analysis compared to other cancer cell lines. Further, TRIB2 expression was analyzed in several *ex-vivo* tissue samples comparing the expression between normal and Melanoma tissue, which significantly supported our *in vitro* results. We observed some minor variation between normal and Melanoma clinical samples when we searched for total AKT with the Melanoma samples showing slighter higher levels compared to normal tissues. In contrast, Melanoma patient samples showed significantly greater levels of phosphorylated-AKT compared to normal samples.

Consistent with this activated AKT pathway, we note the significantly higher level of phosphorylated-FOXO3a. We also note that one of our normal samples showed highly phosphorylated FOXO3a. Consistent with this, we observe significantly higher protein levels of FasL and BIM in normal samples. Identical to AKT, we also note the elevated level of phosphorylated p70S6K in Melanoma samples. This could be due to cancer cells needing to evade apoptosis and constitutively drive cell division, particularly in the late stage of disease.

Finally, based on these results, we propose two mechanisms as a result of this investigation: (Figure 5.1) without TRIB2 over expression – PI3K inhibition and (Figure 5.2) following TRIB2 over expression.
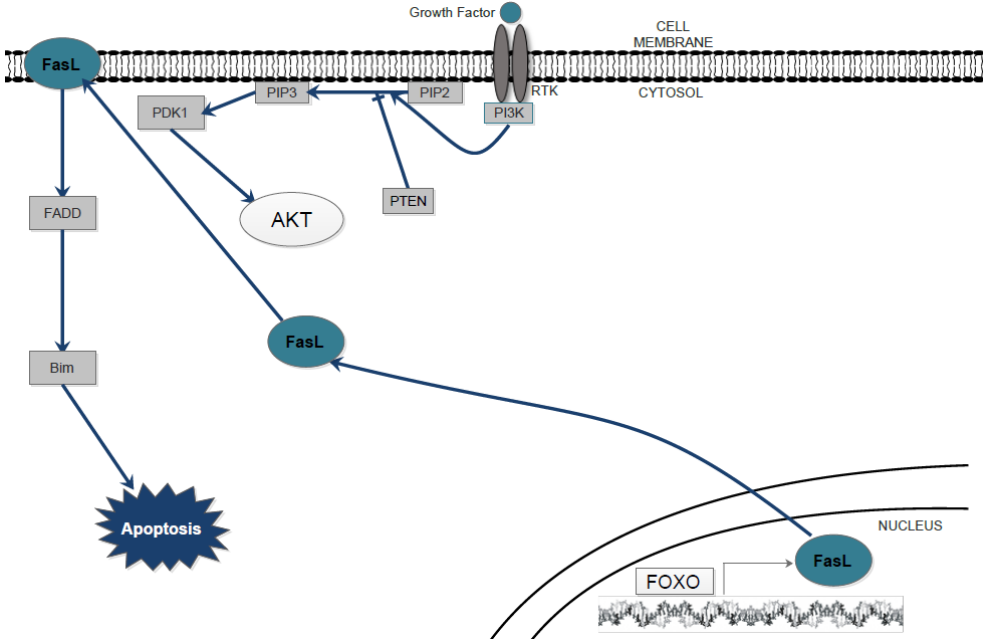
Figure 5.1: Proposed mechanism for the PTEN/PI3K/AKT pathway, without TRIB2 over expression, due to PI3K inhibition.
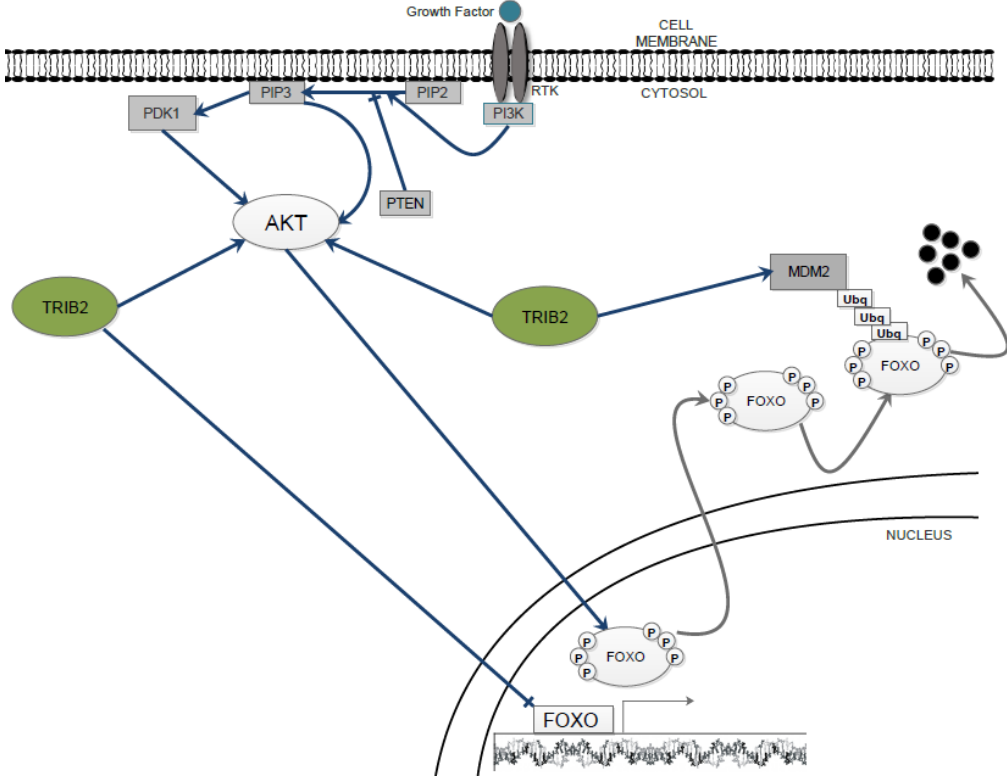
Figure 5.2: Proposed mechanism for the PTEN/PI3K/AKT pathway, with TRIB2 over expression and, consequently, the phosphorilation of FOXO.

5.1. Future Directions.

There are numerous experimentations that could be performed to corroborate these findings. We will expand our studies in order to investigate more PI3K inhibitors, testing more potent and newly developed compounds, and in order to understand thoroughly how TRIB2 is regulated. Considering that, currently, we have data which demonstrate that TRIB2 is stabilized through PI3K inhibition, in the future the direction of our investigation will be in order to study the protein stabilization of TRIB2 and its mRNA's half life. Additionally, we want to study if and how the TRIB2 is degraded in the proteossome. This is very interesting because the TRIB2 binds to an E3 ubiquitin ligase, which is an enzyme that targets specific protein substrates for degradation by the proteossome.

On the other hand, we want to investigate more and profoundly how the TRIB2 affects the AKT pathway and signaling. In order to do that, we will have to study different pathways, like the PI3K and the mTOR pathways, and to study if TRIB2 affects AKT directly and/or it acts by deregulating PTEN. The clarification of how TRIB2 affects the AKT pathway will bring, hopefully, answers that will allow us to investigate novel therapies in order to overcome drug resistance. The main objectives from now on will be investigate: novel therapeutic methods to overcome drug-resistance, personalized methods of predicting when patients would benefit most from treatment with PI3K/AKT pathway inhibitors and the optimization of treatments and clinical trial design by the differentiation of patients in terms of drug effectiveness for disease treatment

Another line of investigation that also need to be expanded, in order to allow us understand how it happens, is the deregulated promoter recruitment displayed by FOXO3a and p53. This is extremely interesting for our group and will continue being very studied in our lab. Our work will also be expanded to include additional Melanoma cell lines and to evaluate FOXO3a and p53 promoter binding from *ex vivo* clinical samples. Thus, further investigation into the role of TRIB2 in the pathogenesis of Melanoma lesions may provide new therapeutic insights into this most aggressive form of skin cancer resistant to all standard anticancer therapies.

CHAPTER 6

REFERENCES

6. <u>REFERENCES</u>

1. Hanahan, D. & Weinberg, R. a. Hallmarks of cancer: The next generation. *Cell* **144,** 646–674 (2011).

2. Vogelstein, B. & Kinzler, K. W. Cancer genes and the pathways they control. *Nat. Med.* **10,** 789–99 (2004).

3. Macaluso, M., Paggi, M. G. & Giordano, A. Genetic and epigenetic alterations as hallmarks of the intricate road to cancer. *Oncogene* **22,** 6472–6478 (2003).

4. Hanahan, D., Weinberg, R. A. & Francisco, S. The Hallmarks of Cancer. *Cell* **100,** 57–70 (2000).

5. Bello, D. M., Ariyan, C. E. & Carvajal, R. D. Melanoma mutagenesis and aberrant cell signaling. *Cancer Control* **20,** 261–281 (2013).

6. Tuong, W., Cheng, L. S. & Armstrong, A. W. Melanoma: Epidemiology, Diagnosis, Treatment, and Outcomes. *Dermatologic Clinics* **30,** 113–124 (2012).

7. Tucker, M. A. Melanoma Epidemiology. *Hematology/Oncology Clinics of North America* **23,** 383–395 (2009).

8. Russo, A. E. *et al.* Melanoma: Molecular pathogenesis and emerging target therapies (review). *International Journal of Oncology* **34,** 1481–1489 (2009).

9. Madhunapantula, S. V, Mosca, P. J. & Robertson, G. P. The Akt signaling pathway: an emerging therapeutic target in malignant melanoma. *Cancer Biol. Ther.* **12,** 1032–1049 (2011).

10. Garbe, C. & Leiter, U. Melanoma epidemiology and trends. *Clin. Dermatol.* **27,** 3–9 (2009).

11. Cho, Y. R. & Chiang, M. P. Epidemiology, Staging (New System), and Prognosis of Cutaneous Melanoma. *Clinics in Plastic Surgery* **37,** 47–53 (2010).

12. Mohr, P., Eggermont, A. M. M., Hauschild, A. & Buzaid, A. Staging of cutaneous melanoma. *Ann. Oncol.* **20,** (2009).

13. Kim, C. J., Reintgen, D. S. & Balch, C. M. The new melanoma staging system. *Cancer Control* **9,** 9–15 (2002).

14. Atallah, E. & Flaherty, L. Treatment of metastatic malignant melanoma. *Curr.Treat.Options.Oncol.* **6,** 185–193 (2005).

15. Bhatia, S., Tykodi, S. S. & Thompson, J. A. Treatment of metastatic melanoma: an overview. *Oncology (Williston Park).* **23,** 488–496 (2009).

16. Rager, E. L., Bridgeford, E. P. & Ollila, D. W. Cutaneous melanoma: Update on prevention, screening, diagnosis, and treatment. *American Family Physician* **72,** 269–276 (2005).

17. Young, A. M., Marsden, J., Goodman, A., Burton, A. & Dunn, J. A. *Prospective randomized comparison of dacarbazine (DTIC) versus DTIC plus interferon-alpha (IFN-alpha) in metastatic melanoma. Clinical oncology (Royal College of Radiologists (Great Britain))* **13,** 458–465 (2001).

18. Tsao, H., Chin, L., Garraway, L. A. & Fisher, D. E. Melanoma: From mutations to medicine. *Genes and Development* **26,** 1131–1155 (2012).

19. K., K. *et al.* Long term safety and efficacy of vemurafenib in the treatment of BRAFV600-mutant advanced melanoma (BRIM-2 study update). *Pigment Cell and Melanoma Research* **25,** 866 (2012).

20. Polak, M. E. *et al.* Mechanisms of local immunosuppression in cutaneous melanoma. *Br. J. Cancer* **96,** 1879–1887 (2007).

21. Tarhini, A. A. & Agarwala, S. S. Interleukin-2 for the treatment of melanoma. *Curr. Opin. Investig. Drugs* **6,** 1234–1239 (2005).

22. Eklund, J. W. & Kuzel, T. M. A review of recent findings involving interleukin-2-based cancer therapy. *Curr. Opin. Oncol.* **16,** 542–546 (2004).

23. Lipson, E. J. & Drake, C. G. Ipilimumab: An anti-CTLA-4 antibody for metastatic melanoma. *Clinical Cancer Research* **17,** 6958–6962 (2011).

24. Arlo J. Miller, M.D., Ph.D., and Martin C. Mihm, Jr., M. D. Mechanisms of disease Melanoma. *new Engl. J. o f Med.* 51–65 (2006). doi:10.1056/NEJMra052166

25. Gray-Schopfer, V., Wellbrock, C. & Marais, R. Melanoma biology and new targeted therapy. *Nature* **445,** 851–857 (2007).

26. Karimkhani, C., Gonzalez, R. & Dellavalle, R. P. A review of novel therapies for melanoma. *American Journal of Clinical Dermatology* **15,** 323–337 (2014).

27. Miller, A. J. & Mihm, M. C. Melanoma. *New England Journal of Medicine* **355,** 51–65 (2006).

28. Knight, S. D. *et al.* Discovery of GSK2126458, a highly potent inhibitor of PI3K and the mammalian target of rapamycin. *ACS Med. Chem. Lett.* **1,** 39–43 (2010).

29. Leung, E., Kim, J. E., Rewcastle, G. W., Finlay, G. J. & Baguley, B. C. Comparison of the effects of the PI3K/mTOR inhibitors NVP-BEZ235 and GSK2126458 on tamoxifen-resistant breast cancer cells. *Cancer Biol. Ther.* **11,** 938–946 (2011).

30. Masuda, M., Shimomura, M., Kobayashi, K., Kojima, S. & Nakatsura, T. Growth inhibition by NVP-BEZ235, a dual PI3K/mTOR inhibitor, in hepatocellular carcinoma cell lines. *Oncol. Rep.* **26,** 1273–1279 (2011).

31. Bosserhoff, A. K. Novel biomarkers in malignant melanoma. *Clin. Chim. Acta.* **367,** 28–35 (2006).

32. Lee, B., Mukhi, N. & Liu, D. Current management and novel agents for malignant melanoma. *Journal of Hematology & Oncology* **5,** 3 (2012).

33.   Gonzalez, E. & McGraw, T. E. The Akt kinases: Isoform specificity in metabolism and cancer. *Cell Cycle* **8,** 2502–2508 (2009).

34.   Altomare, D. A. & Testa, J. R. Perturbations of the AKT signaling pathway in human cancer. *Oncogene* **24,** 7455–7464 (2005).

35.   Davies, M. A. *et al.* A novel AKT3 mutation in melanoma tumours and cell lines. *Br. J. Cancer* **99,** 1265–1268 (2008).

36.   Rajasekhar, V. K. *et al.* Oncogenic Ras and Akt signaling contribute to glioblastoma formation by differential recruitment of existing mRNAs to polysomes. *Mol. Cell* **12,** 889–901 (2003).

37.   Kelly, E., Won, A., Refaeli, Y. & Van Parijs, L. IL-2 and related cytokines can promote T cell survival by activating AKT. *J. Immunol.* **168,** 597–603 (2002).

38.   Berna, M. J. *et al.* Gastrointestinal growth factors and hormones have divergent effects on Akt activation. *Cell. Signal.* **21,** 622–638 (2009).

39.   Bellacosa, A. *et al.* Akt activation by growth factors is a multiple-step process: the role of the PH domain. *Oncogene* **17,** 313–325 (1998).

40.   Huang, B. X., Akbar, M., Kevala, K. & Kim, H. Y. Phosphatidylserine is a critical modulator for Akt activation. *J. Cell Biol.* **192,** 979–992 (2011).

41.   Li, Y., Dowbenko, D. & Lasky, L. A. AKT/PKB phosphorylation of p21Cip/WAF1 enhances protein stability of p21Cip/WAF1 and promotes cell survival. *J. Biol. Chem.* **277,** 11352–11361 (2002).

42.   Vazquez, F. & Devreotes, P. Regulation of PTEN function as a PIP3 gatekeeper through membrane interaction. *Cell Cycle* **5,** 1523–1527 (2006).

43.   Carnero, A., Blanco-Aparicio, C., Renner, O., Link, W. & Leal, J. F. The PTEN/PI3K/AKT signalling pathway in cancer, herapeutic implications. *Curr Cancer Drug Targets* **8,** 187–198 (2008).

44.   Chalhoub, N. & Baker, S. J. PTEN and the PI3-kinase pathway in cancer. *Annu. Rev. Pathol.* **4,** 127–150 (2009).

45.   Yin, Y. & Shen, W. H. PTEN: a new guardian of the genome. *Oncogene* **27,** 5443–5453 (2008).

46.   Fresno Vara, J. A. *et al.* PI3K/Akt signalling pathway and cancer. *Cancer Treat. Rev.* **30,** 193–204 (2004).

47.   Osaki, M., Oshimura, M. & Ito, H. PI3K-Akt pathway: its functions and alterations in human cancer. *Apoptosis* **9,** 667–676 (2004).

48.   Kruse, J. P. & Gu, W. Modes of p53 Regulation. *Cell* **137,** 609–622 (2009).

49.   Franke, T. F. PI3K/Akt: getting it right matters. *Oncogene* **27,** 6473–6488 (2008).

50.   Haupt, S., Berger, M., Goldberg, Z. & Haupt, Y. Apoptosis - the p53 network. *J. Cell Sci.* **116,** 4077–4085 (2003).

51. Manfredi, J. J. The Mdm2-p53 relationship evolves: Mdm2 swings both ways as an oncogene and a tumor suppressor. *Genes and Development* **24,** 1580–1589 (2010).

52. Muller, P. a J. & Vousden, K. H. P53 Mutations in Cancer. *Nat. Cell Biol.* **15,** 2–8 (2013).

53. Beckerman, R. & Prives, C. Transcriptional regulation by p53. *Cold Spring Harbor perspectives in biology* **2,** (2010).

54. Tang, Y., Zhao, W., Chen, Y., Zhao, Y. & Gu, W. Acetylation Is Indispensable for p53 Activation. *Cell* **133,** 612–626 (2008).

55. Peyssonnaux, C. & Eychène, A. The Raf/MEK/ERK pathway: New concepts of activation. *Biology of the Cell* **93,** 53–62 (2001).

56. McCubrey, J. A. *et al.* Roles of the RAF/MEK/ERK and PI3K/PTEN/AKT pathways in malignant transformation and drug resistance. *Adv. Enzyme Regul.* **46,** 249–279 (2006).

57. McCubrey, J. A. *et al.* Roles of the Raf/MEK/ERK pathway in cell growth, malignant transformation and drug resistance. *Biochimica et Biophysica Acta - Molecular Cell Research* **1773,** 1263–1284 (2007).

58. Zhang, X., Tang, N., Hadden, T. J. & Rishi, A. K. Akt, FoxO and regulation of apoptosis. *Biochimica et Biophysica Acta - Molecular Cell Research* **1813,** 1978–1986 (2011).

59. Zanella, F. *et al.* Human TRIB2 is a repressor of FOXO that contributes to the malignant phenotype of melanoma cells. *Oncogene* **29,** 2973–2982 (2010).

60. Greer, E. L. & Brunet, A. FOXO transcription factors at the interface between longevity and tumor suppression. *Oncogene* **24,** 7410–7425 (2005).

61. Keeshan, K. *et al.* Transformation by Tribbles homolog 2 (Trib2) requires both the Trib2 kinase domain and COP1 binding. *Blood* **116,** 4948–4957 (2010).

62. Yokoyama, T. & Nakamura, T. Tribbles in disease: Signaling pathways important for cellular function and neoplastic transformation. *Cancer Sci.* **102,** 1115–1122 (2011).

63. Dedhia, P. H. *et al.* Differential ability of Tribbles family members to promote degradation of C/EBP?? and induce acute myelogenous leukemia. *Blood* **116,** 1321–1328 (2010).

64. Grandinetti, K. B. *et al.* Overexpression of TRIB2 in human lung cancers contributes to tumorigenesis through downregulation of C/EBPα. *Oncogene* **30,** 3328–3335 (2011).

65. Grandinetti, K. *et al.* Overexpression of TRIB2 in human lung cancers contributes to tumorigenesis through downregulation of C/EBPα. *Oncogene* **30,** 3328–3335 (2012).

66. Qiao, Y., Zhang, Y. & Wang, J. Ubiquitin E3 ligase SCF (β-TRCP) regulates TRIB2 stability in liver cancer cells. *Biochem. Biophys. Res. Commun.* **441,** 555–559 (2013).

67. Wang, J. *et al.* Impaired phosphorylation and ubiquitination by p70 S6 kinase (p70S6K) and smad ubiquitination regulatory factor 1 (Smurf1) promote tribbles homolog 2 (TRIB2) stability and carcinogenic property in liver cancer. *J. Biol. Chem.* **288,** 33667–33681 (2013).

CHAPTER 7

APPENDIX

SANTA CRUZ BIOTECHNOLOGY, INC.

Akt1 (C-20): sc-1618

SANTA CRUZ® BIOTECHNOLOGY

The Power to Question

BACKGROUND

The serine/threonine kinase Akt family contains several members, including Akt1 (also designated PKB or RacPK), Akt2 (also designated PKBβ or RacPK-β) and Akt3 (also designated PKBγ or thyoma viral proto-oncogene 3), which exhibit sequence homology with the protein kinase A and C families and are encoded by the c-Akt proto-oncogene. All members of the Akt family have a Pleckstrin homology domain. Akt1 and Akt2 are activated by PDGF stimulation. This activation is dependent on PDGFR-β tyrosine residues 740 and 751, which bind the subunit of the phosphatidylinositol 3-kinase (PI 3-kinase) complex. Activation of Akt1 by Insulin or Insulin-growth factor-1 (IGF-1) results in phosphorylation of both Thr 308 and Ser 473. Phosphorylation of both residues is important to generate a high level of Akt1 activity, and the phosphorylation of Thr 308 is not dependent on phosphorylation of Ser 473 *in vivo*. Thus, Akt proteins become phosphorylated and activated in Insulin/IGF-1-stimulated cells by an upstream kinase(s). The activation of Akt1 and Akt2 is inhibited by the PI kinase inhibitor Wortmannin, suggesting that the protein signals downstream of the PI kinases.

SOURCE

Akt1 (C-20) is available as either goat (sc-1618) or rabbit (sc-1618-R) polyclonal affinity purified antibody raised against a peptide mapping at the C-terminus of Akt1 of human origin.

PRODUCT

Each vial contains 200 µg IgG in 1.0 ml of PBS with < 0.1% sodium azide and 0.1% gelatin.

Blocking peptide available for competition studies, sc-1618 P, (100 µg peptide in 0.5 ml PBS containing < 0.1% sodium azide and 0.2% BSA).

Available as phycoerythrin conjugate for flow cytometry, sc-1618 PE, 100 tests; and as agarose conjugate for immunoprecipitation, sc-1618 AC, 500 µg/0.25 ml agarose in 1 ml.

APPLICATIONS

Akt1 (C-20) is recommended for detection of Akt1 and, to a lesser extent, Akt2 and Akt3 of mouse, rat, human and *Xenopus laevis* origin by Western Blotting (starting dilution 1:200, dilution range 1:100-1:1000), immunoprecipitation [1-2 µg per 100-500 µg of total protein (1 ml of cell lysate)], immunofluorescence (starting dilution 1:50, dilution range 1:50-1:500), flow cytometry (1 µg per 1 x 10^6 cells) and solid phase ELISA (starting dilution 1:30, dilution range 1:30-1:3000).

Akt1 (C-20) is also recommended for detection of Akt1 and, to a lesser extent, Akt2 and Akt3 in additional species, including equine, canine, bovine, porcine and avian.
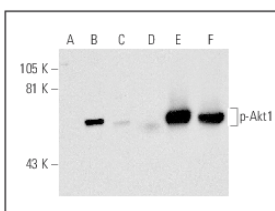
Molecular Weight of Akt1: 62 kDa.

Positive Controls: Akt1 (h): 293T Lysate: sc-158248, HeLa whole cell lysate: sc-2200 or IMR-32 cell lysate: sc-2409.

STORAGE

Store at 4° C, **DO NOT FREEZE**. Stable for one year from the date of shipment. Non-hazardous. No MSDS required.

RESEARCH USE

For research use only, not for use in diagnostic procedures.

DATA

Western blot analysis of Akt1 phosphorylation in non-transfected: sc-117752 (**A,D**), untreated human Akt1 transfected: sc-158248 (**B,E**) and lambda protein phosphatase (sc-200312A) treated human Akt1 transfected: sc-158248 (**C,F**) 293T whole cell lysates. Antibodies tested include p-Akt1 (Thr 308): sc-135650 (**A-C**) and Akt1 (C-20): sc-1618 (**D-F**).
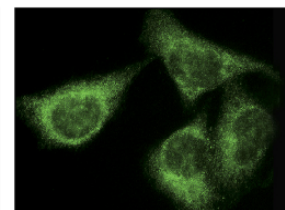
Akt1 (C-20): sc-1618. Immunofluorescence staining of methanol-fixed HeLa cells showing cytoplasmic localization.

SELECT PRODUCT CITATIONS

1. Datta, S.R., et al. 1997. Akt phosphorylation of Bad couples survival signals to the cell intrinsic death machinery. Cell 91: 231-241.

2. Sun, S., et al. 2012. The ATP-P2X7 signaling axis is dispensable for obesity-associated inflammasome activation in adipose tissue. Diabetes 61: 1471-1478.

3. Li, M., et al. 2012. HBcAg induces PD-1 upregulation on CD4+T cells through activation of JNK, ERK and PI3K/AKT pathways in chronic hepatitis-B-infected patients. Lab. Invest. 92: 295-304.

4. Razolli, D.S., et al. 2012. Hypothalamic action of glutamate leads to body mass reduction through a mechanism partially dependent on JAK2. J. Cell. Biochem. 113: 1182-1189.

5. Urtasun, R., et al. 2012. Osteopontin, an oxidant stress sensitive cytokine, up-regulates collagen-I via integrin $\alpha_V\beta_3$ engagement and PI3K/pAkt/NFκB signaling. Hepatology 55: 594-608.

6. Cintra, D.E., et al. 2012. Unsaturated fatty acids revert diet-induced hypothalamic inflammation in obesity. PLoS ONE 7: e30571.

7. Ramis, G., et al. 2012. EGFR inhibition in glioma cells modulates Rho signaling to inhibit cell motility and invasion and cooperates with temozolomide to reduce cell growth. PLoS ONE 7: e38770.

8. Sarró, E., et al. 2012. A pharmacologically-based array to identify targets of cyclosporine A-induced toxicity in cultured renal proximal tubule cells. Toxicol. Appl. Pharmacol. 258: 275-287.

9. Jang, J.Y., et al. 2012. Aqueous fraction from *Cuscuta japonica* seed suppresses melanin synthesis through inhibition of the p38 mitogen-activated protein kinase signaling pathway in B16F10 cells. J. Ethnopharmacol. 141: 338-344.

10. Jia, Y. 2012. Endogenous erythropoietin signaling facilitates skeletal muscle repair and recovery following pharmacologically induced damage. FASEB J. 26: 2847-2858.

Santa Cruz Biotechnology, Inc. 1.800.457.3801 831.457.3800 fax 831.457.3801 **Europe** +00800 4573 8000 49 6221 4503 0 **www.scbt.com**

Figure A. 1: Datasheet of Total Akt antibody (http://www.scbt.com/).

SANTA CRUZ BIOTECHNOLOGY, INC.

p-Akt1/2/3 (Ser 473)-R: sc-7985-R

SANTA CRUZ® BIOTECHNOLOGY

The Power to Question

BACKGROUND

The serine/threonine kinase Akt family contains several members, including Akt1 (also designated PKB or RacPK), Akt2 (also designated PKBβ or RacPK-β) and Akt 3 (also designated PKBγ or thyoma viral proto-oncogene 3), which exhibit sequence homology with the protein kinase A and C families and are encoded by the c-Akt proto-oncogene. All members of the Akt family have a Pleckstrin homology domain. Akt1 and Akt2 are activated by PDGF stimulation. This activation is dependent on PDGFR-β tyrosine residues 740 and 751, which bind the subunit of the phosphatidylinositol 3-kinase (PI 3-kinase) complex. Activation of Akt1 by Insulin or Insulin-growth factor-1(IGF-1) results in phosphorylation of both Thr 308 and Ser 473. Akt proteins become phosphorylated and activated in Insulin/IGF-1-stimulated cells by an upstream kinase(s), and the activation of Akt1 and Akt2 is inhibited by the PI kinase inhibitor Wortmannin. Taken together, this data strongly suggests that the protein signals downstream of the PI kinases. Akt3 is phosphorylated on a serine residue in response to Insulin. However, the activation of Akt3 by Insulin is inhibited by prior activation of protein kinase C via a mechanism that does not require the presence of the PH domain. Akt3 is expressed in 3T3-L1 fibroblasts, adipocytes and skeletal muscle and may be involved in various biological processes, including adipocyte and muscle differentiation, glycogen synthesis, glucose uptake, apoptosis and cellular proliferation.

SOURCE

p-Akt1/2/3 (Ser 473)-R is a rabbit polyclonal antibody raised against a short amino acid sequence containing Ser 473 phosphorylated Akt1 of human origin.

PRODUCT

Each vial contains 200 µg IgG in 1.0 ml of PBS with < 0.1% sodium azide and 0.1% gelatin.

Blocking peptide available for competition studies, sc-7985 P, (100 µg peptide in 0.5 ml PBS containing < 0.1% sodium azide and 0.2% BSA).

APPLICATIONS

p-Akt1/2/3 (Ser 473)-R is recommended for detection of Ser 473 phosphorylated Akt1 and correspondingly Ser 474 phosphorylated Akt2 and correspondingly Ser 472 phosporylated Akt3 of mouse, rat, human and *Xenopus laevis* origin by Western Blotting (starting dilution 1:200, dilution range 1:100-1:1000), immunoprecipitation [1-2 µg per 100-500 µg of total protein (1 ml of cell lysate)], immunofluorescence (starting dilution 1:50, dilution range 1:50-1:500) and solid phase ELISA (starting dilution 1:30, dilution range 1:30-1:3000).

p-Akt1/2/3 (Ser 473)-R is also recommended for detection of correspondingly phosphorylated Akt1, Akt2 and Akt3 in additional species, including bovine, porcine and avian.

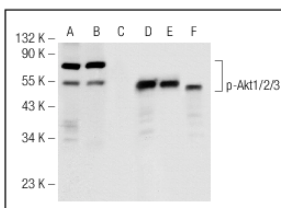Molecular Weight of p-Akt1: 62 kDa.

Molecular Weight of p-Akt2: 56 kDa.

Molecular Weight of p-Akt3: 62 kDa.

Positive Controls: A-431 whole cell lysate: sc-2201, Jurkat whole cell lysate: sc-2204 or HeLa + heat shock cell lysate: sc-2272.

STORAGE

Store at 4° C, **DO NOT FREEZE**. Stable for one year from the date of shipment. Non-hazardous. No MSDS required.

DATA

Western blot analysis of Akt1/2/3 phosphorylation in untreated (**A,D**), calyculin treated (**B,E**) and calyculin and lambda protein phosphatase (sc-200312A) treated (**C,F**) Jurkat whole cell lysates. Antibodies tested include p-Akt1/2/3 (Ser 473)-R: sc-7985-R (**A,B,C**) and Akt1 (C-20): sc-1618 (**D,E,F**).
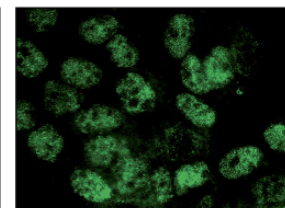
p-Akt1/2/3 (Ser 473)-R: sc-7985-R. Immunofluorescence staining of methanol-fixed A-431 cells showing nuclear localization.

SELECT PRODUCT CITATIONS

1. Contos, J.J., et al. 2002. Characterization of lpa₂ (EDG-4) and lpa₁/lpa₂ (EDG-2/EDG-4) lysophosphatidic acid receptor knockout mice: signaling deficits without obvious phenotypic abnormality attributable to lpa₂. Mol. Cell. Biol. 22: 6921-6929.

2. He, Y.Y., et al. 2003. Epidermal growth factor receptor downregulation induced by UVA in human keratinocytes does not require the receptor kinase activity. J. Biol. Chem. 278: 42457-42465.

3. Singh, M.K., et al. 2003. High-fat diet and leptin treatment alter skeletal muscle Insulin-stimulated phosphatidylinositol 3-kinase activity and glucose transport. Metab. Clin. Exp. 52: 1196-1205.

4. Yaspelkis, B.B., III, et al. 2004. Chronic leptin treatment enhances Insulin-stimulated glucose disposal in skeletal muscle of high-fat fed rodents. Life Sci. 74: 1801-1816.

5. De Souza, C.T., et al. 2005. Short-term inhibition of peroxisome proliferator-activated receptor-γ coactivator-1α expression reverses diet-induced diabetes mellitus and hepatic steatosis in mice. Diabetologia 48: 1860-1871.

6. Singleton, P.A., et al. 2006. Transactivation of sphingosine 1-phosphate receptors is essential for vascular barrier regulation. Novel role for hyaluronan and CD44 receptor family. J. Biol. Chem. 281: 34381-34393.

7. Nincheri, P., et al. 2010. Sphingosine kinase-1/S1P1 signalling axis negatively regulates mitogenic response elicited by PDGF in mouse myoblasts. Cell. Signal. 22: 1688-1699.

8. Alexandru, N., et al. 2011. Platelet activation in hypertension associated with hypercholesterolemia: effects of irbesartan. J. Thromb. Haemost. 9: 173-184.

RESEARCH USE

For research use only, not for use in diagnostic procedures.

Santa Cruz Biotechnology, Inc.   1.800.457.3801   831.457.3800   fax 831.457.3801   **Europe**   +00800 4573 8000   49 6221 4503 0   **www.scbt.com**

Figure A. 2: Datasheet of phospho-Akt antibody (http://www.scbt.com/).

SANTA CRUZ BIOTECHNOLOGY, INC.

FKHRL1 (N-16): sc-9813

SANTA CRUZ® BIOTECHNOLOGY
The Power to Question

BACKGROUND

FKHRL1 (forkhead in rhabdomyosarcoma-like 1), also known as FOXO3 (forkhead box O3) or FOXO3A, is a 673 amino acid transcriptional activator that belongs to the FKHR subfamily of forkhead transcription factors. Transcriptional activation of FKHR proteins is regulated by the serine/threonine kinase Akt1, which phosphorylates FKHRL1 at Threonine 32 and Serine 253. Phosphorylation by Akt1 negatively regulates FKHRL1 by promoting its export from the nucleus. Phosphorylated FKHRL1 associates with 14-3-3 proteins and this complex is retained in the cytoplasm. Growth factor withdrawal stimulates FKHRL1 dephosphorylation and nuclear translocation, leading to FKHR-induced gene-specific transcriptional activation. Within the nucleus, dephosphorylated FKHRL1 triggers apoptosis by inducing the expression of genes that are critical for cell death.

CHROMOSOMAL LOCATION

Genetic locus: FOXO3 (human) mapping to 6q21; Foxo3 (mouse) mapping to 10 B2.

SOURCE

FKHRL1 (N-16) is an affinity purified goat polyclonal antibody raised against a peptide mapping at the N-terminus of FKHRL1 of human origin.

PRODUCT

Each vial contains 200 µg IgG in 1.0 ml of PBS with < 0.1% sodium azide and 0.1% gelatin.

Blocking peptide available for competition studies, sc-9813 P, (100 µg peptide in 0.5 ml PBS containing < 0.1% sodium azide and 0.2% BSA).

Available as TransCruz reagent for Gel Supershift and ChIP applications, sc-9813 X, 200 µg/0.1 ml.

APPLICATIONS

FKHRL1 (N-16) is recommended for detection of FKHRL1 of mouse, rat and human origin by Western Blotting (starting dilution 1:200, dilution range 1:100-1:1000), immunoprecipitation [1-2 µg per 100-500 µg of total protein (1 ml of cell lysate)], immunofluorescence (starting dilution 1:50, dilution range 1:50-1:500), immunohistochemistry (including paraffin-embedded sections) (starting dilution 1:50, dilution range 1:50-1:500) and solid phase ELISA (starting dilution 1:30, dilution range 1:30-1:3000).

FKHRL1 (N-16) is also recommended for detection of FKHRL1 in additional species, including bovine and porcine.

Suitable for use as control antibody for FKHRL1 siRNA (h): sc-37887, FKHRL1 siRNA (m): sc-37888, FKHRL1 shRNA Plasmid (h): sc-37887-SH, FKHRL1 shRNA Plasmid (m): sc-37888-SH, FKHRL1 shRNA (h) Lentiviral Particles: sc-37887-V and FKHRL1 shRNA (m) Lentiviral Particles: sc-37888-V.
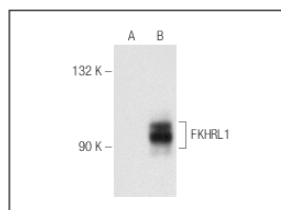
FKHRL1 (N-16) X TransCruz antibody is recommended for Gel Supershift and ChIP applications.
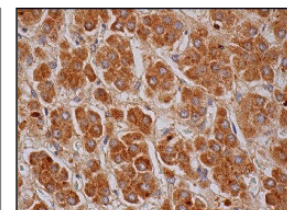
Molecular Weight (predicted) of FKHRL1: 71 kDa.

Molecular Weight (observed) of FKHRL1: 87-99 kDa.

STORAGE

Store at 4° C, **DO NOT FREEZE**. Stable for one year from the date of shipment. Non-hazardous. No MSDS required.

DATA

FKHRL1 (N-16): sc-9813. Western blot analysis of FKHRL1 expression in non-transfected: sc-117752 (**A**) and mouse FKHRL1 transfected: sc-178617 (**B**) 293T whole cell lysates.

FKHRL1 (N-16): sc-9813. Immunoperoxidase staining of formalin fixed, paraffin-embedded human adrenal gland tissue showing cytoplasmic staining of glandular cells.

SELECT PRODUCT CITATIONS

1. Ghosh, A.K., et al. 2001. A nucleoprotein complex containing CCAAT/enhancer-binding protein β interacts with an insulin response sequence in the insulin-like growth factor-binding protein-1 gene and contributes to insulin-regulated gene expression. J. Biol. Chem. 276: 8507-8515.

2. Nadal, A., et al. 2002. Down-regulation of the mitochondrial 3-hydroxy-3-methylglutaryl-CoA synthase gene by insulin: the role of the forkhead transcription factor FKHRL1. Biochem. J. 366: 289-297.

3. Li, L., et al. 2003. Caveolin-1 maintains activated Akt in prostate cancer cells through scaffolding domain binding site interactions with and inhibition of serine/threonine protein phosphatases PP1 and PP2A. Mol. Cell. Biol. 23: 9389-9404.

4. Xiang, Y., et al. 2012. Calorie restriction increases primordial follicle reserve in mature female chemotherapy-treated rats. Gene 493: 77-82.

5. Kornfeld, S.F., et al. 2012. Differential expression of mature microRNAs involved in muscle maintenance of hibernating little brown bats, *Myotis lucifugus*: a model of muscle atrophy resistance. Genomics Proteomics Bioinformatics 10: 295-301.

RESEARCH USE

For research use only, not for use in diagnostic procedures.

PROTOCOLS

See our web site at www.scbt.com or our catalog for detailed protocols and support products.

Figure A. 3: Datasheet of Total FOXO antibody (http://www.scbt.com/).

SANTA CRUZ BIOTECHNOLOGY, INC.

p-FKHRL1 (Ser 253): sc-101683

SANTA CRUZ®
BIOTECHNOLOGY

The Power to Question

BACKGROUND

FKHRL1 (for forkhead in rhabdomyosarcoma) is a member of the FKHR sub-family of forkhead transcription factors. Transcriptional activation of FKHR proteins is regulated by the serine/threonine kinase Akt1, which phospho-rylates FKHRL1 at Threonine 32 and Serine 253. Phosphorylation by Akt1 negatively regulates FKHRL1 by promoting its export from the nucleus. Phosphorylated FKHRL1 associates with 14-3-3 proteins and this complex is retained in the cytoplasm. Growth factor withdrawal stimulates FKHRL1 dephosphorylation and nuclear translocation, leading to FKHR-induced gene-specific transcriptional activation. Within the nucleus, dephosphorylated FKHRL1 triggers apoptosis by inducing the expression of genes that are critical for cell death.

REFERENCES

1. Galili, N., Davis, R.J., Fredericks, W.J., Mukhopadhyay, S., Rauscher, F.J. III, Emanuel, B.S., Rovera, G. and Barr, F.G. 1993. Fusion of a forkhead domain gene to Pax-3 in the solid tumour alveolar rhabdomyosarcoma. Nat. Genet. 5: 230-235.

2. Anderson, M.J., Viars, C.S., Czekay, S., Cavenee, W.K. and Arden, K.C. 1998. Cloning and characterization of three human forkhead genes that comprise an FKHR-like gene subfamily. Genomics 47: 187-199.

3. Biggs, W.H. III, Meisenhelder, J., Hunter, T., Cavenee, W.K. and Arden, K.C. 1999. Protein kinase B/Akt-mediated phosphorylation promotes nuclear exclusion of the winged helix transcription factor FKHR1. Proc. Natl. Acad. Sci. USA 96: 7421-7426.

4. Brunet, A., Bonni, A., Zigmond, M.J., Lin, M.Z., Juo, P., Hu, L.S., Anderson, M.J., Arden, K.C., Blenis, J. and Greenberg, M.E. 1999. Akt promotes cell survival by phosphorylating and inhibiting a forkhead transcription factor. Cell 96: 857-868.

5. Tang, E.D., Nunez, G., Barr, F.G. and Guan, K.L. 1999. Negative regulation of the forkhead transcription factor FKHR by Akt. J. Biol. Chem. 274: 16741-16746.

CHROMOSOMAL LOCATION

Genetic locus: FOXO3A (human) mapping to 6q21; Foxo3a (mouse) mapping to 10 B2.

SOURCE

p-FKHRL1 (Ser 253) is a rabbit polyclonal antibody raised against a short amino acid sequence containing phosphorylated Ser 253 of FKHRL1 of human origin.

PRODUCT

Each vial contains 100 µg IgG in 1.0 ml of PBS with < 0.1% sodium azide and 0.1% gelatin.

STORAGE

Store at 4° C, **DO NOT FREEZE**. Stable for one year from the date of shipment. Non-hazardous. No MSDS required.

APPLICATIONS

p-FKHRL1 (Ser 253) is recommended for detection of Ser 253 phosphorylated FKHRL1 of human origin and correspondingly phosphorylated Ser 253 of mouse and rat origin by Western Blotting (starting dilution 1:200, dilution range 1:100-1:1000), immunoprecipitation [1-2 µg per 100-500 µg of total protein (1 ml of cell lysate)], immunofluorescence and immunohistochem-istry (including paraffin-embedded sections) (starting dilution 1:50, dilution range 1:50-1:500).

Suitable for use as control antibody for FKHRL1 siRNA (h): sc-37887, FKHRL1 siRNA (m): sc-37888, FKHRL1 shRNA Plasmid (h): sc-37887-SH, FKHRL1 shRNA Plasmid (m): sc-37888-SH, FKHRL1 shRNA (h) Lentiviral Particles: sc-37887-V and FKHRL1 shRNA (m) Lentiviral Particles: sc-37888-V.

Molecular Weight of p-FKHRL1: 97 kDa.

Positive Controls: NIH/3T3 + serum cell lysate: sc-2248, NIH/3T3 + serum cell lysate: sc-2248 or HeLa + serum-starved cell lysate: sc-24693.

DATA
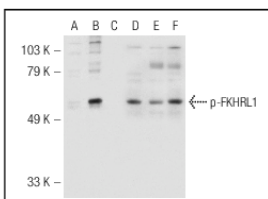
Western blot analysis of FKHRL1 phosphorylation in untreated (**A,D**), serum starved and serum treated (**B,E**) and serum starved, serum treated and lambda protein phosphatase (sc-200312A) treated (**C,F**) HeLa whole cell lysates. Antibodies tested include p-FKHRL1 (Ser 253): sc-101683 (**A,B,C**) and FKHRL1 (H-144): sc-11351 (**D,E,F**).
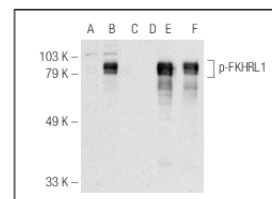
Western blot analysis of FKHRL1 phosphorylation in non-transfected: sc-117752 (**A,D**), untreated mouse FKHRL1 transfected: sc-178617 (**B,E**) and lambda protein phosphatase (sc-200312A) treated mouse FKHRL1 transfected: sc-178617 (**C,F**) 293T whole cell lysates. Antibodies tested include p-FKHRL1 (Ser 253): sc-101683 (**A,B,C**) and FKHRL1 (m): 293T Lysate: sc-11351 (**D,E,F**).
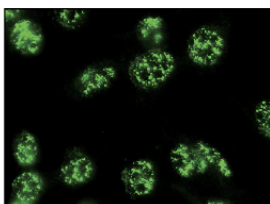
p-FKHRL1 (Ser 253): sc-101683. Immunofluorescence staining of methanol-fixed NIH/3T3 cells showing nuclear localization.
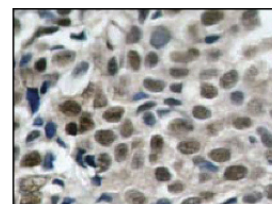
p-FKHRL1 (Ser 253): sc-101683. Immunoperoxidase staining of formalin-fixed, paraffin-embedded human breast carcinoma tissue showing nuclear staining.

RESEARCH USE

For research use only, not for use in diagnostic procedures.

PROTOCOLS

See our web site at www.scbt.com or our catalog for detailed protocols and support products.

Santa Cruz Biotechnology, Inc. 1.800.457.3801 831.457.3800 fax 831.457.3801 **Europe** +00800 4573 8000 49 6221 4503 0 **www.scbt.com**

Figure A. 4: Datasheet of phospho-FOXO antibody (http://www.scbt.com/).

SANTA CRUZ BIOTECHNOLOGY, INC.

FAS-L (C-178): sc-6237

SANTA CRUZ®
BIOTECHNOLOGY
The Power to Question

BACKGROUND

Cytotoxic T lymphocyte (CTL)-mediated cytotoxicity constitutes an important component of specific effector mechanisms in immuno-surveillance against virus-infected or transformed cells. Two mechanisms appear to account for this activity, one of which is the perforin-based process. Independently, a FAS-based mechanism involves the transducing molecule FAS (also designated Apo-1) and its ligand (FAS-L). The human FAS protein is a cell surface glycoprotein that belongs to a family of receptors that includes CD40, nerve growth factor receptors and tumor necrosis factor receptors. The FAS antigen is expressed on a broad range of lymphoid cell lines, certain of which undergo apoptosis in response to treatment with antibody to FAS. These findings strongly imply that targeted cell death is potentially mediated by the inter-cellular interactions of FAS with its ligand or effectors, and that FAS may be critically involved in CTL-mediated cytotoxicity.

CHROMOSOMAL LOCATION

Genetic locus: FASLG (human) mapping to 1q24.3; Fasl (mouse) mapping to 1 H2.1.

SOURCE

FAS-L (C-178) is a rabbit polyclonal antibody raised against amino acids 100-278 mapping at the C-terminus of FAS-L of rat origin.

PRODUCT

Each vial contains 200 µg IgG in 1.0 ml of PBS with < 0.1% sodium azide and 0.1% gelatin.

Available as agarose conjugate for immunoprecipitation, sc-6237 AC, 500 µg/0.25 ml agarose in 1 ml.

APPLICATIONS

FAS-L (C-178) is recommended for detection of FAS-L of mouse, rat and human origin by Western Blotting (starting dilution 1:200, dilution range 1:100-1:1000), immunoprecipitation [1-2 µg per 100-500 µg of total protein (1 ml of cell lysate)], immunofluorescence (starting dilution 1:50, dilution range 1:50-1:500) and solid phase ELISA (starting dilution 1:30, dilution range 1:30-1:3000).

Suitable for use as control antibody for FAS-L siRNA (h): sc-29313, FAS-L siRNA (m): sc-35358, FAS-L shRNA Plasmid (h): sc-29313-SH, FAS-L shRNA Plasmid (m): sc-35358-SH, FAS-L shRNA (h) Lentiviral Particles: sc-29313-V and FAS-L shRNA (m) Lentiviral Particles: sc-35358-V.

Molecular Weight of soluble FAS-L: 26 kDa.

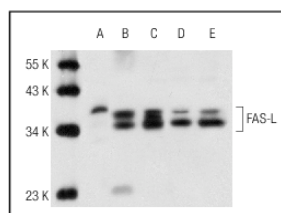Molecular Weight of FAS-L membrane: 40 kDa.

Positive Controls: HL-60 whole cell lysate: sc-2209, Jurkat whole cell lysate: sc-2204 or K-562 whole cell lysate: sc-2203.

STORAGE

Store at 4° C, **DO NOT FREEZE**. Stable for one year from the date of shipment. Non-hazardous. No MSDS required.

RESEARCH USE

For research use only, not for use in diagnostic procedures.

DATA

FAS-L (C-178): sc-6237. Western blot analysis of FAS-L expression in AML-193 (**A**), HL-60 (**B**), K-562 (**C**), CCRF-CEM (**D**) and Jurkat (**E**) whole cell lysates.

SELECT PRODUCT CITATIONS

1. Chen, M.K., et al. 1999. FAS-mediated induction of hepatocyte apoptosis in a neurobalstoma and hepatocyte coculture model. J. Surg. Res. 84: 82-87.

2. Wang, Y., et al. 2008. Protective effect of a standardized Ginkgo extract (ginaton) on renal ischemia/reperfusion injury via suppressing the activation of JNK signal pathway. Phytomedicine 15: 923-931.

3. Liu, Q.B., et al. 2010. The induction of reactive oxygen species and loss of mitochondrial Omi/HtrA2 is associated with S-nitrosoglutathione-induced apoptosis in human endothelial cells. Toxicol. Appl. Pharmacol. 244: 374-384.

4. Williams, K.E., et al. 2010. Lumican reduces tumor growth via induction of fas-mediated endothelial cell apoptosis. Cancer Microenviron. 4: 115-126.

5. Pan, J., et al. 2010. Small peptide inhibitor of JNKs protects against MPTP-induced nigral dopaminergic injury via inhibiting the JNK-signaling pathway. Lab. Invest. 90: 156-167.

6. Qi, S.H., et al. 2010. Neuroprotection of ethanol against ischemia/reperfusion-induced brain injury through decreasing c-Jun N-terminal kinase 3 (JNK3) activation by enhancing GABA release. Neuroscience 167: 1125-1137.

7. Jin, X., et al. 2010. Apoptosis-inducing activity of the antimicrobial peptide cecropin of *Musca domestica* in human hepatocellular carcinoma cell line BEL-7402 and the possible mechanism. Acta Biochim. Biophys. Sin. 42: 259-265.

8. Li, C., et al. 2010. Coactivation of GABA receptors inhibits the JNK3 apoptotic pathway via disassembly of GluR6-PSD-95-MLK3 signaling module in KA-induced seizure. Epilepsia 51: 391-403.

9. Zhang, J., et al. 2011. Activation of GluR6-containing kainate receptors induces ubiquitin-dependent Bcl-2 degradation via denitrosylation in the rat hippocampus after kainate treatment. J. Biol. Chem. 286: 7669-7680.

Figure A. 5: Datasheet of Faz-L antibody (http://www.scbt.com/).

SANTA CRUZ BIOTECHNOLOGY, INC.

MDM2 (C-18): sc-812

SANTA CRUZ®
BIOTECHNOLOGY

The Power to Question

BACKGROUND

p53 is the most commonly mutated gene in human cancer identified to date. Expression of p53 leads to inhibition of cell growth by preventing progression of cells from G_1 to S phase of the cell cycle. Most importantly, p53 functions to cause arrest of cells in the G_1 phase of the cell cycle following any exposure of cells to DNA-damaging agents. The MDM2 (murine double minute-2) protein was initially identified as an oncogene in a murine transformation system. MDM2 functions to bind p53 and block p53-mediated transactivation of cotransfected reporter constructs. The MDM2 gene is amplified in a high percentage of human sarcomas that retain wildtype p53 and tumor cells that overexpress MDM2 can tolerate high levels of p53 expression. These findings argue that MDM2 overexpression represents at least one mechanism by which p53 function can be abrogated during tumorigenesis.

CHROMOSOMAL LOCATION

Genetic locus: MDM2 (human) mapping to 12q15; Mdm2 (mouse) mapping to 10 D2.

SOURCE

MDM2 (C-18) is an affinity purified rabbit polyclonal antibody raised against a peptide mapping within the C-terminus of MDM2 of human origin.

PRODUCT

Each vial contains 200 µg IgG in 1.0 ml of PBS with < 0.1% sodium azide and 0.1% gelatin.

Blocking peptide available for competition studies, sc-812 P, (100 µg peptide in 0.5 ml PBS containing < 0.1% sodium azide and 0.2% BSA).

APPLICATIONS

MDM2 (C-18) is recommended for detection of MDM2 of mouse, rat and human origin by Western Blotting (starting dilution 1:100, dilution range 1:50-1:500), immunoprecipitation [1-2 µg per 100-500 µg of total protein (1 ml of cell lysate)], immunofluorescence (starting dilution 1:25, dilution range 1:25-1:250) and solid phase ELISA (starting dilution 1:30, dilution range 1:30-1:3000).

MDM2 (C-18) is also recommended for detection of MDM2 in additional species, including equine, canine, bovine, porcine, avian and feline.

Suitable for use as control antibody for MDM2 siRNA (h): sc-29394, MDM2 siRNA (m): sc-37263, MDM2 shRNA Plasmid (h): sc-29394-SH, MDM2 shRNA Plasmid (m): sc-37263-SH, MDM2 shRNA (h) Lentiviral Particles: sc-29394-V and MDM2 shRNA (m) Lentiviral Particles: sc-37263-V.

Molecular Weight of MDM2: 90 kDa.

Molecular Weight of MDM2 cleavage product: 60 kDa.

Positive Controls: A-673 cell lysate: sc-2414, RAW 264.7 whole cell lysate: sc-2211 or MCF7 whole cell lysate: sc-2206.
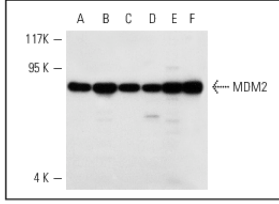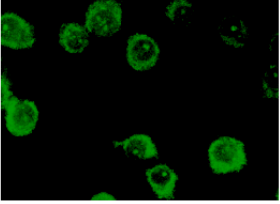
STORAGE

Store at 4° C, **DO NOT FREEZE**. Stable for one year from the date of shipment. Non-hazardous. No MSDS required.

RESEARCH USE

For research use only, not for use in diagnostic procedures.

DATA

MDM2 (C-18): sc-812. Western blot analysis of MDM2 expression in MCF7 (**A**), V-205 (**B**), A-673 (**C**), RAW 264.7 (**D**), Jurkat (**E**) and MDA-MB-468 (**F**) whole cell lysates.

MDM2 (C-18): sc-812. Immunofluorescence staining of methanol-fixed RAW 264.7 cells showing cytoplasmic localization.

SELECT PRODUCT CITATIONS

1. Carroll, P.E., et al. 1999. Centrosome hyperamplification in human cancer: chromosome instability by p53 mutation and/or MDM2 overexpression. Oncogene 18: 1935-1944.

2. Eischen, C.M., et al. 2001. Bax loss impairs Myc-induced apoptosis and circumvents the selection of p53 mutations during Myc-mediated lymphomagenesis. Mol. Cell. Biol. 21: 7653-7662.

3. Samuels-Lev, Y., et al. 2001. ASPP proteins specifically stimulate the apoptotic function of p53. Mol. Cell 8: 781-794.

4. Steinman, H.A., et al. 2004. An alternative splice form of MDM2 induces p53-independent cell growth and tumorigenesis. J. Biol. Chem. 279: 4877-4886.

5. Perucca-Lostanlen, D., et al. 2004. Distinct MDM2 and p14 ARF expression and centrosome amplification in well-differentiated liposarcomas. Genes Chromosomes Cancer 39: 99-109.

6. Eischen, C.M., et al. 2004. Loss of one allele of ARF rescues MDM2 haploinsufficiency effects on apoptosis and lymphoma development. Oncogene 23: 8931-8940.

7. Gladden, A.B., et al. 2006. Expression of constitutively nuclear cyclin D1 in murine lymphocytes induces B-cell lymphoma. Oncogene 25: 998-1007.

8. Gorrini, C., et al. 2007. Tip60 is a haplo-insufficient tumour suppressor required for an oncogene-induced DNA damage response. Nature 448: 1063-1067.

9. Kulikov, R., et al. 2010. Mdm2 facilitates the association of p53 with the proteasome. Proc. Natl. Acad. Sci. USA 107: 10038-10043.

10. Arrate, M.P., et al. 2010. MicroRNA biogenesis is required for Myc-induced B-cell lymphoma development and survival. Cancer Res. 70: 6083-6092.

11. Ta, V.B., et al. 2010. Malignant transformation of Slp65-deficient pre-B cells involves disruption of the Arf-Mdm2-p53 tumor suppressor pathway. Blood 115: 1385-1393.

Santa Cruz Biotechnology, Inc.   1.800.457.3801   831.457.3800   fax 831.457.3801   **Europe**   +00800 4573 8000   49 6221 4503 0   **www.scbt.com**

Figure A. 6: Datasheet of MDM2 antibody (http://www.scbt.com/).

SANTA CRUZ BIOTECHNOLOGY, INC.

PTEN (A2B1): sc-7974

SANTA CRUZ®
BIOTECHNOLOGY

The Power to Question

BACKGROUND

As human tumors progress to advanced stages, one genetic alteration that occurs at high frequency is a loss of heterozygosity (LOH) at chromosome 10q23.31. Mapping of homozygous deletions on this chromosome led to the isolation of the PTEN gene, also designated MMAC1 (for mutated in multiple advanced cancers) and TEP1. This candidate tumor suppressor gene exhibits a high frequency of mutations in human glioblastomas and is also mutated in other cancers, including sporadic brain, breast, kidney and prostate cancers. PTEN has been associated with Cowden disease, an autosomal dominant cancer predisposition syndrome. The PTEN gene product is a putative protein tyrosine phosphatase that is localized to the cytoplasm, and it shares extensive homology with the cytoskeletal proteins tensin and auxilin. Gene transfer studies have indicated that the phosphatase domain of PTEN is essential for growth suppression of glioma cells.

CHROMOSOMAL LOCATION

Genetic locus: PTEN (human) mapping to 10q23.31; Pten (mouse) mapping to 19 C1.

SOURCE

PTEN (A2B1) is a mouse monoclonal antibody raised against amino acids 388-400 of PTEN of human origin.

PRODUCT

Each vial contains 200 µg IgG$_1$ in 1.0 ml of PBS with < 0.1% sodium azide and 0.1% gelatin.

Blocking peptide available for competition studies, sc-7974 P, (100 µg peptide in 0.5 ml PBS containing < 0.1% sodium azide and 0.2% BSA).

Available as agarose conjugate for immunoprecipitation, sc-7974 AC, 500 µg/ 0.25 ml agarose in 1 ml; and as HRP conjugate for Western blotting, sc-7974 HRP, 200 µg/1 ml.

APPLICATIONS

PTEN (A2B1) is recommended for detection of PTEN of mouse, rat and human origin by Western Blotting (starting dilution 1:200, dilution range 1:100-1:1000), immunoprecipitation [1-2 µg per 100-500 µg of total protein (1 ml of cell lysate)], immunofluorescence (starting dilution 1:50, dilution range 1:50-1:500) and solid phase ELISA (starting dilution 1:30, dilution range 1:30-1:3000).

Suitable for use as control antibody for PTEN siRNA (h): sc-29459, PTEN siRNA (m): sc-36326, PTEN siRNA (r): sc-61873, PTEN shRNA Plasmid (h): sc-29459-SH, PTEN shRNA Plasmid (m): sc-36326-SH, PTEN shRNA Plasmid (r): sc-61873-SH, PTEN shRNA (h) Lentiviral Particles: sc-29459-V, PTEN shRNA (m) Lentiviral Particles: sc-36326-V and PTEN shRNA (r) Lentiviral Particles: sc-61873-V.

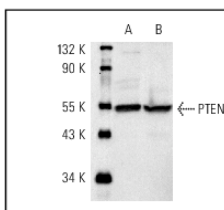Molecular Weight of PTEN: 55 kDa.

STORAGE

Store at 4° C, **DO NOT FREEZE**. Stable for one year from the date of shipment. Non-hazardous. No MSDS required.
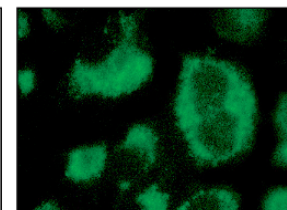
RESEARCH USE

For research use only, not for use in diagnostic procedures.

DATA

PTEN (A2B1): sc-7974. Western blot analysis of PTEN expression in A-431 (**A**) and KNRK (**B**) whole cell lysates.

PTEN (A2B1): sc-7974. Immunofluorescence staining of methanol-fixed HeLa cells showing cytoplasmic localization.

SELECT PRODUCT CITATIONS

1. Huang, J. and Kontos, C.D. 2002. PTEN modulates vascular endothelial growth factor-mediated signaling and angiogenic effects. J. Biol. Chem. 277: 10760-10766.

2. Altomare, D.A., et al. 2002. Frequent activation of AKT2 kinase in human pancreatic carcinomas. J. Cell. Biochem. 87: 470-476.

3. Pernicová, Z., et al. 2011. Androgen depletion induces senescence in prostate cancer cells through down-regulation of Skp2. Neoplasia 13: 526-536.

4. Lehman, J.A., et al. 2011. Induction of apoptotic genes by a p73-phos phatase and tensin homolog (p73-PTEN) protein complex in response to genotoxic stress. J. Biol. Chem. 286: 36631-36640.

5. Cao, X., et al. 2011. WW domain-containing E3 ubiquitin protein ligase 1 (WWP1) delays cellular senescence by promoting p27(Kip1) degradation in human diploid fibroblasts. J. Biol. Chem. 286: 33447-33456.

6. Godfrey, R., et al. 2012. Cell transformation by FLT3 ITD in acute myeloid leukemia involves oxidative inactivation of the tumor suppressor protein-tyrosine phosphatase DEP-1/ PTPRJ. Blood 119: 4499-4511.

7. Yuan, H., et al. 2012. Stem cell antigen-1 deficiency enhances the chemo-preventive effect of peroxisome proliferator-activated receptorγ activation. Cancer Prev. Res. 5: 51-60.

8. Riggio, M., et al. 2012. PI3K/AKT pathway regulates phosphorylation of steroid receptors, hormone independence and tumor differentiation in breast cancer. Carcinogenesis 33: 509-518.

9. González-Rodríguez, A., et al. 2012. Essential role of protein tyrosine phosphatase 1B in obesity-induced inflammation and peripheral Insulin resistance during aging. Aging Cell 11: 284-296.

10. Berglund, F.M., et al. 2012. Disruption of epithelial architecture caused by loss of PTEN or by oncogenic mutant p110α/PIK3CA but not by HER2 or mutant AKT1. Oncogene. E-published.

Figure A. 7: Datasheet of PTEN antibody (http://www.scbt.com/).

SANTA CRUZ BIOTECHNOLOGY, INC.

p53 (DO-1): sc-126

BACKGROUND

p53, a DNA-binding, oligomerization domain- and transcription activation domain-containing tumor suppressor, upregulates growth arrest and apoptosis-related genes in response to stress signals, thereby influencing programmed cell death, cell differentiation, and cell cycle control mechanisms. p53 localizes to the nucleus, yet can be chaperoned to the cytoplasm by the negative regulator, MDM2. MDM2 is an E3 ubiquitin ligase that is upregulated in the presence of active p53, where it poly-ubiquitinates p53 for proteasome targeting. p53 fluctuates between latent and active DNA-binding conformations and is differentially activated through posttranslational modifications, including phosphorylation and acetylation. Mutations in the DNA-binding domain (DBD) of p53, amino acids 110-286, can compromise energetically-favorable association with *cis* elements and are implicated in several human cancers.

CHROMOSOMAL LOCATION

Genetic locus: TP53 (human) mapping to 17p13.1.

SOURCE

p53 (DO-1) is a mouse monoclonal antibody raised against amino acids 11-25 of p53 of human origin.

PRODUCT

Each vial contains 200 μg IgG$_{2a}$ in 1.0 ml of PBS with < 0.1% sodium azide and 0.1% gelatin.

Available as TransCruz reagent for Gel Supershift and ChIP applications, sc-126 X, 200 μg/0.1 ml; as agarose conjugate for immunoprecipitation, sc-126 AC, 500 μg/ 0.25 ml agarose in 1 ml; as HRP conjugate for Western blotting, sc-126 HRP, 200 μg/ml; as either fluorescein (sc-126 FITC) or rhodamine (sc-126 TRITC) conjugates for use in immunofluorescence, 200 μg/ml; as phycoerythrin (sc-126 PE) or PerCP-Cy5.5 (sc-126 PCPC5) conjugates for flow cytometry, 100 tests; and as Alexa Fluor® 405 (sc-126 AF405), Alexa Fluor® 488 (sc-126 AF488) or Alexa Fluor® 647 (sc-126 AF647) conjugates for flow cytometry or immunofluorescence; 100 μg/2 ml.

Alexa Fluor® is a trademark of Molecular Probes, Inc., Oregon, USA

APPLICATIONS

p53 (DO-1) is recommended for detection of wild type and mutant p53 under denaturing and non-denaturing conditions of human origin by Western Blotting (starting dilution 1:200, dilution range 1:100-1:1000), immunoprecipitation [1-2 μg per 100-500 μg of total protein (1 ml of cell lysate)], immunofluorescence (starting dilution 1:50, dilution range 1:50-1:500), immunohistochemistry (in-cluding paraffin-embedded sections) (starting dilution 1:50, dilution range 1:50-1:500) and flow cytometry (1 μg per 1 x 10^6 cells).

Suitable for use as control antibody for p53 siRNA (h): sc-29435, p53 shRNA Plasmid (h): sc-29435-SH and p53 shRNA (h) Lentiviral Particles: sc-29435-V.
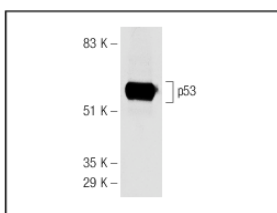
p53 (DO-1) X TransCruz antibody is recommended for Gel Supershift and ChIP applications.
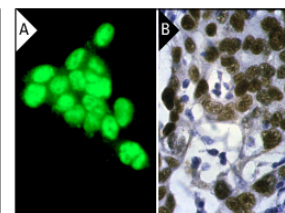
Molecular Weight of p53: 53 kDa.

STORAGE

Store at 4° C, **DO NOT FREEZE**. Stable for one year from the date of shipment. Non-hazardous. No MSDS required.

DATA

p53 (DO-1): sc-126. Western blot analysis of p53 expression in A-431 whole cell lysate.

p53 (DO-1): sc-126. Immunofluorescence staining of methanol-fixed A-431 cells showing nuclear localization (**A**). Immunoperoxidase staining of formalin-fixed, paraffin-embedded human breast carcinoma tissue. Note intense nuclear staining of ductal epithelia (**B**).

SELECT PRODUCT CITATIONS

1. Dierov, J., et al. 1999. Retinoic acid modulates a bimodal effect on cell cycle progression in human adult T-cell leukemia cells. Clin. Cancer Res. 5: 2540-2547.

2. Burns, T.F., et al. 2013. Inhibition of TWIST1 leads to activation of oncogene-induced senescence in oncogene-driven non-small cell lung cancer. Mol. Cancer Res. 11: 329-338.

3. Tao, T., et al. 2013. Def defines a conserved nucleolar pathway that leads p53 to proteasome-independent degradation. Cell Res. 23: 620-634.

4. Wang, M. and Li, S. 2013. Bladder polypoid cystitis-derived A20 associates with tumorigenesis. Cell Biochem. Biophys. 67: 669-673.

5. Vatsyayan, R., et al. 2013. Nutlin-3 enhances sorafenib efficacy in renal cell carcinoma. Mol. Carcinog. 52: 39-48.

6. Zajkowicz, A., et al. 2013. Nutlin-3a, an MDM2 antagonist and p53 activator, helps to preserve the replicative potential of cancer cells treated with a genotoxic dose of resveratrol. Mol. Biol. Rep. 40: 5013-5026.

7. Martin, N., et al. 2013. Interplay between Homeobox proteins and Polycomb repressive complexes in p16^{INK4a} regulation. EMBO J. 32: 982-995.

8. Yang, Y., et al. 2013. Cleavage of the BRCT tandem domains of nibrin by the 657del5 mutation affects the DNA damage response less than the Arg215Trp mutation. IUBMB Life 10: 853-861.

9. Basile, V., et al. 2013. bis-Dehydroxy-Curcumin triggers mitochondrial-associated cell death in human colon cancer cells through ER-stress induced autophagy. PLoS One 8: e53664.

10. Tang, Q., et al. 2013. Resveratrol-induced apoptosis is enhanced by inhibition of autophagy in esophageal squamous cell carcinoma. Cancer Lett. 336: 325-337.

RESEARCH USE

For research use only, not for use in diagnostic procedures.

Figure A. 8: Datasheet of P53 antibody (http://www.scbt.com/).

SANTA CRUZ BIOTECHNOLOGY, INC.

Bim (H-191): sc-11425

SANTA CRUZ® BIOTECHNOLOGY

The Power to Question

BACKGROUND

Pro-apoptotic Bcl-2 family members promote cell death by neutralizing their anti-apoptotic relatives, which otherwise maintain cell viability by regulating caspase activity. Bim belongs to the BH3-only subgroup of Bcl-2 related proteins and exists in three distinct isoforms, Bim_S (short), Bim_L (long) and Bim_{EL} (extra long). ERK1/2 phosphorylates Bim_{EL}, resulting in rapid degradation of the isoform via the proteasome pathway. At least three sites for ERK1/2 phosphorylation exist on Bim_{EL}, whereas ERK1/2 does not effect Bim_S or Bim_L, implying a unique role for Bim_{EL} in cell survival signaling.

CHROMOSOMAL LOCATION

Genetic locus: BCL2L11 (human) mapping to 2q13; Bcl2l11 (mouse) mapping to 2 F1.

SOURCE

Bim (H-191) is a rabbit polyclonal antibody raised against amino acids 4-195 of Bim_{EL} of human origin.

PRODUCT

Each vial contains 200 µg IgG in 1.0 ml of PBS with < 0.1% sodium azide and 0.1% gelatin.

APPLICATIONS

Bim (H-191) is recommended for detection of Bim_{EL}, Bim_L and Bim_S of mouse, rat and human origin by Western Blotting (starting dilution 1:200, dilution range 1:100-1:1000), immunoprecipitation [1-2 µg per 100-500 µg of total protein (1 ml of cell lysate)], immunofluorescence (starting dilution 1:50, dilution range 1:50-1:500), immunohistochemistry (including paraffin-embedded sections) (starting dilution 1:50, dilution range 1:50-1:500) and solid phase ELISA (starting dilution 1:30, dilution range 1:30-1:3000).

Suitable for use as control antibody for Bim siRNA (h): sc-29802, Bim siRNA (m): sc-29803, Bim shRNA Plasmid (h): sc-29802-SH, Bim shRNA Plasmid (m): sc-29803-SH, Bim shRNA (h) Lentiviral Particles: sc-29802-V and Bim shRNA (m) Lentiviral Particles: sc-29803-V.

Molecular Weight of Bim_S: 19 kDa.

Molecular Weight of Bim_L: 21 kDa.

Molecular Weight of Bim_{EL}: 24 kDa.

Positive Controls: HuT 78 whole cell lysate: sc-2208 or HL-60 whole cell lysate: sc-2209.

STORAGE

Store at 4° C, **DO NOT FREEZE**. Stable for one year from the date of shipment. Non-hazardous. No MSDS required.

PROTOCOLS

See our web site at www.scbt.com or our catalog for detailed protocols and support products.

RESEARCH USE

For research use only, not for use in diagnostic procedures.

DATA
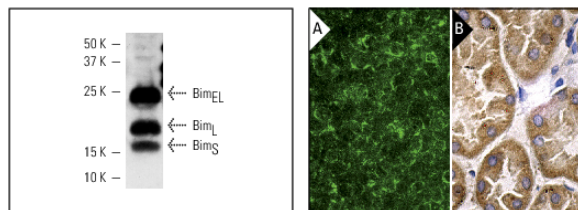
Bim (FL-198): sc-11425. Western blot analysis of Bim isoform expression in HuT 78 whole cell lysate.

Bim (H-191): sc-11425. Immunofluorescence staining of normal mouse lymph node frozen section showing cytoplasmic staining (**A**). Immunoperoxidase staining of formalin fixed, paraffin-embedded human kidney tissue showing cytoplasmic staining of cells in tubules (**B**).

SELECT PRODUCT CITATIONS

1. Qin, J.Z., et al. 2004. p53-independent NOXA induction overcomes apoptotic resistance of malignant melanomas. Mol. Cancer Ther. 3: 895-902.

2. Castera, L., et al. 2009. Apoptosis-related mitochondrial dysfunction defines human monocyte-derived dendritic cells with impaired immuno-stimulatory capacities. J. Cell. Mol. Med. 13: 1321-1335.

3. Tong, D.D., et al. 2009. RUNX3 inhibits cell proliferation and induces apoptosis by TGF-β-dependent and -independent mechanisms in human colon carcinoma cells. Pathobiology 76: 163-169.

4. Yu, C.Z., et al. 2009. Neuroprotection against transient focal cerebral ischemia and oxygen-glucose deprivation by interference with GluR6-PSD95 protein interaction. Neurochem. Res. 34: 2008-2021.

5. Di Leva, G., et al. 2010. MicroRNA cluster 221-222 and estrogen receptor α interactions in breast cancer. J. Natl. Cancer Inst. 102: 706-721.

6. Lai, K.W., et al. 2010. MicroRNA-130β regulates the tumour suppressor RUNX3 in gastric cancer. Eur. J. Cancer 46: 1456-1463.

7. Wood, K.L., et al. 2010. The small heat shock protein 27 is a key regulator of CD8+ CD57+ lymphocyte survival. J. Immunol. 184: 5582-5588.

8. Latré de Laté, P., et al. 2010. Glucocorticoid-induced leucine zipper (GILZ) promotes the nuclear exclusion of FOXO3 in a Crm1-dependent manner. J. Biol. Chem. 285: 5594-5605.

9. Stühmer, T., et al. 2010. Preclinical anti-myeloma activity of the novel HDAC-inhibitor JNJ-26481585. Br. J. Haematol. 149: 529-536.

10. Kim, K.D., et al. 2011. ORAI1 deficiency impairs activated T cell death and enhances T cell survival. J. Immunol. 187: 3620-3630.

11. Essafi, M., et al. 2011. Cell-penetrating TAT-FOXO3 fusion proteins induce apoptotic cell death in leukemic cells. Mol. Cancer Ther. 10: 37-46.

12. Liao, M., et al. 2011. Role of bile salt in regulating Mcl-1 phosphorylation and chemoresistance in hepatocellular carcinoma cells. Mol. Cancer 10: 44.

Figure A. 9: Datasheet of BIM antibody (http://www.scbt.com/).

SANTA CRUZ BIOTECHNOLOGY, INC.

PRAS40 (H-216): sc-67042

SANTA CRUZ® BIOTECHNOLOGY

The Power to Question

BACKGROUND

Akt, also known as protein kinase B is one of the major downstream targets of the phosphatidylinositol 3-kinase pathway. This protein kinase has been implicated in Insulin signaling, stimulation of cellular growth, inhibition of apoptosis and transformation of cells. The proline-rich Akt substrate PRAS40, also designated AKT1S1, becomes phosphorylated by activated Akt on Ser or Thr residues in the motif RXRXX(S/T). Phosphorylated PRAS40 subsequently binds 14-3-3 in a sequence-specific manner, thereby inducing such changes as alteration of protein subcellular localization and regulation of intrinsic enzymatic activity. Studies also suggest that PRAS40 phosphorylation and its interaction with pAkt and 14-3-3 may play an important role in neuroprotection mediated by NGF in apoptotic neuronal cell death after cerebral ischemia. PRAS40 maps to human chromosome 19q13.33.

REFERENCES

1. Cahill, C.M., et al. 2001. Phosphatidylinositol 3-kinase signaling inhibits DAF-16 DNA binding and function via 14-3-3-dependent and 14-3-3 independent pathways. J. Biol. Chem. 276: 13402-13410.

2. Liu, M.Y., et al. 2002. 14-3-3 interacts with the tumor suppressor tuberin or Akt phosphorylation site(s). Cancer Res. 22: 6475-6480.

3. Chen, H.K., et al. 2003. Interaction of Akt-phosphorylated ataxin-1 with 14-3-3 mediates neurodegeneration in spinocerebellar ataxia type 1. Cell 113: 457-468.

4. Kovacina, K.S., et al. 2003. Identification of a proline-rich Akt substrate as a 14-3-3 binding partner. J. Biol. Chem. 278: 10189-10194.

5. Saito, A., et al. 2004. Neuroprotective role of a proline-rich Akt substrate in apoptotic neuronal cell death after stroke: relationships with nerve growth factor. J. Neurosci. 24: 1584-1593.

6. Chan, P.H. 2004. Mitochondria and neuronal death/survival signaling pathways in cerebral ischemia. Neurochem. Res. 29: 1943-1949.

7. Jiang, Y., et al. 2005. Apoptosis and inhibition of the phosphatidylinositol 3-kinase/Akt signaling pathway in the anti-profliferative actions of dehydroepiandrosterone. J. Gastroenterol. 40: 490-497.

8. Reddy, P., et al. 2005. Formation of E-cadherin-mediated cell-cell adhesion activates AKT and mitogen activated protein kinase via phosphatidylinositol 3 kinase and ligand-independent activation of epidermal growth factor receptor in ovarian cancer cells. Mol. Endocrinol. 19: 2564-2578.

9. Suga, H., et al. 2005. Possible involvement of phosphatidylinositol 3-kinase/Akt signal pathway in vasopressin-induced HSP27 phosphorylation in aortic smooth muscle A10 cells. Arch. Biochem. Biophys. 438: 137-145.

CHROMOSOMAL LOCATION

Genetic locus: AKT1S1 (human) mapping to 19q13.33; Akt1s1 (mouse) mapping to 7 B4.

SOURCE

PRAS40 (H-216) is a rabbit polyclonal antibody raised against amino acids 61-256 mapping at the C-terminus of PRAS40 of human origin.

PRODUCT

Each vial contains 200 µg IgG in 1.0 ml of PBS with < 0.1% sodium azide and 0.1% gelatin.

APPLICATIONS

PRAS40 (H-216) is recommended for detection of PRAS40 of mouse, rat and human origin by Western Blotting (starting dilution 1:200, dilution range 1:100-1:1000), immunoprecipitation [1-2 µg per 100-500 µg of total protein (1 ml of cell lysate)], immunofluorescence (starting dilution 1:50, dilution range 1:50-1:500) and solid phase ELISA (starting dilution 1:30, dilution range 1:30-1:3000).
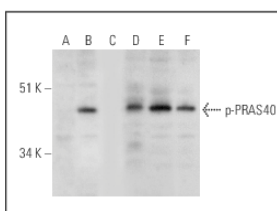
Suitable for use as control antibody for PRAS40 siRNA (h): sc-44635, PRAS40 siRNA Plasmid (h): sc-44635-SH and PRAS40 shRNA (h) Lentiviral Particles: sc44635-V.
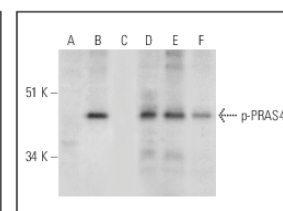
Molecular Weight of PRAS40: 40 kDa.

Positive Controls: Hela whole cell lysate: sc-2200.

RECOMMENDED SECONDARY REAGENTS

To ensure optimal results, the following support (secondary) reagents are recommended: 1) Western Blotting: use goat anti-rabbit IgG-HRP: sc-2004 (dilution range: 1:2000-1:100,000) or Cruz Marker™ compatible goat anti-rabbit IgG-HRP: sc-2030 (dilution range: 1:2000-1:5000), Cruz Marker™ Molecular Weight Standards: sc-2035, TBS Blotto A Blocking Reagent: sc-2333 and Western Blotting Luminol Reagent: sc-2048. 2) Immunoprecipitation: use Protein A/G PLUS-Agarose: sc-2003 (0.5 ml agarose/2.0 ml). 3) Immunofluorescence: use goat anti-rabbit IgG-FITC: sc-2012 (dilution range: 1:100-1:400) or goat anti-rabbit IgG-TR: sc-2780 (dilution range: 1:100-1:400) with UltraCruz™ Mounting Medium: sc-24941.

DATA

Western blot analysis of PRAS40 phosphorylation in untreated (**A,D**), EGF treated (**B,E**) and EGF and lambda protein phosphatase (sc-200312A) treated (**C,F**) HeLa whole cell lysates. Antibodies tested include p-PRAS40 (Thr 246): sc-32629 (**A,B,C**) and PRAS40 (H-216): sc-67042 (**D,E,F**).

Western blot analysis of PRAS40 phosphorylation in untreated (**A,D**), insulin treated (**B,E**) and insulin and lambda protein phosphatase (sc-200312A) treated (**C,F**) HeLa whole cell lysates. Antibodies tested include p-PRAS40 (Thr 246): sc-32629 (**A,B,C**) and PRAS40 (H-216): sc-67042 (**D,E,F**).

STORAGE

Store at 4° C, **DO NOT FREEZE**. Stable for one year from the date of shipment. Non-hazardous. No MSDS required.

RESEARCH USE

For research use only, not for use in diagnostic procedures.

Santa Cruz Biotechnology, Inc.   1.800.457.3801   831.457.3800   fax 831.457.3801   **Europe**   +00800 4573 8000   49 6221 4503 0   **www.scbt.com**

Figure A. 10: Datasheet of Total PRAS40 antibody (http://www.scbt.com/).

SANTA CRUZ BIOTECHNOLOGY, INC.

p-PRAS40 (Thr 246): sc-32629

SANTA CRUZ® BIOTECHNOLOGY

The Power to Question

BACKGROUND

Akt, also known as protein kinase B, is one of the major downstream targets of the phosphatidylinositol 3-kinase pathway. This protein kinase has been implicated in Insulin signaling, stimulation of cellular growth, inhibition of apoptosis and transformation of cells. The proline-rich Akt substrate PRAS40, also designated AKT1S1, becomes phosphorylated by activated Akt on serine or threonine residues in the motif RXRXX(S/T). Phosphorylated PRAS40 subsequently binds 14-3-3 in a sequence-specific manner, thereby inducing such changes as alteration of protein subcellular localization and regulation of intrinsic enzymatic activity. Studies also suggest that PRAS40 phosphorylation and its interaction with p-Akt and 14-3-3 may play an important role in neuroprotection mediated by NGF in apoptotic neuronal cell death after cerebral ischemia. PRAS40 maps to human chromosome 19q13.33.

REFERENCES

1. Cahill, C.M., et al. 2001. Phosphatidylinositol 3-kinase signaling inhibits DAF-16 DNA binding and function via 14-3-3 dependent and 14-3-3 independent pathways. J. Biol. Chem. 276: 13402-13410.

2. Liu, M.Y., et al. 2002. 14-3-3 interacts with the tumor suppressor tuberin or Akt phosphorylation site(s). Cancer Res. 22: 6475-6480.

3. Chen, H.K., et al. 2003. Interaction of Akt-phosphorylated ataxin-1 with 14-3-3 mediates neurodegeneration in spinocerebellar ataxia type 1. Cell 113: 457-468.

4. Kovacina, K.S., et al. 2003. Identification of a proline-rich Akt substrate as a 14-3-3 binding partner. J. Biol. Chem. 278: 10189-10194.

5. Atsushi, S., et al. 2004. Neuroprotective role of a proline-rich Akt substrate in apoptotic neuronal cell death after stroke: relationships with nerve growth factor. J. Neurosci. 24: 1584-1593.

CHROMOSOMAL LOCATION

Genetic locus: AKT1S1 (human) mapping to 19q13.33.

SOURCE

p-PRAS40 (Thr 246) is a rabbit polyclonal antibody raised against a short amino acid sequence containing Thr 246 phosphorylated PRAS40 of human origin.

PRODUCT

Each vial contains 200 µg IgG in 1.0 ml of PBS with < 0.1% sodium azide and 0.1% gelatin.

Blocking peptide available for competition studies, sc-32629 P, (100 µg peptide in 0.5 ml PBS containing < 0.1% sodium azide and 0.2% BSA).

STORAGE

Store at 4° C, **DO NOT FREEZE**. Stable for one year from the date of shipment. Non-hazardous. No MSDS required.

RESEARCH USE

For research use only, not for use in diagnostic procedures.

APPLICATIONS

p-PRAS40 (Thr 246) is recommended for detection of Thr 246 phosphorylated PRAS40 of human origin by Western Blotting (starting dilution 1:200, dilution range 1:100-1:1000), immunoprecipitation [1-2 µg per 100-500 µg of total protein (1 ml of cell lysate)], immunofluorescence (starting dilution 1:50, dilution range 1:50-1:500) and solid phase ELISA (starting dilution 1:30, dilution range 1:30-1:3000).

p-PRAS40 (Thr 246) is also recommended for detection of correspondingly phosphorylated PRAS40 in additional species, including equine, canine, bovine and porcine.
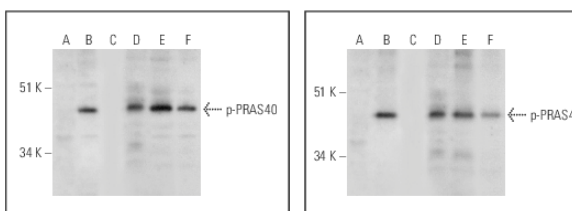
Suitable for use as control antibody for PRAS40 siRNA (h): sc-44635, PRAS40 shRNA Plasmid (h): sc-44635-SH and PRAS40 shRNA (h) Lentiviral Particles: sc-44635-V.

Molecular Weight of p-PRAS40: 40 kDa.

Positive Controls: Hela whole cell lysate: sc-2200.

RECOMMENDED SECONDARY REAGENTS

To ensure optimal results, the following support (secondary) reagents are recommended: 1) Western blotting: use goat anti-rabbit IgG-HRP: sc-2004 (dilution range: 1:2000-1:100,000) or Cruz Marker™ compatible goat anti-rabbit IgG-HRP: sc-2030 (dilution range: 1:2000-1:5000), Cruz Marker™ Molecular Weight Standards: sc-2035, TBS Blotto B Blocking Reagent: sc-2335 (use 50 mM NaF, sc-24988, as diluent), Western Blotting Luminol Reagent: sc-2048 and Lambda Phosphatase: sc-200312A. 2) Immunoprecipitation: use Protein A/G PLUS-Agarose: sc-2003 (0.5 ml agarose/2.0 ml). 3) Immunofluorescence: use goat anti-rabbit IgG-FITC: sc-2012 (dilution range: 1:100-1:400) or goat anti-rabbit IgG-TR: sc-2780 (dilution range: 1:100-1:400) with UltraCruz™ Mounting Medium: sc-24941.

DATA

Western blot analysis of PRAS40 phosphorylation in untreated (**A**,**D**), EGF treated (**B**,**E**) and EGF and lambda protein phosphatase (sc-200312A) treated (**C**,**F**) HeLa whole cell lysates. Antibodies tested include p-PRAS40 (Thr 246): sc-32629 (**A**,**B**,**C**) and PRAS40 (H-216): sc-67042 (**D**,**E**,**F**).

Western blot analysis of PRAS40 phosphorylation in untreated (**A**,**D**), insulin treated (**B**,**E**) and insulin and lambda protein phosphatase (sc-200312A) treated (**C**,**F**) HeLa whole cell lysates. Antibodies tested include p-PRAS40 (Thr 246): sc-32629 (**A**,**B**,**C**) and PRAS40 (H-216): sc-67042 (**D**,**E**,**F**).

SELECT PRODUCT CITATIONS

1. Wu, C.W. and Storey, K.B. 2012. Regulation of the mTOR signaling network in hibernating thirteen-lined ground squirrels. J. Exp. Biol. 215: 1720-1727.

Figure A. 11: Datasheet of phospho-PRAS40 antibody (http://www.scbt.com/).

SANTA CRUZ BIOTECHNOLOGY, INC.

p70 S6 kinase α (C-18): sc-230

SANTA CRUZ® BIOTECHNOLOGY

The Power to Question

BACKGROUND

In studies to elucidate key regulatory pathways in signal transduction, several protein serine/threonine (Ser/Thr) kinases have been identified, including two distinct families of 40S ribosomal protein S6 Ser/Thr kinases present in somatic animal cells, designated p70 S6 kinase and p90 Rsk kinase. p90 Rsk kinase is maximally activated within minutes of addition of growth factors or phorbol ester to cultured cells followed by activation of p70 S6 kinase. Both enzymes are regulated by serine/threonine phosphorylation, suggesting that specific kinases may exist upstream in the signaling pathway that regulate these kinases. In fact, evidence suggests that one such family of activating enzymes includes the members of the ERK MAP kinase family. The ERK MAP kinases are, in turn, regulated by phosphorylation at threonine and tyrosine residues by a protein kinase designated MEK.

CHROMOSOMAL LOCATION

Genetic locus: RPS6KB1 (human) mapping to 17q23.1; Rps6kb1 (mouse) mapping to 11 C.

SOURCE

p70 S6 kinase α (C-18) is an affinity purified rabbit polyclonal antibody raised against a peptide mapping at the C-terminus of p70 S6 kinase α of rat origin.

PRODUCT

Each vial contains 200 µg IgG in 1.0 ml of PBS with < 0.1% sodium azide and 0.1% gelatin.

Blocking peptide available for competition studies, sc-230 P, (100 µg peptide in 0.5 ml PBS containing < 0.1% sodium azide and 0.2% BSA).

APPLICATIONS

p70 S6 kinase α (C-18) is recommended for detection of p70 S6 kinase α of mouse, rat, human, chicken and *Xenopus laevis* origin by Western Blotting (starting dilution 1:200, dilution range 1:100-1:1000), immunoprecipitation [1-2 µg per 100-500 µg of total protein (1 ml of cell lysate)], immunofluorescence (starting dilution 1:50, dilution range 1:50-1:500), immunohistochemistry (including paraffin-embedded sections) (starting dilution 1:50, dilution range 1:50-1:500) and solid phase ELISA (starting dilution 1:30, dilution range 1:30-1:3000).

p70 S6 kinase α (C-18) is also recommended for detection of p70 S6 kinase α in additional species, including equine, canine, bovine, porcine and avian.

Suitable for use as control antibody for p70 S6 kinase α siRNA (h): sc-36165, p70 S6 kinase α siRNA (m): sc-36166, p70 S6 kinase α shRNA Plasmid (h): sc-36165-SH, p70 S6 kinase α shRNA Plasmid (m): sc-36166-SH, p70 S6 kinase α shRNA (h) Lentiviral Particles: sc-36165-V and p70 S6 kinase α shRNA (m) Lentiviral Particles: sc-36166-V.
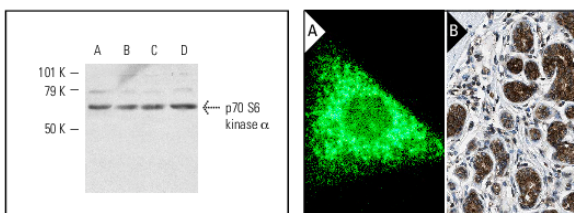
Molecular Weight of p70 S6 kinase α: 70 kDa.

Positive Controls: HeLa whole cell lysate: sc-2200, NIH/3T3 whole cell lysate: sc-2210 or KNRK whole cell lysate: sc-2214.

STORAGE

Store at 4° C, **DO NOT FREEZE**. Stable for one year from the date of shipment. Non-hazardous. No MSDS required.

DATA

p70 S6 kinase α (C-18): sc-230. Western blot analysis of p70 S6 kinase α expression in HeLa (**A**), NIH/3T3 (**B**) and KNRK (**C**) whole cell lysates and rat liver tissue (**D**).

p70 S6 kinase α (C-18): sc-230. Immunofluorescence staining of methanol-fixed KNRK rat cells (**A**). Immunoperoxidase staining of formalin fixed, paraffin-embedded human breast tissue showing cytoplasmic and nuclear staining of glandular cells. Kindly provided by The Swedish Human Protein Atlas (HPA) program (**B**).

SELECT PRODUCT CITATIONS

1. Rommel, C., et al. 2001. Mediation of IGF-1-induced skeletal myotube hypertrophy by PI 3-kinase/Akt/mTOR and PI 3-kinase/Akt/GSK-3 pathways. Nat. Cell Biol. 11: 1009-1013.

2. Bodine, S.C., et al. 2001. Akt/mTOR pathway is a crucial regulator of skeletal muscle hypertrophy and can prevent muscle atrophy *in vivo*. Nat. Cell Biol. 11: 1014-1019.

3. Zhao, Y., et al. 2011. DEPTOR, an mTOR inhibitor, is a physiological substrate of SCFβTrCP E3 ubiquitin ligase and regulates survival and autophagy. Mol. Cell 44: 304-316.

4. Sanchez, A.M, et al. 2012. AMPK promotes skeletal muscle autophagy through activation of forkhead FoxO3a and interaction with Ulk1. J. Cell. Biochem. 113: 695-710.

5. Wang, Z., et al. 2012. Inhibition of mammalian target of rapamycin signaling by CCI-779 (temsirolimus) induces growth inhibition and cell cycle arrest in Cashmere goat fetal fibroblasts *(Capra hircus)*. DNA Cell Biol. 31: 1095-1099.

6. Chen, W., et al. 2012. Developmental transition of pectoralis muscle from atrophy in late-term duck embryos to hypertrophy in neonates. Exp. Physiol. 97: 861-872.

7. Diez, H., et al. 2012. Specific roles of Akt iso forms in apoptosis and axon growth regulation in neurons. PLoS ONE 7: e32715.

8. Zanou, N., et al. 2012. Trpc1 ion channel modulates phosphatidylinositol 3-kinase/Akt pathway during myoblast differentiation and muscle regeneration. J. Biol. Chem. 287: 14524-14534.

9. Liu, J., et al. 2013. Metformin inhibits renal cell carcinoma *in vitro* and *in vivo* xenograft. Urol. Oncol. 31: 264-270.

RESEARCH USE

For research use only, not for use in diagnostic procedures.

Figure A. 12: Datasheet of Total p70S6K antibody (http://www.scbt.com/).

SANTA CRUZ BIOTECHNOLOGY, INC.

Actin (I-19): sc-1616

BACKGROUND

All eukaryotic cells express Actin, which often constitutes as much as 50% of total cellular protein. Actin filaments can form both stable and labile structures and are crucial components of microvilli and the contractile apparatus of muscle cells. While lower eukaryotes, such as yeast, have only one Actin gene, higher eukaryotes have several isoforms encoded by a family of genes. At least six types of Actin are present in mammalian tissues and fall into three classes. α Actin expression is limited to various types of muscle, whereas β and γ are the principle constituents of filaments in other tissues. Members of the small GTPase family regulate the organization of the Actin cytoskeleton. Rho controls the assembly of Actin stress fibers and focal adhesion, Rac regulates Actin filament accumulation at the plasma membrane and Cdc42 stimulates formation of filopodia.

SOURCE

Actin (I-19) is available as either goat (sc-1616) or rabbit (sc-1616-R) polyclonal affinity purified antibody raised against a peptide mapping at the C-terminus of Actin of human origin.

PRODUCT

Each vial contains 200 µg IgG in 1.0 ml of PBS with < 0.1% sodium azide and 0.1% gelatin.

Blocking peptide available for competition studies, sc-1615 P, (100 µg peptide in 0.5 ml PBS containing < 0.1% sodium azide and 0.2% BSA).

Available as TransCruz reagent for ChIP application, sc-1615 X, 200 µg/0.1 ml; as agarose conjugate for immunoprecipitation, sc-1615 AC, 500 µg/0.25 ml agarose in 1 ml; as HRP conjugate for Western blotting, sc-1615 HRP, 200 µg/1 ml; as rhodamine (sc-1615 TRITC) conjugate for immunofluorescence, 200 µg/1 ml; as phycoerythrin (sc-1615 PE) or fluorescein (sc-1615 FITC) conjugates for flow cytometry, 100 tests; and as Alexa Fluor® 405 (sc-1615 AF405), Alexa Fluor® 488 (sc-1615 AF488) or Alexa Fluor® 647 (sc-1615 AF647) conjugates for flow cytometry or immunofluorescence; 100 µg/2 ml.

Alexa Fluor® is a trademark of Molecular Probes, Inc., Oregon, USA

APPLICATIONS

Actin (I-19) is recommended for detection of a broad range of Actin isoforms of mouse, rat, human, Drosophila melanogaster, Xenopus laevis, zebrafish and Caenorhabditis elegans origin by Western Blotting (starting dilution 1:200, dilution range 1:100-1:1000), immunoprecipitation [1-2 µg per 100-500 µg of total protein (1 ml of cell lysate)], immunofluorescence (starting dilution 1:50, dilution range 1:50-1:500), flow cytometry (1 µg per 1 x 10⁶ cells) and solid phase ELISA (starting dilution 1:30, dilution range 1:30-1:3000).

Actin (I-19) is also recommended for detection of a broad range of Actin isoforms in additional species, including equine, canine, bovine, porcine and avian.
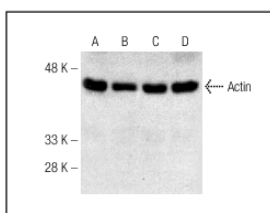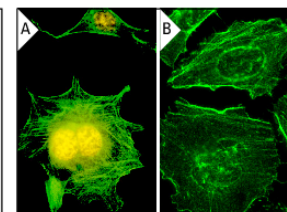
Molecular Weight of Actin: 43 kDa.

STORAGE

Store at 4° C, **DO NOT FREEZE**. Stable for one year from the date of shipment. Non-hazardous. No MSDS required.

RESEARCH USE

For research use only, not for use in diagnostic procedures.

DATA

Actin (I-19): sc-1616. Western blot analysis of Actin expression in C32 (**A**), BC₃HI (**B**), Sol 8 (**C**) and L8 (**D**) whole cell lysates.

Actin (I-19): sc-1616. Immunofluorescence staining of methanol-fixed NIH/3T3 cells showing cytoskeletal fluorescein immunostaining of actin filaments. Note nuclear rhodamine immunostaining with PCNA (PC-10): sc-56 (**A**). Immunofluorescence staining of methanol-fixed HeLa cells showing cytoskeletal localization (**B**).

SELECT PRODUCT CITATIONS

1. Pogorzelska, E., et al. 1990. Modification of the test for determining bacterial capacity for nitrate reduction. Rocz. Panstw. Zakl. Hig. 41: 58-62.

2. Chung, L.C., et al. 2012. L-Mimosine blocks cell proliferation via upregulation of B-cell translocation gene 2 and N-myc downstream regulated gene 1 in prostate carcinoma cells. Am. J. Physiol., Cell Physiol. 302: C676-C685.

3. Scotti, L., et al. 2013. Involvement of the ANGPTs/Tie-2 system in ovarian hyperstimulation syndrome (OHSS). Mol. Cell. Endocrinol. 365: 223-230.

4. Alvarez, Z., et al. 2013. The effect of the composition of PLA films and lactate release on glial and neuronal maturation and the maintenance of the neuronal progenitor niche. Biomaterials 34: 2221-2233.

5. Garcia-Yague, A.J., et al. 2013. Nuclear import and export signals control the subcellular localization of Nurr1 in response to oxidative stress. J. Biol. Chem. 288: 5506-5517.

6. Kaur, J. and Tikoo, K. 2013. Evaluating cell specific cytotoxicity of differentially charged silver nanoparticles. Food Chem. Toxicol. 51: 1-14.

7. Miranda-Goncalves, V., et al. 2013. Monocarboxylate transporters (MCTs) in gliomas: expression and exploitation as therapeutic targets. Neuro Oncol. 15: 172-188.

8. Faouzi, M., et al. 2013. ORAI3 silencing alters cell proliferation and cell cycle progression via c-myc pathway in breast cancer cells. Biochim. Biophys. Acta 1833: 752-760.

9. Lutz, D., et al. 2013. Generation and nuclear translocation of sumoylated transmembrane fragment of cell adhesion molecule L1. J. Biol. Chem. 287: 17161-17175.

10. García-Corzo, L., et al. 2013. Dysfunctional Coq9 protein causes predominant encephalomyopathy associated with CoQ deficiency. Hum. Mol. Genet. 22: 1233-1248.

Santa Cruz Biotechnology, Inc.   1.800.457.3801   831.457.3800   fax 831.457.3801   **Europe**   +00800 4573 8000   49 6221 4503 0   **www.scbt.com**

Figure A. 13: Datasheet of Actin antibody (http://www.scbt.com/).

SANTA CRUZ BIOTECHNOLOGY, INC.

caspase-3 (E-8): sc-7272

SANTA CRUZ®
BIOTECHNOLOGY
The Power to Question

BACKGROUND

Caspase-3, also known as apopain, SCA-1, Yama and CPP32, is an aspartate-specific cysteine protease that belongs to the ICE subfamily of caspases. Caspase-3 is expressed in cells as an inactive precursor from which the p17 and p11 subunits of the mature caspase-3 are proteolytically generated during apoptosis. The caspase-3 precursor is first cleaved at Asp 175-Ser 176 to produce the p11 subunit and the p20 peptide. Subsequently, the p20 peptide is cleaved at Asp 28-Ser 29 to generate the mature p17 subunit. The active caspase-3 enzyme is a heterodimer composed of two p17 and two p11 sub-units. At the onset of apoptosis, caspase-3 proteolytically cleaves PARP at a Asp 216-Gly 217 bond. During the execution of the apoptotic cascade, acti-vated caspase-3 releases SREBP from the membrane of the ER in a proteo-lytic reaction that is distinct from their normal sterol-dependent activation. Caspase-3 cleaves and activates SREBPs between the basic helix-loop-helix leucine zipper domain and the membrane attachment domain. Caspase-3 also cleaves and activates caspase-6, -7 and -9. The human caspase-3 gene en-codes a cytoplasmic protein that is highly expressed in lung, spleen, heart, liver, kidney and cells of the immune system.

CHROMOSOMAL LOCATION

Genetic locus: CASP3 (human) mapping to 4q35.1.

SOURCE

caspase-3 (E-8) is a mouse monoclonal antibody raised against amino acids 1-277 representing full length caspase-3 of human origin.

PRODUCT

Each vial contains 200 μg IgG$_{2a}$ in 1.0 ml of PBS with < 0.1% sodium azide and 0.1% gelatin.

Available as agarose conjugate for immunoprecipitation, sc-7272 AC, 500 μg/ 0.25 ml agarose in 1 ml; as HRP conjugate for Western Blotting, sc-7272 HRP, 200 μg/1 ml; as fluorescein (sc-7272 FITC) or rhodamine (sc-7272 TRITC) conjugates for immunofluorescence, 200 μg/1 ml and as phycoerythrin (sc-7272 PE) or fluorescein (sc-7272 FITC) conjugates for flow cytometry, 100 tests; and as Alexa Fluor® 405 (sc-7272 AF405), Alexa Fluor® 488 (sc-7272 AF488) or Alexa Fluor® 647 (sc-7272 AF647) conjugates for flow cytometry or immunofluorescence; 100 μg/2 ml.

Alexa Fluor® is a trademark of Molecular Probes, Inc., Oregon, USA

APPLICATIONS

caspase-3 (E-8) is recommended for detection of caspase-3 and full length procaspase-3 of human origin by Western Blotting (starting dilution 1:200, dilution range 1:100-1:1000), immunoprecipitation [1-2 μg per 100-500 μg of total protein (1 ml of cell lysate)], immunofluorescence (starting dilution 1:50, dilution range 1:50-1:500), immunohistochemistry (including paraffin-embedded sections) (starting dilution 1:50, dilution range 1:50-1:500), flow cytometry (1 μg per 1 x 10^6 cells) and solid phase ELISA (starting dilution 1:30, dilution range 1:30-1:3000).

Suitable for use as control antibody for caspase-3 siRNA (h): sc-29237, caspase-3 shRNA Plasmid (h): sc-29237-SH and caspase-3 shRNA (h) Lentiviral Particles: sc-29237-V.

STORAGE

Store at 4° C, **DO NOT FREEZE**. Stable for one year from the date of shipment. Non-hazardous. No MSDS required.

DATA

caspase-3 (E-8): sc-7272. Western blot analysis of caspase-3 expression in non-transfected 293T: sc-117752 (**A**), human caspase-3 transfected 293T: sc-113427 (**B**) and Jurkat (**C**) whole cell lysates.

caspase-3 (E-8): sc-7272.Immunofluorescence staining of methanol-fixed HuT 78 cells showing cytoplasmic staining (**A**). Immunoperoxidase staining of formalin fixed, paraffin-embedded human duodenum tissue showing cytoplasmic staining of glandular cells (**B**).

SELECT PRODUCT CITATIONS

1. Tseng, C., et al. 2002. Microtubule damaging agents induce apoptosis in HL 60 cells and G$_2$/M cell cycle arrest in HT 29 cells. Toxicology 175: 123-142.

2. Wu, S., et al. 2002. Adriamycin-induced cardiomyocyte and endothelial cell apoptosis: *in vitro* and *in vivo* studies. J. Mol. Cell. Cardiol. 34: 1595-1607.

3. Qin, J.Z., et al. 2002. Regulation of apoptosis by p53 in UV-irradiated human epidermis, psoriatic plaques and senescent keratinocytes. Oncogene 21: 2991-3002.

4. Franklin, C.C., et al. 2002. Caspase-3-dependent cleavage of the glutamate-L-cysteine ligase catalytic subunit during apoptotic cell death. Am. J. Pathol. 160: 1887-1894.

5. Marisavljevic, D., et al. 2002. Biological and clinical significance of clonogenic assays in patients with myelodysplastic syndromes. Med. Oncol. 19: 249-259.

6. Stauber, R.H., et al. 2012. A combination of a ribonucleotide reductase inhibitor and histone deacetylase inhibitors downregulates EGFR and triggers BIM-dependent apoptosis in head and neck cancer. Oncotarget 3: 31-43.

7. Ginter, T., et al. 2012. Histone deacetylase inhibitors block IFNγ-induced STAT1 phosphorylation. Cell. Signal. 24: 1453-1460.

8. Khan, S., et al. 2012. A novel cyano derivative of 11-keto-β-boswellic acid causes apoptotic death by disrupting PI3K/AKT/Hsp-90 cascade, mitochondrial integrity, and other cell survival signaling events in HL-60 cells. Mol. Carcinog. 51: 679-695.

9. Pietschmann, K., et al. 2012. Differential regulation of PML-RARα stability by the ubiquitin ligases SIAH1/SIAH2 and TRIAD1. Int. J. Biochem. Cell Biol. 44: 132-138.

RESEARCH USE

For research use only, not for use in diagnostic procedures.

Santa Cruz Biotechnology, Inc. 1.800.457.3801 831.457.3800 fax 831.457.3801 **Europe** +00800 4573 8000 49 6221 4503 0 **www.scbt.com**

Figure A. 14: Datasheet of Caspase-3 antibody (http://www.scbt.com/).

SANTA CRUZ BIOTECHNOLOGY, INC.

cleaved caspase-3 p11 (h176)-R: sc-22171-R

SANTA CRUZ BIOTECHNOLOGY
The Power to Question

BACKGROUND

Caspase-3, also known as apopain, SCA-1, Yama and CPP32, is an aspartate-specific cysteine protease that belongs to the ICE subfamily of caspases. Caspase-3 is expressed in cells as an inactive precursor from which the p17 and p11 subunits of the mature caspase-3 are proteolytically generated during apoptosis. The caspase-3 precursor is first cleaved at Asp-175-Ser-176 to produce the p11 subunit and the p20 peptide. Subsequently, the p20 peptide is cleaved at Asp-28-Ser-29 to generate the mature p17 subunit. The active caspase-3 enzyme is a heterodimer composed of two p17 and two p11 subunits. At the onset of apoptosis, caspase-3 proteolytically cleaves PARP at a Asp-216-Gly-217 bond. During the execution of the apoptotic cascade, activated caspase-3 releases SREBP from the membrane of the ER in a proteolytic reaction that is distinct from their normal sterol-dependent activation. Caspase-3 cleaves and activates SREBPs between the basic helix-loop-helix leucine zipper domain and the membrane attachment domain. Caspase-3 also cleaves and activates caspase-6, -7 and -9. The human caspase-3 gene encodes a cytoplasmic protein that is highly expressed in lung, spleen, heart, liver, kidney and cells of the immune system.

CHROMOSOMAL LOCATION

Genetic locus: CASP3 (human) mapping to 4q35.1.

SOURCE

cleaved caspase-3 p11 (h176)-R is a rabbit polyclonal antibody raised against a short amino acid sequence containing the neoepitope at Ser 176 of caspase-3 p11 of human origin.

PRODUCT

Each vial contains 200 µg IgG in 1.0 ml of PBS with < 0.1% sodium azide and 0.1% gelatin.

Blocking peptide available for competition studies, sc-22171 P, (100 µg peptide in 0.5 ml PBS containing < 0.1% sodium azide and 0.2% BSA).

APPLICATIONS

cleaved caspase-3 p11 (h176)-R is recommended for detection of the p11 subunit of caspase-3 of human origin by Western Blotting (starting dilution 1:200, dilution range 1:100-1:1000), immunofluorescence (starting dilution 1:50, dilution range 1:50-1:500) and solid phase ELISA (starting dilution 1:30, dilution range 1:30-1:3000); non cross-reactive with full length caspase-3.

Suitable for use as control antibody for caspase-3 siRNA (h): sc-29237, caspase-3 shRNA Plasmid (h): sc-29237-SH and caspase-3 shRNA (h) Lentiviral Particles: sc-29237-V.

Molecular Weight of procaspase-3: 32 kDa.

Molecular Weight of caspase-3 subunits: 11/17/20 kDa.

Positive Controls: MOLT-4 cell lysate: sc-2233 or CCRF-CEM cell lysate: sc-2225.

RESEARCH USE

For research use only, not for use in diagnostic procedures.

SELECT PRODUCT CITATIONS

1. Lepelletier, Y., et al. 2007. Prevention of mantle lymphoma tumor establishment by routing transferrin receptor toward lysosomal compartments. Cancer Res. 67: 1145-1154.

2. Qiu, W., et al. 2008. Retinoblastoma protein modulates gankyrin-MDM2 in regulation of p53 stability and chemosensitivity in cancer cells. Oncogene 27: 4034-4043.

3. Amendola, D., et al. 2009. Myc down-regulation affects cyclin D1/cdk4 activity and induces apoptosis via Smac/Diablo pathway in an astrocytoma cell line. Cell Prolif. 42: 94-109.

4. Hamano, Y., et al. 2010. Low-dose darbepoetin α attenuates progression of a mouse model of aristolochic acid nephropathy through early tubular protection. Nephron Exp. Nephrol. 114: e69-e81.

5. Zhang, A., et al. 2010. EIF2α and caspase-12 activation are involved in oxygen-glucose-serum deprivation/restoration-induced apoptosis of spinal cord astrocytes. Neurosci. Lett. 478: 32-36.

6. Löhr, J.M., et al. 2010. Autoantibodies against the exocrine pancreas in autoimmune pancreatitis: gene and protein expression profiling and immunoassays identify pancreatic enzymes as a major target of the inflammatory process. Am. J. Gastroenterol. 105: 2060-2071.

7. Bonilla-Porras, A.R., et al. 2011. Vitamin K3 and vitamin C alone or in combination induced apoptosis in leukemia cells by a similar oxidative stress signalling mechanism. Cancer Cell Int. 11: 19.

8. Anitha, P., et al. 2011. Ellagic acid coordinately attenuates Wnt/β-catenin and NFκB signaling pathways to induce intrinsic apoptosis in an animal model of oral oncogenesis. Eur. J. Nutr. 52: 75-84.

9. Thiyagarajan, P., et al. 2011. Dietary chlorophyllin inhibits the canonical NFκB signaling pathway and induces intrinsic apoptosis in a hamster model of oral oncogenesis. Food Chem. Toxicol. 50: 867-876.

10. Jiang, Y., et al. 2011. Drug transporter-independent liver cancer cell killing by a marine steroid methyl spongoate via apoptosis induction. J. Biol. Chem. 286: 26461-26469.

11. Pan, H., et al. 2011. Salvianolic acid A demonstrates cardioprotective effects in rat hearts and cardiomyocytes after ischemia/reperfusion injury. J. Cardiovasc. Pharmacol. 58: 535-542.

12. Driák, D., et al. 2011. Changes in expression of some apoptotic markers in different types of human endometrium. Folia Biol. 57: 104-111.

13. Huang, W., et al. 2012. Sirt1 overexpression protects murine osteoblasts against TNF-α-induced injury in vitro by suppressing the NFκB signaling pathway. Acta Pharmacol. Sin. 33: 668-674.

14. Zhu, H., et al. 2012. Impaired N-cadherin-mediated adhesion increases the risk of inducible ventricular arrhythmias in isolated rat hearts. Sci. Res. Essays 7: 2983-2991.

STORAGE

Store at 4° C, **DO NOT FREEZE**. Stable for one year from the date of shipment. Non-hazardous. No MSDS required.

Santa Cruz Biotechnology, Inc.   1.800.457.3801   831.457.3800   fax 831.457.3801   **Europe**   +00800 4573 8000   49 6221 4503 0   **www.scbt.com**

Figure A. 15: Datasheet of Cleaved Caspase-3 antibody (http://www.scbt.com/).

SANTA CRUZ BIOTECHNOLOGY, INC.

PDK1 (C-20): sc-7140

SANTA CRUZ®
BIOTECHNOLOGY
The Power to Question

BACKGROUND

Mitochondrial pyruvate dehydrogenase (PDH) catalyzes the oxidative decarboxylation of pyruvate and plays a central role in the regulation of homeostasis of carbohydrate fuels in mammals. PDH activity is controlled by a phosphorylation/dephosphorylation cycle, in which phosphorylation leads to inactivation and dephosphorylation leads to reactivation of PDH. The phosphorylation of PDH is catalyzed by pyruvate dehydrogenase kinase (PDK), the activity of which is stimulated by the products of PDH catalysis. PDK1 consists of α and β subunits. The kinase activity resides in the α subunit. Three PDK isoenzymes have been identified in humans (PDK1, 2 and 3) and two have been identified in rodent (PDK1 and 2).

REFERENCES

1. Linn, T.C., et al. 1969. α-keto acid dehydrogenase complexes. X. Regulation of the activity of the pyruvate dehydrogenase complex from beef kidney mitochondria by phosphorylation and dephosphorylation. Proc. Natl. Acad. Sci. USA 62: 234-241.

2. Hucho, F., et al. 1972. α-keto acid dehydrogenase complexes. XVII. Kinetic and regulatory properties of pyruvate dehydrogenase kinase and pyruvate dehydrogenase phosphatase from bovine kidney and heart. Arch. Biochem. Biophys. 151: 328-340.

3. Cate, R.L., et al. 1978. A unifying mechanism for stimulation of mammalian pyruvate dehydrogenase(a) kinase by reduced nicotinamide adenine dinucleotide, dihydrolipamide, acetyl coenzyme A, or pyruvate. J. Biol. Chem. 253: 496-503.

4. Stepp, L.R., et al. 1983. Purification and properties of pyruvate dehydrogenase kinase from bovine kidney. J. Biol. Chem. 258: 9454-9458.

CHROMOSOMAL LOCATION

Genetic locus: PDK1 (human) mapping to 2q31.1; Pdk1 (mouse) mapping to 2 C3.

SOURCE

PDK1 (C-20) is an affinity purified goat polyclonal antibody raised against a peptide mapping at the C-terminus of PDK1 of human origin.

PRODUCT

Each vial contains 200 µg IgG in 1.0 ml of PBS with < 0.1% sodium azide and 0.1% gelatin.

Blocking peptide available for competition studies, sc-7140 P, (100 µg peptide in 0.5 ml PBS containing < 0.1% sodium azide and 0.2% BSA).

STORAGE

Store at 4° C, **DO NOT FREEZE**. Stable for one year from the date of shipment. Non-hazardous. No MSDS required.

RESEARCH USE

For research use only, not for use in diagnostic procedures.

APPLICATIONS

PDK1 (C-20) is recommended for detection of precursor and mature PDK1 of mouse, rat and human origin by Western Blotting (starting dilution 1:200, dilution range 1:100-1:1000), immunoprecipitation [1-2 µg per 100-500 µg of total protein (1 ml of cell lysate)], immunofluorescence (starting dilution 1:50, dilution range 1:50-1:500) and solid phase ELISA (starting dilution 1:30, dilution range 1:30-1:3000).

PDK1 (C-20) is also recommended for detection of precursor and mature PDK1 in additional species, including equine, canine, bovine, porcine and avian.

Suitable for use as control antibody for PDK1 siRNA (h): sc-36203, PDK1 siRNA (m): sc-36204, PDK1 shRNA Plasmid (h): sc-36203-SH, PDK1 shRNA Plasmid (m): sc-36204-SH, PDK1 shRNA (h) Lentiviral Particles: sc-36203-V and PDK1 shRNA (m) Lentiviral Particles: sc-36204-V.

Molecular Weight of PDK1: 49 kDa.

Positive Controls: PDK1 (h): 293T Lysate: sc-113873 or rat heart extract: sc-2393.

RECOMMENDED SECONDARY REAGENTS

To ensure optimal results, the following support (secondary) reagents are recommended: 1) Western Blotting: use donkey anti-goat IgG-HRP: sc-2020 (dilution range: 1:2000-1:100,000) or Cruz Marker™ compatible donkey anti-goat IgG-HRP: sc-2033 (dilution range: 1:2000-1:5000), Cruz Marker™ Molecular Weight Standards: sc-2035, TBS Blotto A Blocking Reagent: sc-2333 and Western Blotting Luminol Reagent: sc-2048. 2) Immunoprecipitation: use Protein A/G PLUS-Agarose: sc-2003 (0.5 ml agarose/2.0 ml). 3) Immunofluorescence: use donkey anti-goat IgG-FITC: sc-2024 (dilution range: 1:100-1:400) or donkey anti-goat IgG-TR: sc-2783 (dilution range: 1:100-1:400) with UltraCruz™ Mounting Medium: sc-24941.
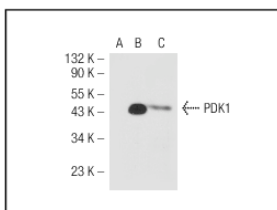
DATA

PDK1 (C-20): sc-7140. Western blot analysis of PDK1 expression in non-transfected: sc-117752 (**A**) and human PDK1 transfected: sc-113873 (**B**) 293T whole cell lysates and rat heart tissue extract (**C**).
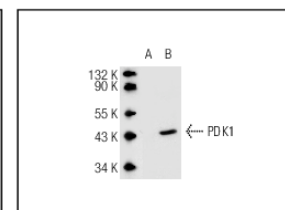
PDK1 (C-20): sc-7140. Western blot analysis of PDK1 expression in non-transfected: sc-117752 (**A**) and human PDK1 transfected: sc-171642 (**B**) 293T whole cell lysates.

SELECT PRODUCT CITATIONS

1. Sikder, D., et al. 2007. The neurohormone orexin stimulates hypoxia-inducible factor-1 activity. Genes Dev. 21: 2995-3005.

2. De Palma, S., et al. 2007. Metabolic modulation induced by chronic hypoxia in rats using a comparative proteomic analysis of skeletal muscle tissue. J. Proteome Res. 6: 1974-1984.

Figure A. 16: Datasheet of Total PDK1 antibody (http://www.scbt.com/).

Phospho-PDK1 (Ser241) Antibody

Store at -20°C

#3061

☐ Small 100 µl
(10 western blots)

☐ Large 300 µl
(30 western blots)

Cell Signaling
TECHNOLOGY®

Orders	■	877-616-CELL (2355)
		orders@cellsignal.com
Support	■	877-678-TECH (8324)
		info@cellsignal.com
Web	■	www.cellsignal.com

rev. 10/12/11

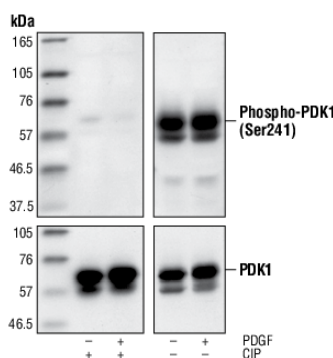This product is intended for research purposes only. This product is not intended to be used for therapeutic or diagnostic purposes in humans or animals.

Entrez-Gene ID #5170
Swiss-Prot Acc. #O15530

Applications	Species Cross-Reactivity*	Molecular Wt.	Source
W, IP Endogenous	H, M, R	58–68 kDa	Rabbit**

Storage: Supplied in 10 mM sodium HEPES (pH 7.5), 150 mM NaCl, 100 µg/ml BSA and 50% glycerol. Store at –20°C. *Do not aliquot the antibody.*

*Species cross-reactivity is determined by western blot.

**Anti-rabbit secondary antibodies must be used to detect this antibody.

Recommended Antibody Dilutions:
Western Blotting 1:1000
Immunoprecipitation 1:100

For application specific protocols please see the web page for this product at www.cellsignal.com.

Please visit www.cellsignal.com for a complete listing of recommended companion products.

Background: Phosphoinositide-dependent protein kinase 1 (PDK1) plays a central role in many signal transduction pathways (1,2), activating Akt and the PKC isoenzymes p70 S6 kinase and RSK (3). Through its effects on these kinases, PDK1 is involved in the regulation of a wide variety of processes, including cell proliferation, differentiation and apoptosis.
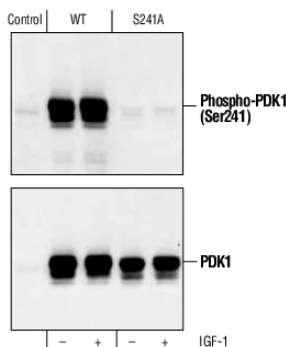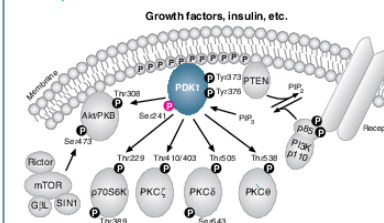
Several serine sites (Ser25, Ser241, Ser393/396 and Ser410) are phosphorylated on PDK1 in unstimulated human embryo kidney 293 cells, as well as IGF-1 stimulated cells (4). Phosphorylation on the activation loop Ser241 by autophosphorylation is necessary for PDK1 activity (4).

Specificity/Sensitivity: Phospho-PDK1 (Ser241) Antibody detects PDK1 only when phosphorylated at Ser241.

Source/Purification: Polyclonal antibodies are produced by immunizing animals with a synthetic phosphopeptide corresponding to residues surrounding Ser241 of human PDK1. Antibodies are purified by protein A and peptide affinity chromatography.

Background References:
(1) Belham, C. et al. (1999) *Curr. Biol.* 9, R93–R96.
(2) Toker, A. and Newton, A.C. (2000) *Cell* 103, 185–188.
(3) Williams, M.R. et al. (2000) *Curr. Biol.* 10, 439–448.
(4) Casamayor, A. et al. (1999) *Biochem. J.* 342, 287–292.

Western blot analysis of extracts from NIH/3T3 cells (starved for 16 hours) treated with PDGF (50 ng/ml), using Phospho-PDK1 (Ser241) Antibody (upper) or control PDK1 antibody (lower). The phospho-specificity of the antibody was confirmed by treating the membrane with calf intestinal alkaline phosphatase (CIP) after Western transfer.

Western blot analysis of extracts from 293 cells transiently transfected with DNA constructs expressing Wild-type PDK1 or S241A mutant PDK1, treated with IGF-1, using Phospho-PDK1 (Ser241) Antibody (upper) or control PDK1 Antibody #3062 (lower). (Cell lysates provided by Dr. M. Scheid, Ontario Cancer Institute, University Health Network, Toronto.)

IMPORTANT: For western blots, incubate membrane with diluted antibody in 5% w/v BSA, 1X TBS, 0.1% Tween-20 at 4°C with gentle shaking, overnight.

Applications Key: W—Western IP—Immunoprecipitation IHC—Immunohistochemistry ChIP—Chromatin Immunoprecipitation IF—Immunofluorescence F—Flow cytometry E-P—ELISA-Peptide

Species Cross-Reactivity Key: H—human M—mouse R—rat Hm—hamster Mk—monkey Mi—mink C—chicken Dm—D. melanogaster X—Xenopus Z—zebrafish B—bovine
Dg—dog Pg—pig Sc—S. cerevisiæ Ce—C. elegans Hr—Horse All—all species expected Species enclosed in parentheses are predicted to react based on 100% homology.

Figure A. 17: Datasheet of p-PDK1 antibody (http://www.cellsignal.com//).

SANTA CRUZ BIOTECHNOLOGY, INC.

14-3-3 σ (N-14): sc-7681

SANTA CRUZ®
BIOTECHNOLOGY
The Power to Question

BACKGROUND

14-3-3 proteins regulate many cellular processes relevant to cancer biology, notably apoptosis, mitogenic signaling and cell cycle checkpoints. Seven isoforms, denoted 14-3-3 β, γ, ε, ζ, η, θ and σ, comprise this family of signaling intermediates. 14-3-3 σ, also known as SFN, stratifin, HME1 or YWHAS, is a secreted adaptor protein that is involved in regulating both general and specific signaling pathways. Expressed predominantly in stratified squamous keratinizing epithelium, 14-3-3 β is able to bind and modify the activity of a large number of proteins, such as KRT17 (Keratin 17), through recognition of a phosphothreonine or phosphoserine motif. When bound to KRT17, for example, 14-3-3 σ acts to stimulate the Akt/mTOR signaling pathway by upregulating protein synthesis and cell growth. 14-3-3 σ also functions to positively mediate IGF-I-induced cell cycle progression and can bind to a variety of translation initiation factors, thus controlling mitotic translation. In response to tumor growth, 14-3-3 σ positively regulates the tumor suppressor p53 and increases the rate of p53-regulated inhibition of G_2/M cell cycle progression. Multiple isoforms of 14-3-3 σ exist due to alternative splicing events.

CHROMOSOMAL LOCATION

Genetic locus: SFN (human) mapping to 1p36.11; Sfn (mouse) mapping to 4 D2.3.

SOURCE

14-3-3 σ (N-14) is an affinity purified goat polyclonal antibody raised against a peptide mapping near the N-terminus of 14-3-3 σ of human origin.

PRODUCT

Each vial contains 200 µg IgG in 1.0 ml of PBS with < 0.1% sodium azide and 0.1% gelatin.

Blocking peptide available for competition studies, sc-7681 P, (100 µg peptide in 0.5 ml PBS containing < 0.1% sodium azide and 0.2% BSA).

APPLICATIONS

14-3-3 σ (N-14) is recommended for detection of 14-3-3 σ of mouse, rat and human origin by Western Blotting (starting dilution 1:200, dilution range 1:100-1:1000), immunoprecipitation [1-2 µg per 100-500 µg of total protein (1 ml of cell lysate)], immunofluorescence (starting dilution 1:50, dilution range 1:50-1:500) and solid phase ELISA (starting dilution 1:30, dilution range 1:30-1:3000).

14-3-3 σ (N-14) is also recommended for detection of 14-3-3 σ in additional species, including equine, canine, bovine and porcine.

Suitable for use as control antibody for 14-3-3 σ siRNA (h): sc-29590, 14-3-3 σ siRNA (m): sc-29591, 14-3-3 σ shRNA Plasmid (h): sc-29590-SH, 14-3-3 σ shRNA Plasmid (m): sc-29591-SH, 14-3-3 σ shRNA (h) Lentiviral Particles: sc-29590-V and 14-3-3 σ shRNA (m) Lentiviral Particles: sc-29591-V.

Molecular Weight of 14-3-3 σ: 30 kDa.

Positive Controls: 14-3-3 σ (h3): 293T Lysate: sc-110782, A-431 whole cell lysate: sc-2201 or HeLa whole cell lysate: sc-2200.

STORAGE

Store at 4° C, **DO NOT FREEZE**. Stable for one year from the date of shipment. Non-hazardous. No MSDS required.

DATA
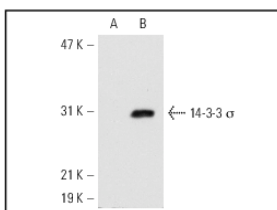
14-3-3 σ (N-14): sc-7681. Western blot analysis of 14-3-3 σ expression in non-transfected: sc-117752 (**A**) and human 14-3-3 σ transfected: sc-110782 (**B**) 293T whole cell lysates.
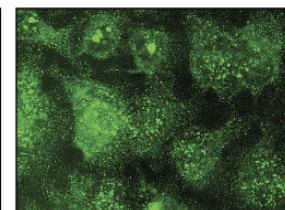
14-3-3 σ (N-14): sc-7681. Immunofluorescence staining of methanol-fixed HeLa cells showing cytoplasmic and nuclear localization.

SELECT PRODUCT CITATIONS

1. Iwata, N., et al. 2000. Frequent hypermethylation of CpG islands and loss of expression of the 14-3-3 gene in human hepatocellular carcinoma. Oncogene 19: 5298-5302.

2. Xin, Y., et al. 2010. 14-3-3σ controls corneal epithelial cell proliferation and differentiation through the Notch signaling pathway. Biochem. Biophys. Res. Commun. 392: 593-598.

3. Mirza, S., et al. 2010. Clinical significance of Stratifin, ERα and PR promoter methylation in tumor and serum DNA in Indian breast cancer patients. Clin. Biochem. 43: 380-386.

4. Suárez-Bonnet, A., et al. 2010. Immunohistochemical localisation of 14-3-3 σ protein in normal canine tissues. Vet. J. 185: 218-221.

5. Jeong, J.H., et al. 2010. p53-independent induction of G_1 arrest and p21$^{WAF1/CIP1}$ expression by ascofuranone, an isoprenoid antibiotic, through downregulation of c-Myc. Mol. Cancer Ther. 9: 2102-2113.

6. Rohaly, G., et al. 2010. Simian virus 40 activates ATR-Δ p53 signaling to override cell cycle and DNA replication control. J. Virol. 84: 10727-10747.

7. Xin, Y., et al. 2011. IKK1 control of epidermal differentiation is modulated by notch signaling. Am. J. Pathol. 178: 1568-1577.

8. Xu, Y., et al. 2011. Multiple pathways were involved in tubeimoside-1-induced cytotoxicity of HeLa cells. J. Proteomics 75: 491-501.

9. Di Costanzo, A., et al. 2011. A dominant mutation etiologic for human tricho-dento-osseous syndrome impairs the ability of DLX3 to downregulate ΔNp63α. J. Cell. Physiol. 226: 2189-2197.

10. Inglés-Esteve, J., et al. 2012. Inhibition of specific NFκB activity contributes to the tumor suppressor function of 14-3-3σ in breast cancer. PLoS ONE 7: e38347.

RESEARCH USE

For research use only, not for use in diagnostic procedures.

Figure A. 18: Datasheet of 14-3-3s antibody (http://www.scbt.com/).